# Identifying significant groundwater recharge areas and modelling surface and subsurface water balance of the Neebing River

by

Tim Vehling

Lakehead University

2024

## Abstract

This study provides a hydrological function assessment of the Neebing River, a stream that starts in a rural context and transitions to an urban environment that has historically been prone to flooding. Hydrological function assessments have been widely used across the globe, but there is limited information on many rivers in northern Ontario's watersheds. Previous hydrological function assessments provide a basis upon which to develop models based on thematic mapping, surface water and groundwater interactions and isotope sampling to enable the mapping of significant groundwater recharge areas (SGRA) in the Neebing watershed. Infiltration rates were modelled based on available topographic, soil and land use data sets. Statistical analyses of climatological and hydrological variables were used to examine surface-subsurface water interactions on a seasonal and annual scale. Stable isotope sampling was used to investigate groundwater-surface water interactions in some detail. Results of the study show that the Neebing River is highly dependent on the contribution of groundwater to streamflow, especially during dry periods and during the winter. The flow dependency on groundwater highlights the relationship between the Neebing River and the SGRAs within its watershed. The present study advances knowledge of the hydrological function of the Neebing River and provides baseline data for future studies of the impacts of climate change and urbanization on this watershed.

## Acknowledgements

I thank the Geography and the Environment department at Lakehead University, especially my supervisors, Dr. Adam Cornwell and Dr. Kamil Zaniewski, for their support and guidance in this research project. I would also like to thank my committee member, Dr. Robert Stewart, for his valuable advice. A special thanks to the Geography and the Environment department technicians Mr. Jason Freeburn and Mr. Reg Nelson. Their help and guidance with the fieldwork, data collection, advice, and expertise in the work with GIS were of great value to this project and greatly appreciated. Additionally, I thank Mr. Graham Saunders for providing the historical climatologic data needed to fill data gaps. I would like to acknowledge that the Ontario Ministry of the Environment, Conservation and Parks funded this project. I thank Pradeep Goel (MECP) for his valuable help. I also would like to thank Lorena Vehling and my children for their endless support.

Table of Contents

## List of Tables



## List of Figures

List of Equations

**CHAPTER 1**

# 1 Introduction

The Neebing River is a stream in northern Ontario with rural headwaters, transitioning to an urban environment before terminating into the McIntyre River within the City of Thunder Bay. The hydrological function assessment of the Neebing River is one of several projects across the province of Ontario to better understand our watersheds, streams, and groundwater-surface water interactions (Persaud et al. 2020; Azarkhish et al. 2021; Philip et al. 2022; Montgomery 2023). A hydrologic function assessment results in an analysis of the catchment area's response to incoming water, how water is stored and eventually released from the catchment. The discharge levels and volumes leaving the catchment can be measured and used to determine the ability to store water and the response to high and low precipitation events. Human development can impact the hydrologic function of a river through urbanization, the channelling of the stream, the reduction of wetlands, and the overall increase in impermeable surfaces in the river basin. This hydrologic function assessment will include mapping significant groundwater recharge areas and modelling surface and subsurface water interactions. These models will be applied on both an annual and seasonal basis to understand changes over time. Furthermore, stable isotopic sampling of hydrogen and oxygen will be used to further investigate the groundwater-surface water interactions. Stable hydrogen and oxygen isotopes are naturally occurring and are commonly used as tracers for estimating streamflow contribution (Kalbus et al. 2006). The results of this project will contribute to our understanding of the Neebing River hydrologic function and its catchment area and provide a baseline for understanding how climate change and future development in this area may impact groundwater.

## 1.1 Research Objectives

The research objectives are to: (1) identify significant groundwater recharge areas (SGRA) within the Neebing River watershed; (2) model the seasonal and annual patterns of climatic and hydrological variables and indicators using correlation analysis, trend analysis, and double-mass balance analysis; (3) to determine the water balance of the Neebing River and to analyze the surface water and groundwater interactions.

The results of this research will improve our understanding of the surface water and groundwater relationship and establish baseline conditions in the Neebing River watershed that can be utilized in future development within the study area. This research will provide a baseline data set to simulate future conditions under changing climatic and hydrologic conditions.

**CHAPTER 2**

# 2 Literature Review

## 2.1 Hydrologic Function

The hydrologic function can be defined as the action of the catchment (also called watershed or basin) on the incoming water (Wagener et al. 2007). The water that enters the catchment in the form of precipitation then undergoes partition in the form of interception, infiltration, and percolation (Wagener et al. 2007). Water is then either directly released or enters the stage of storage, where it can be stored in vegetation, snow, groundwater, lake, channel, soil moisture, and saturated zone storage (Wagener et al. 2007). The storage time of water greatly varies with the storage location and the geographical characteristics of the catchment (Wagener et al. 2007). Eventually, water reaches the stage of release when it exits the catchment through evapotranspiration, streamflow, or groundwater flow (Wagener et al. 2007). Barbier et al. define the interactions between the system's components as functions (1997). Furthermore, the hydrologic function can include a watershed's ecologic and wetland functions (McLaughlin and Cohen 2013). Hydrologic function assessments are used to analyze how the water travels through the catchment and its individual components.

Hydrological function assessments have been conducted in various settings to examine different aspects of a catchment area. Garrett et al. investigated groundwater-surface water interactions and used a hydrograph separation method (End-Member Mixing Analysis or EMMA) to determine the main contributing sources for streamflow (Garrett et al. 2012). This study from South Carolina found precipitation, groundwater and streambed groundwater as the main sources of streamflow (Garrett et al. 2012). Runoff from precipitation was identified as the primary contribution to streamflow during rainfall events (Garrett et al. 2012).

The hydrologic function assessment conducted by McLaughlin and Cohen (2013) in Florida investigated the hydrologic regime, groundwater, and evapotranspiration rates in eleven wetlands. The analysis used the Uniform Mitigation Assessment Method (UMAM), Florida's official wetland assessment tool and the White method to investigate the groundwater (White 1932; McLaughlin and Cohen 2013). The study found that human developments can disrupt wetland services and that especially evapotranspiration is affected by changes in land use (McLaughlin and Cohen 2013).

The effectiveness of water management practices can be tested and modelled using GIS software. Raster spatial analysis of Geo-Information System (RGIS-HM) can capture the impact of small-scale flood mitigation elements that were previously not possible with models such as Soil and Water Assessment Tool (SWAT) or HEC-HMS (the Hydrologic Modelling System from the Hydrologic Engineering Center by the US Army Corps of Engineering) (Tarigan 2016). These discrete smaller flood mitigation elements include infiltration wells, farm reservoirs, and silt pits. Tarigan (2016) used a RGIS-HM model to model flood events, and the results were then validated with the measurements of a flood event from the study area in West Java, Indonesia.

Fleury et al. (2009) modelled the hydrologic function of a karst aquifer. They used a reservoir model to simulate the function of the aquifer that divides the aquifer into saturated and unsaturated infiltration zones. The Lez River water level in southern France is dependent on the saturation of the infiltration zones of the aquifer. This model can simulate different saturation levels and, therefore, could be used for water resource management and flood mitigation (Fleury et al. 2009).

One example of a hydrologic function that describes ecologic and wetland function is by Brinson (1993). This study suggests a new grouping of wetlands for biochemical functioning by the exchange of nutrients and sediments in specific sections of the wetland instead of categorizing them as sinks or sources of a specific component (Brinson 1993). Besides the well-established functions of wetlands as water storage, Brison highlights the retaining function of nutrients and sediments in wetlands (Brinson 1993). Other ecological wetland functions include flood-flow alteration and habitat preservation (Brinson 1993). Hydrologic functions vary among catchment areas and provide valuable environmental services.

The water storage capabilities of a catchment area are vital for natural flood protection and are one aspect of hydrologic function. Anthropogenic changes to the catchment through urbanization can lead to changes in hydrologic function (Taylor and Roth 1979). Urban development can lead to increased direct runoff in response to snowmelt events (Taylor and Roth 1979). A changing climate can also contribute to changes in the catchment's hydrologic function and streamflow discharge (Lister et al. 1999; Persaud et al. 2020; Philip et al. 2022). Data analyses from previous decades suggest more substantial impacts of climate change on the hydrologic function of streams located in southern Ontario compared to streams located in northern Ontario (Azarkhish et al. 2021). One recent study found that a changing climate is more likely to impact surface water compared to groundwater (Persaud et al. 2020). Therefore, changes in climatic conditions can cause significant changes in a catchment area that hydrological function assessments can detect.

## 2.2 Thematic Mapping

The *"Delineation of Significant Groundwater Recharge Areas: Supplemental Technical Guide"* (AquaResource Inc. 2012) that was prepared for the Ontario Ministry of Natural Resources provides a guideline for the identification of significant groundwater recharge areas and the necessary steps that the Conservation Authorities took during that process. The methodology in this report can be adapted and used to identify significant groundwater recharge areas in the Neebing River watershed. The Ontario Ministry for the Environment report "*Stormwater Management Planning and Design Manual"* (Ontario Ministry of the Environment 2003) provides detailed infiltration values for different groundcovers and soil types. This information will be used to identify significant groundwater recharge areas. A non-linear regression model was used to estimate the infiltration value for the derived slope values to produce a topography-related factor grid, as suggested by the Niagara Conservation Authority and Aqua Resource Inc. in the *Significant Groundwater Recharge Area Delineation Niagara Peninsula Source Protection Area* report (2009).

A significant groundwater recharge area can be defined in two ways. Rule 44(1) of the technical rules under the Clean Water Act (Ontario Ministry of the Environment 2013) states that an area that has an infiltration rate that is greater by a factor of 1.15 than the average infiltration rate of the full watershed can be identified as an SGRA (Ontario Ministry of the Environment 2013). Alternatively, an SGRA can be defined, under Rule44(2), as an area that annually recharges 55% or more to an aquifer, where the annual

evapotranspiration of the whole related groundwater recharge area is subtracted from the annual precipitation of the whole related groundwater recharge area (Ontario Ministry of the Environment 2013). The definition in rule 44(1) is usually used in areas where recharge rates are similar and can distinguish between high and low recharge rates in a given area. In contrast, the second definition, in Rule 44(2), is used in areas that vary greatly in the range of recharge rates (AquaResource Inc. 2012). The supplemental technical guide for the delineation of SGRAs in Ontario lists reports by conservation authorities in Ontario and the preferred rule they followed in their identification of SGRAs (AquaResource Inc. 2012). Rule 44(1) has been used more often with regional differences (AquaResource Inc. 2012). Rule 44(2) has been used more commonly in eastern Ontario, and Rule 44(1) was used more commonly in Southern Ontario, whereas in northern Ontario both rules were used (AquaResource Inc. 2012). The Lakehead Region Conservation Authority (LRCA) used Rule 44(1) for SGRA delineation in the Thunder Bay area in 2008 (Gartner Lee Limited 2008). Therefore, Rule 44(1) was deemed more suitable for identifying SGRAs in this study.

## 2.3 Statistical Analysis

Mills and Post (2018) assessed the hydrologic function in the Nottawasaga Valley in Ontario. The two major components of this function assessment were a thematic land use evaluation and a statistical analysis (Mills and Post 2018). Mills and Post's approach will be used as an example for the hydrological function assessment of the Neebing River. Their report utilized the Thornwaite-Mather approach to describe the water balance and gives an example for the estimate of baseflow derived from streamflow (Mills and Post 2018). Cuddy, Chan, and Post (2013) also, cite the Thornwaite-Mather approach as a commonly used tool in their description of a general water balance model in the hydrological assessment submission guidelines to the Ontario Conservation Authorities. This approach will also be used in the Neebing River hydrologic function assessment to estimate the water balance.

The methodology of using Spearman's Rank, Kendall's Rank, linear regression, and the Mann-Kendall trend test used by Mills and Post (2018) was also used by Gao et al. (2010). In their study, Gao et al. analyzed hydrologic data, such as streamflow discharge, precipitation, and groundwater level, in a time-series format. The correlation analysis was conducted to evaluate the relationships between the different hydrologic variables (Gao et al. 2010). The Mann-Kendall trend test was used for trend detection to evaluate if the data is trending in a particular direction (Gao et al. 2010).

Piggot et al. (2005) describe modifications to the UKIH (United Kingdom Institute of Hydrology) method to address issues regarding the "less than optimal results" that were obtained using the original method. The UKIH method identifies and interpolates turning points within a time series of streamflow data. Daily streamflow averages are used in this method, and the time series is sequenced into five-day segments. Within each segment, the minimum value for streamflow value is identified as a potential turning point and compared to the minimum value from the previous and subsequent segments. This sequence of successive turning points is then used in the interpolation to estimate the variability in baseflow over time. Piggott et al. (2005) suggested changes to the UKIH method; the first addresses the interpolated values for baseflow values that surpass the observed streamflow values. Limiting the baseflow values to be no greater than the observed streamflow values delivers results that are objectively

more realistic compared to results from the original method. The change also decreases the dependency of estimated baseflow values on the arbitrary start of the segmentation period (2005).

The SepHydro hydrograph separation tool is an alternative tool designed for baseflow estimation (Danielescu et al. 2018). This online tool allows the user to choose different baseflow separation methods, upload their input data and export results in the form of graphs, tables, and descriptive statistics (Danielescu et al.,2018). These methods are based on different mathematical models and can require different kinds of input data. The baseflow separation methods that are available are:

- the Lyne and Hollick method,
- Chapman method,
- Eckhardt method,
- Pettyjohn and Henning - fixed interval method,
- Pettyjohn and Henning - sliding interval method,
- Pettyjohn and Henning - local minimum method,
- TR-55 method, Szilagyi method,
- Boughton method,
- Furey and Gupta method, and
- Chapman and Maxwell method (Danielescu et al. 2018).

The online tool is freely available and part of the Hydrology Tool Set (HTS), which was developed by the Canadian Rivers Institute (CRI), the University of New Brunswick (UNB), Agriculture and Agri-Food Canada (AAFC), and Environment and Climate Change Canada (ECCC).

Although different methodologies exist for baseflow separation, the method described by (Eckhardt 2005) was chosen for the Neebing River because of the available data and the accessible online tool SepHydro using Eckhardt (2005). May et al. (2023) Other recent work in Ontario (e.g. May et al. (2023) use Eckhardt's methodology of baseflow separation. For the recession constant α, a master recession curve was established in Matlab using the HYDRORECESSION tool by Arciniega-Esparza et al. (2017). Using this methodology, May et al. (2023) found an α value of 0.77, which is lower than other articles in the literature suggested.

Arciniega-Esparza et al. (2017) describe the tool they developed to help with recession analysis using a graphical interface within the Matlab software. This toolbox can analyze segments of the hydrograph recession and model recession curves using three models (Arciniega-Esparza et al. 2017). May et al. (2023) used this tool successfully for the estimation of the recession constant α (May et al. 2023). This tool is a good option for the recession analysis to estimate the recession constant α as it has been used for this purpose before. Furthermore, Matlab is a software tool available on the internet, and it is free to use when signing in as a student. However, this Matlab toolbox was not operational when tried for this study and only led to repeated error messages. Therefore, the method suggested by Eckhardt (2008) was successfully used as an alternative.

For this study, therefore, the SepHydro tool using the (Eckhardt 2005) method was used due to the availability of the required input data, free access to the software program on the internet, and ease of use and its very accessible interface. The results are comparable with other methods and the literature suggests this as a feasible option. Xie et al. (2020) compared four graphical and five digital filter methods for baseflow separation, including the UKIH method, and found that the Eckhardt (2005) method

performed best independent of catchment characteristics. These findings included baseflow separation analysis from 1815 catchments in the continental United States (Xie et al. 2020).

## 2.4 Stable Isotope Sampling

A methodology component that is different from the previously mentioned approaches is the validation of groundwater contribution to streamflow by stable isotope analysis of hydrogen and oxygen. Stable isotopes are commonly used to analyze groundwater contribution to streamflow, as groundwater usually contains less $\delta^{2}H$ and $\delta^{18}O$ compared to surface water (Kalbus et al. 2006; Ferronsky and Polyakov 2012). Stable isotopes can also aid in identifying seasonal variability in streamflow contribution (Jung et al. 2021). The *"Sampling Procedures for Isotope Hydrology"* by the International Atomic Energy Agency's (IAEA) Water Resource Programme outlines the sampling methodologies for taking water samples. Water samples are taken directly from the moving stream water using 50 ml polyethylene bottles with a cone-shaped lid. This lid type is used to prevent headspace in the sampling bottle, as evaporation is the main concern with water sampling of stable isotopes. Once the sampling bottle is filled with the water sample, the lid is tightly secured, and the bottle is clearly marked with an identification number, location, date, and time. The samples are stored in a cool and dark place before being shipped to the Integrative Watershed Research Center at Nipissing University for stable isotope analysis.

**CHAPTER 3**

# 3 Description of Study Area

## 3.1 General Description

The study area of the Neebing River drainage basin includes areas within the City of Thunder Bay, the Municipality of Oliver Paipoonge, and the Township of Ware (Lakehead Region Conservation Authority and KGS Group 2018). It includes the three major branches of the Neebing River, the northern branch, the western branch, and Pennock Creek. The entire study area is 233 km$^2$ in size. Figure 3.1 below shows the study area and the location of the Environment and Climate Change Canada (ECCC) weather station and Water Survey of Canada (WSC) hydrometric station locations.

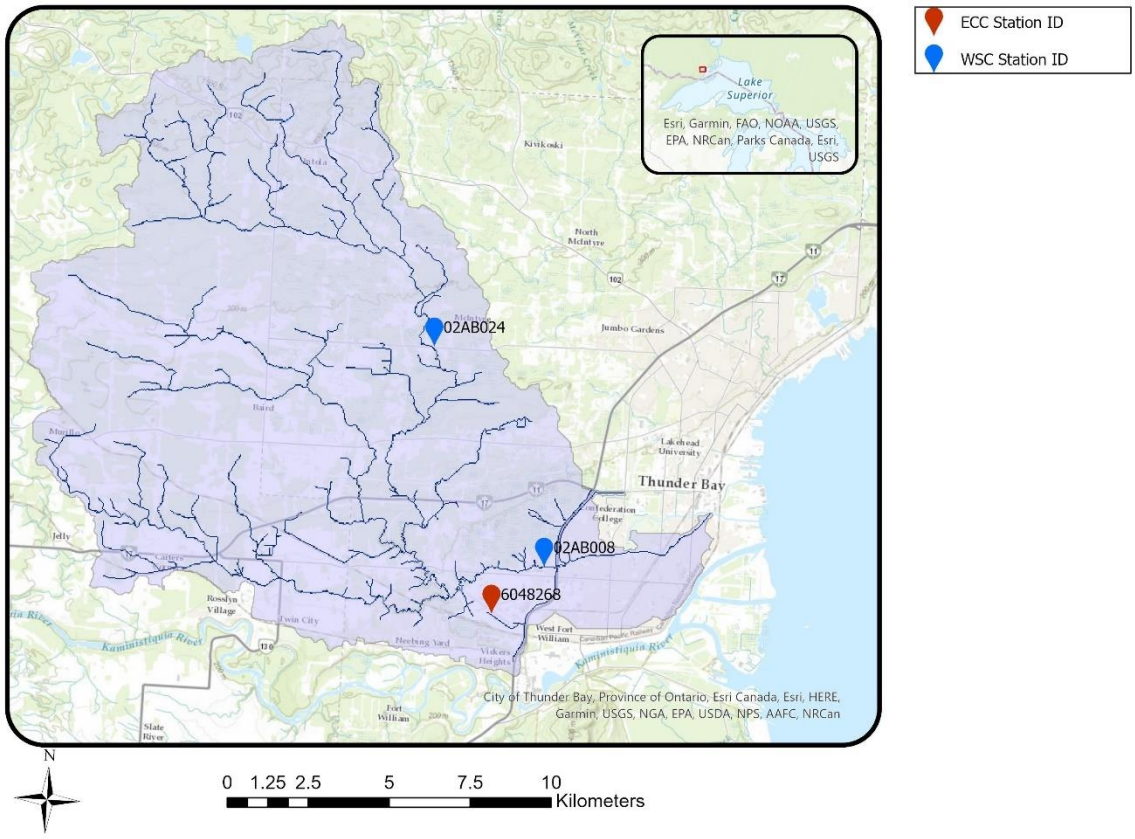


*Figure 3.1. Neebing River study area*

The Northern branch is the largest by drainage area and joins together with the Western branch near Arthur Street West (Lakehead Region Conservation Authority and KGS Group 2018). Pennock Creek is the smallest branch by drainage area and drains the southern part of the watershed (Lakehead Region Conservation Authority and KGS Group 2018). Pennock Creek joins the Neebing River just west of the

Thunder Bay International Airport. The Neebing McIntyre Floodway was constructed between 1978 and 1983 to help reduce the impact of flood events along the lower Neebing River (Macdonald 2014; Lakehead Region Conservation Authority 2024). During the last flood events in 1997, 2008, and 2012, the floodway operated successfully, preventing large-scale riverine flooding on the lower Neebing River (Lakehead Region Conservation Authority 2024). The following Table 3.1 derived from the Ministry of Natural Resource and Forestry (MNRF) Ontario Flow Assessment Tool (OFAT), shows stream characteristics of the Neebing River:

*Table 3.1. Characteristics of the Neebing River Watershed (OMNRF - Provincial Mapping Unit 2023)*

| | |
|---|---|
| Drainage Area | 233.2 $km^2$ |
| Length of Main Channel | 45.2 km |
| Slope of Main Channel | 0.69 % |
| Mean Slope | 3.0 % |
| Maximum Elevation | 501.3 m |
| Annual Mean Temperature | 2.9 °C |
| Annual Precipitation | 707 mm |

## 3.2 Climate

The Neebing River experiences a warm-summer humid continental climate and can be classified as Dfb under the Köppen climate classification (Rohli and Vega 2018). The proximity to Lake Superior has a moderating effect that is lessened with distance to lake. The lake effect can cause cooler conditions near Lake Superior in the summer and warmer conditions during the late fall and winter before the lake freezes over. The continental location causes long and cold winters with snow precipitation. The prevailing wind direction is westerly winds due to Neebing River's location in the mid-latitudes. The Neebing River drainage basin is located in parts within the City of Thunder Bay and the ECCC meteorological station, Thunder Bay CS, lies within the watershed. Therefore, the historic data from this station is most appropriate to describe the atmospheric conditions for the Neebing River.

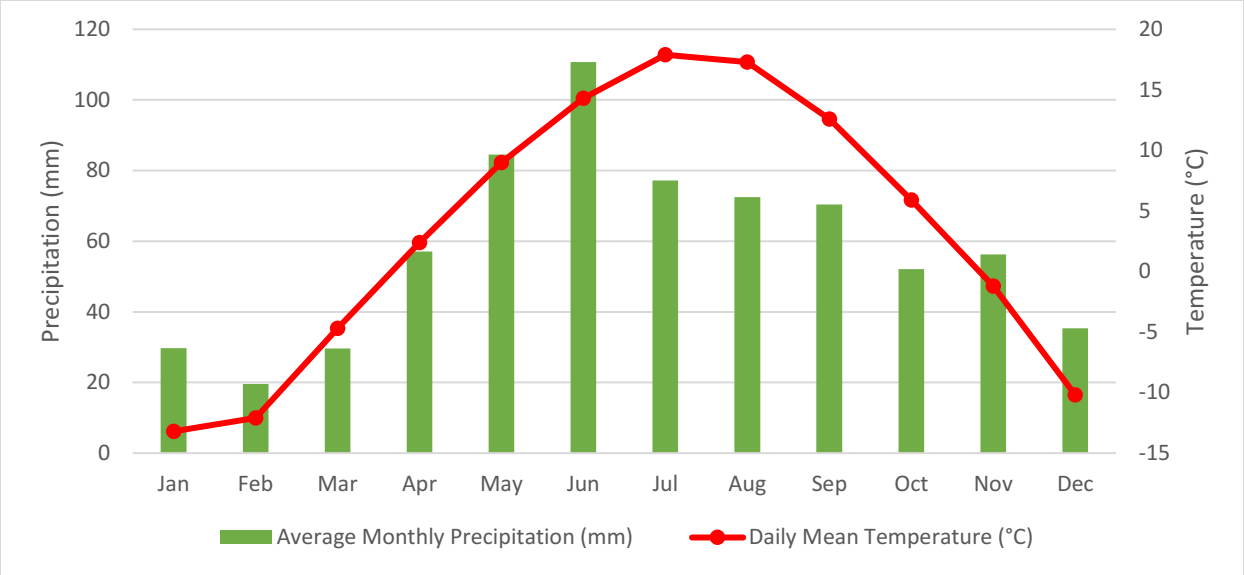


*Figure 3.2. Average monthly precipitation and daily mean temperature for Thunder Bay CS, 2008-2017, Environment and Climate Change Canada*

## 3.3 Hydrology

The Neebing River basin drains an area of approximately 233 km$^2$ with an average slope of the main channel of 0.69% (Ontario Ministry of Natural Resources and ForestryMNRF - Provincial Mapping Unit 2023). Water levels vary greatly between the different seasons in the Neebing River. High flow events are usually observed during the spring freshet, whereas low flow is observed during the late summer months.

Only the area upstream from the WSC station near Arthur Street was used as a study area for the statistical analysis and water balance calculations. This location was chosen as there is no historical data record of the Neebing River at its mouth, where it drains into the McIntyre River before reaching Lake Superior. This is a drainage area of 208 km$^2$. Figure 3.3 shows the overall study area of the Neebing River watershed and the adjusted area upstream of the WSC station near Arthur Street.

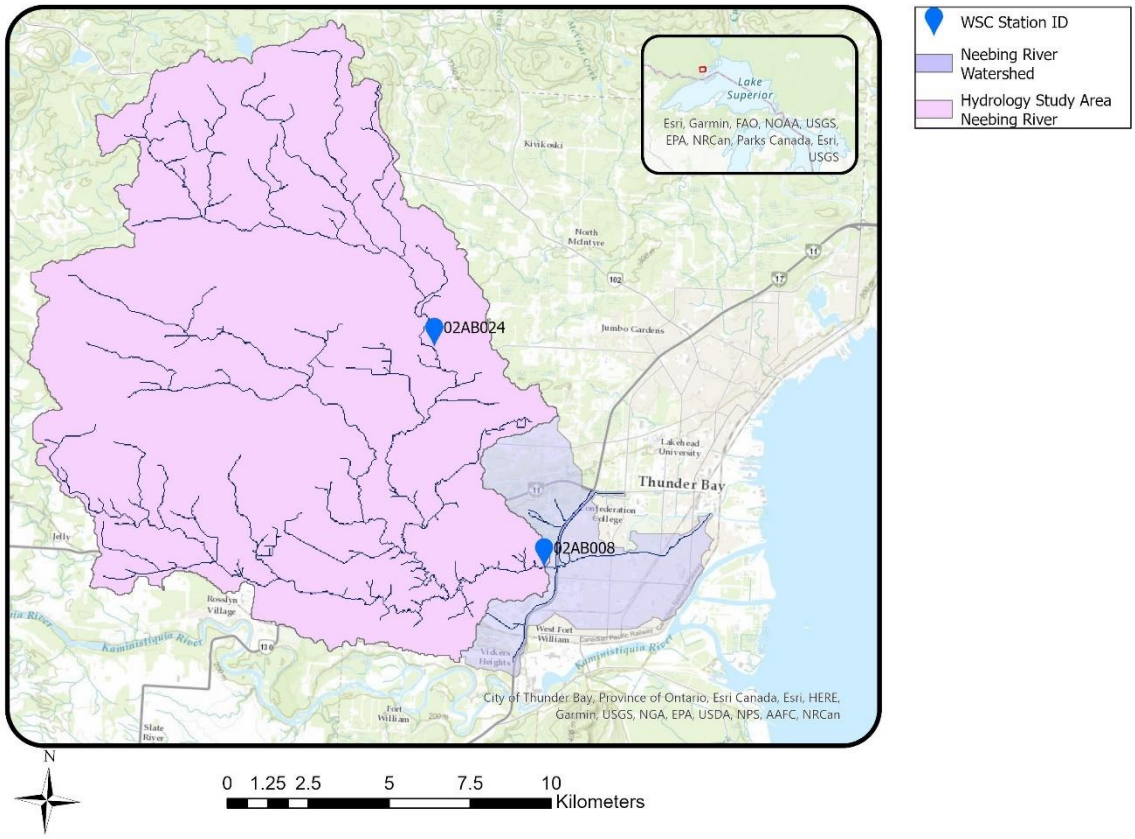


*Figure 3.3. Neebing River hydrology study area*

## 3.4 Land Use

Land use and cover vary greatly within the Neebing River watershed. Table 3.2 below illustrates the landcover types present and how common they are within the Neebing River basin. Forest vegetation is dominant in the areas to the north and northwest; the most dominant tree species include red pine (Pinus resinosa), white pine (Pinus strobus), Jackpine (Pinus banksiana), white birch (Betula papyrifera), white spruce (Picea glauca), black spruce (Picea mariana), and Trembling aspen (Populus tremuloides) (Gartner Lee Limited 2008). Closer to the City of Thunder Bay and more central within the watershed, the amount of agricultural land use increases. Also, the presence of rural dwellings and infrastructure increases with closer proximity to Thunder Bay. Once the Neebing River reaches the city and the more densely populated areas, it enters an urban environment through the mouth of the Neebing River at the McIntyre River.

*Table 3.2. Landcover in the Neebing River basin*

| **Landcover** | **Percentage** |
|---|---|
| Clear Open Water | 0.5 |

| | |
|---|---|
| Bog | 0.6 |
| Sparse Treed | 36.7 |
| Deciduous Treed | 19.8 |
| Mixed Treed | 17.2 |
| Coniferous Treed | 3.5 |
| Community/Infrastructure | 18.3 |
| Agriculture and Undifferentiated Rural Land Use | 3.3 |

**CHAPTER 4**

# 4 Methodology

## 4.1 Significant groundwater recharge areas (SGRA) mapping

The methodology developed and utilized by the Niagara Conservation Authority and AquaResource Inc. (2009) was adapted for this research. The infiltration factor values used by the Niagara Conservation Authority are based on two Ontario provincial manuals and guidelines (Ontario Ministry of Environment and Energy 1995; Ontario Ministry of the Environment 2003). Differences in geographical and geological settings between the Neebing watershed and the Niagara region are accounted for by the differences in infiltration factor values for different soil and landcover types.

Three factors, slope, landcover-based infiltration layer and soil type, were required for this analysis. The GIS (Geographic Information System) software packages ArcPro and QGIS were used to prepare the input layers. The input data, Provincial Digital Elevation Model (PDEM) and Soil Survey Complex data were downloaded from the Ontario GeoHub (Ontario Ministry of Natural Resources 2022) and the stream and landcover information were downloaded from the Ontario Flow Assessment Tool (Ontario Ministry of Natural Resources and Forestry - Provincial Mapping Unit 2023). This input data includes a provincial digital elevation model, a soil layer, and the landcover layer. All input layers were transformed into raster layers (if not already raster) and were converted to 15 m by 15 m raster cells. Input layers for the parameters were input in the same raster format and cell size. For each cell, the infiltration index was calculated as the sum of three infiltration factors based on the characteristics of its input layers. The Ontario provincial government has set out rules and guidelines for the delineation of significant groundwater recharge areas (Ontario Ministry of the Environment 2013). These rules were followed using the methodology used by Niagara Conservation Authority (Niagara Conservation Authority and AquaResource Inc. 2009).

Slope data was derived from the PDEM using ArcPro. Infiltration factors from Ontario Ministry of Environment and Energy (1995) were assigned as shown in Table 4.1.(Ontario Ministry of Environment and Energy 1995).

*Table 4.1. Topographic Infiltration Factors* (Ontario Ministry of Environment and Energy 1995)

| **Description of Area** | **Infiltration Factor** |
|---|---|
| Flat land, average slope not exceeding 0.6 m per km | 0.3 |
| Rolling land, average slope of 2.8 to 3.8 m per km | 0.2 |
| Hilly land, average slope of 20 to 47 m per km | 0.1 |

The slope values necessary for identifying the SGRAs were derived from the provincial DEM. The steeper the slope, the lower the infiltration value. Water can more easily infiltrate the ground on surfaces with a gentle slope or are flat.

A non-linear regression model has been used to assign an infiltration factor to any given slope that is present within the study area.

*Equation 1. Topographic Infiltration Factor*

$TIV = 0.1298\ x^{-0.253}$

where:

TIV : Topography infiltration factor (unitless)

X : slope in degrees

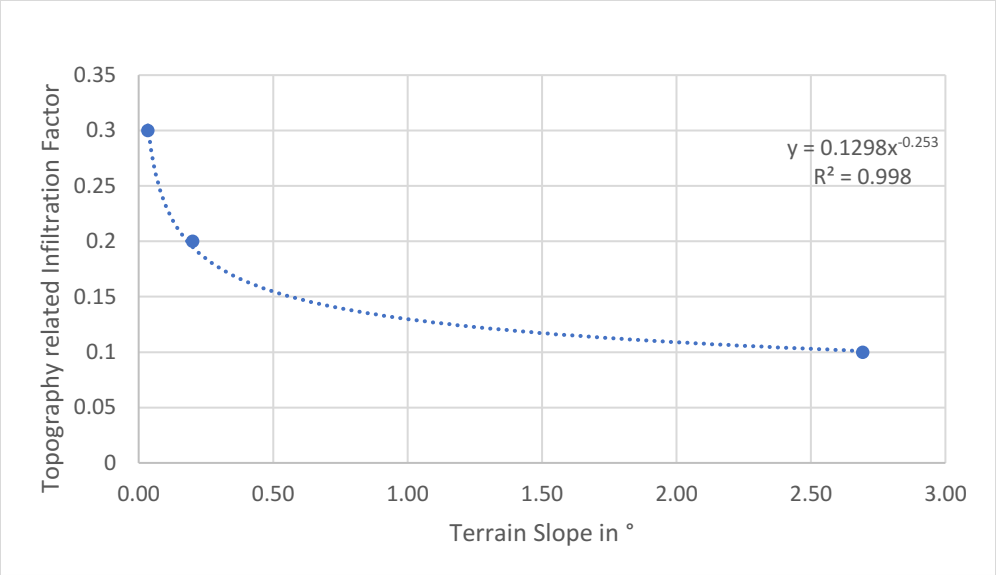


*Figure 4.1. Topography related infiltration factor as a function of terrain slope*

A landcover-based infiltration layer was generated using the infiltration factors shown in Table 4.2. The landcover information was categorized using the landcover infiltration factors developed by the provincial government (Ontario Ministry of Environment and Energy 1995; Ontario Ministry of the Environment 2003) and provided by the Niagara Peninsula Conservation Authority (Niagara Conservation Authority and AquaResource Inc. 2009) (Ontario Ministry of Environment and Energy 1995; Ontario Ministry of the Environment 2003).

*Table 4.2. Landcover infiltration value (Niagara Conservation Authority and AquaResource Inc. 2009)*

| Landcover | Infiltration Factor | Landcover | Infiltration Factor |
|---|---|---|---|
| Annual Crop | 0.1 | Mixed Agriculture | 0.15 |
| Bog | 0.15 | Mixed Crop | 0.15 |
| Built Up Impervious | 0 | Mixed Forest | 0.2 |
| Built Up Pervious | 0.05 | Monoculture | 0.1 |
| Deciduous Forest | 0.2 | Perennial Crop | 0.15 |
| Extraction- Rock (Sand and Gravel) | 0 (0.2) | Plantations | 0.2 |

| | | | |
|---|---|---|---|
| Forest | 0.2 | Rural Land Use | 0.15 |
| Hedge Rows | 0.2 | Transportation | 0 |
| Idle Land | 0.15 | Vineyards | 0.15 |
| Marsh | 0.15 | | |

Soil types in groundwater recharge areas were used to assign infiltration factors based on the same sources (Ontario Ministry of Environment and Energy 1995; Niagara Conservation Authority and AquaResource Inc. 2009). The infiltration factors are listed in Table 4.3 (Ontario Ministry of Environment and Energy 1995).

*Table 4.3. Soil infiltration factors (Ontario Ministry of Environment and Energy 1995)*

| **Description of Area** | **Infiltration Factor** |
|---|---|
| Tight impervious clay | 0.1 |
| Medium combination of clay and loam | 0.2 |
| Open sandy loam | 0.4 |

The three data layers were combined to create the infiltration index grid, identifying areas according to the infiltration index. This scale is unitless and indicates that areas that were assigned a higher value have a greater capacity for water to infiltrate into the ground, and areas with a lower value have a reduced capacity for water to infiltrate into the ground. Therefore, a high infiltration index is correlated to small or no slope, coarse soil material and a permeable land cover. A low infiltration index is correlated to a great slope, fine soil material, and impermeable land cover types. Precipitation not stored in the soil or vegetation is not considered part of runoff or evapotranspiration. The infiltration index grid, therefore, determines the infiltration rate depending on location.

The SGRAs were determined from the three input layers based on topography, land cover, and soils. Based on the input information, three infiltration factor grids were created. These single-variable infiltration factor grids were then added together to form one total infiltration index grid. To identify the SGRAs that contribute above-average amounts to groundwater recharge, an infiltration index grid was created that only contains the SGRAs that contribute 1.15 times above the average contribution.

## 4.2 Statistical Analysis

Seasonal and annual patterns of the climatic and hydrologic variables and indicators listed in Table 4.4 were evaluated using Spearman's Rank, Kendall's Rank and linear regression for correlation analysis, utilizing the SPSS software package. Trend analysis of the hydrologic parameters was determined using the Mann-Kendall trend test in software R. The double-mass balance analysis was conducted using Microsoft Excel.

The modelling of surface and sub-surface water balance requires several climatic and hydrologic variables and indicators (Table 4.4). This temporal analysis ideally includes data from 10 consecutive years. A correlation analysis using linear regression, Mann-Kendall trend test, Spearman's rank and Kendall's rank

will be used to identify any relationship between the variables on both a seasonal and annual time scale. The correlation analysis was completed using SPSS using Spearman's Rank, Kendall's Rank, and linear regression. The Mann-Kendall trend test was conducted with R. The study period used was 2008-2017. This study period was selected based on the availability of consecutive data from the climate and hydrological stations in the Neebing River watershed. The data for the variables listed in Table 4.4 was acquired from these stations. The variables and indicators used for this analysis were based on those used previously by Mills and Post (2018).

*Table 4.4. Variables and indicators for statistical analysis (Mills and Post 2018)*

| Type | Variable/Indicator | Metric | Time period |
|---|---|---|---|
| Climate | Precipitation | Total | Annual |
| | Potential Evapotranspiration | Total | Annual |
| | Climate Moisture Index | P-PET | Annual |
| | Temperature | Average | Annual |
| | | 7-day max | Annual, seasonal |
| | | 7-day min | Annual, seasonal |
| | Hydrologic Release | 3-day max | Annual, seasonal |
| | | 7-day min | Annual, seasonal |
| | | Total | Seasonal |
| Surface water | Surface water discharge | 3-day max | Annual, seasonal |
| | | 7-day min | Annual, seasonal |
| | Water yield | Total | Annual, seasonal |
| | Baseflow yield | Total | Annual, seasonal |
| | Flashiness | Richards-Baker Flashiness Index | Annual |
| | Extreme flows | $<10^{th}$: $>90^{th}$ exceedance percentile | Annual |
| Groundwater | Groundwater level | 3-day max | Annual, seasonal |
| | | 7-day min | Annual, seasonal |

### 4.2.1 Variable Definitions

Seasonal data analysis was grouped according to month, so that December, January, and February are included in "Winter"; March, April, and May are "Spring"; June, July, and August are "Summer"; and September, October, and November are "Fall". This grouping is most appropriate for the local climatic conditions and is also used by the Canadian Seasonal and Interannual Prediction System (Merryfield et al. 2013; Diro et al. 2024).

Precipitation records were obtained from the Environment and Climate Change Canada (ECCC) station located within the Neebing River watershed. The total precipitation value per year was used for the annual time scale (Mills and Post 2018). The seasonal contribution of precipitation to streamflow is significantly influenced by the climatic conditions. As such, most of the precipitation is stored as snow cover during the cold winter months and released in the spring freshet (Mills and Post 2018). This difference will be considered in the hydrological release analysis outlined below.

Evapotranspiration is one of the ways for water to leave the system and must be considered when calculating the water balance (Mills and Post 2018). Potential evapotranspiration (PET) is the amount of evapotranspiration that could occur under atmospheric conditions if the water supply would not be limited (Mills and Post 2018). The Thornthwaite method can be used calculating potential evapotranspiration by using the following formula (Thornthwaite 1948):

*Equation 2. Potential Evapotranspiration*

$E_i$=16(10$T_i$/$I$)$^a$

Where:

$E_i$ = potential evapotranspiration for month $i$ (mm/month),

$T_i$ = mean monthly temperature (°C),

$I$ = local heat index $\sum_{i=1}^{12}(Ti\ /5)^{1.514}$,

$a$= $(0.675 * I^3 - 77.1 * I^2 + 17920 * I + 492390)10^{-6}$

The potential evapotranspiration is calculated for the annual analysis.

The Climate Moisture Index is the total precipitation minus the total potential evapotranspiration (Hogg 1997). A water surplus is indicated by a positive Climate Moisture Index value whereas a negative value demonstrates water deficit (Mills and Post 2018). The role of the Climate Moisture Index in this model was to provide a baseline of whether climatic conditions were responsible for adding water to or taking water out of the system. If the value for the Climate Moisture Index stays constant but the groundwater and surface water interaction changes, it is an indicator of anthropogenic changes in the hydrology (Mills and Post 2018). The Climate Moisture Index was calculated for the annual analysis.

Temperature data is recorded by climate stations in the Neebing River watershed. Following the approach of Mills and Post (2018), a multi-day rolling average was used for the annual average to decrease the impact of outliers. The daily mean temperature was averaged for seven consecutive days. For the seasonal analysis, the seasonal minimum and maximum values of the seven-day averages were used.

The hydrologic release was used to estimate the contribution to the streamflow by water that was temporarily stored during the winter months in the snow cover. The following formula from Brown and Braaten (1998) was utilized in this study to model hydrologic release:

*Equation 3. Hydrologic Release*

$M$=$k$[(1.88+0.007$R$)(9/5$T$)+1.27] $T$ > 0°C

Where:

$M$ = snowmelt water (mm/day),

$k$ = locally calibrated snowmelt factor,

$T$ = mean daily air temperature (°C),

$R$ = total daily snowfall (mm snow water equivalent).

For this analysis, the snowmelt factor was set at 1. The mean daily temperature and snowfall information were retrieved from ECCC data, and other local records provided by local climatologist Graham Saunders (Saunders 2022) were used to fill data gaps. Data gaps were mostly present in the snow on the ground information. Hydrologic release analysis was conducted on a seasonal and annual temporal scale.

The surface water discharge was analysed for seasonal and annual patterns. The annual and seasonal maximum discharge values were calculated using 3-day average daily discharge values. The annual and seasonal minimum discharge values were calculated using the 7-day average daily values. Drought events tend to be longer in duration compared to flood events, therefore a 7-day time period was used to capture minimum flow periods and a 3-day time period was used to capture peak flow events (Mills and Post 2018). In addition, the corresponding day-of-year timing of multi-day minimum and maximum events was captured to identify shifting trends on an annual basis (Mills and Post 2018). Analysing the seasonal and annual streamflow patterns allowed for the distinction between precipitation and snowmelt events (Mills and Post 2018).

Water yield was calculated using the following equation:(2018)

*Equation 4. Water Yield*

$$yield = \frac{Q * 86400000}{A}$$

Where:

$yield$ = streamflow or baseflow in mm/day,

$Q$ = daily average streamflow/baseflow discharge in $m^3/s$,

$A$ = (sub)watershed contributing area in $m^2$,

86400000 = conversion factor between m/s to mm/day.

Baseflow is the part of the streamflow that is fed by groundwater discharge (Mills and Post 2018), and daily baseflow can be derived from daily streamflow data (Piggott, Moin, and Southam (2005). Eckhardt's (2005) methodology of baseflow separation uses a two-parameter tool: the maximum value of the baseflow index ($BFI_{max}$) and the recession constant (α). This model works under the assumption that the contribution of an aquifer to baseflow is linearly proportional to its storage. The $BFI_{max}$ value is not measurable, but Eckhardt suggests that a range of values can be associated with a certain type of catchments that share hydrological and hydrogeological characteristics (Eckhardt 2005). The recession constant can be established by a recession analysis. Eckhardt provides the following equation to establish the baseflow separation:

*Equation 5. Baseflow (Eckhardt)*

$$b_t = \frac{(1 - BFI_{max}) * \ \alpha * b_{t-1} + (1 - \alpha) * BFI_{max} * Q_t}{1 - \alpha * BFI_{max}}$$

Where:

*b*: baseflow $m^3/s$

$Q$: streamflow $m^3/s$

$t$: the time (e.g., day) for which the baseflow is calculated

α: groundwater recession constant [values between 0 and 1]

$BFI_{max}$: long-term ratio of baseflow to total streamflow [values between 0 and 1].

The average BFI value for the Thunder Bay area that was used to test this methodology is 0.761; calculated values for the Lakehead Region vary between 0.70 and 0.89 (Neff et al. 2005). This range was established in the paper *Baseflow in the Great Lakes Basin* by Neff et al. (2005), where the authors established BFI values for the entire Great Lakes basin. Neff et. al used different hydrograph separation models and stream gauge data from Ontario and eight US. States that share the Great Lakes coast (Illinois, Indiana, Michigan, Minnesota, New York, Ohio, Pennsylvania, and Wisconsin). The hydrograph separation models that were used in that analysis are HYSEP methods (Sloto and Crouse 1996), PART (Rutledge 1998), BFLOW (Arnold and Allen 1999), and UKIH (Piggott et al. 2005). The article provides BFI values for all areas in the Great Lakes basin.

The online tool SepHydro (Danielescu et al. 2018) was used to calculate the baseflow separation using the Eckhardt (2005) methodology. The inputs required are discharge, precipitation, α (the recession constant), and $BFI_{max}$ (the long-term ratio of baseflow to total streamflow) (Danielescu et al. 2018). The discharge and precipitation data used for this trial were acquired from the Water Survey of Canada (WSC) and Environment and Climate Change Canada (ECCC), respectively. A $BFI_{max}$ value of 0.761 was used, which is in the range of $BFI_{max}$ values that were established by the Neff et al. (2005) report and was the value for the Thunder Bay area.

Eckhardt's (2008) proposed method of recession analysis was used to estimate the recession constant (α) required for the baseflow estimation. In the estimate of the recession constant, all streamflow values that are part of a recession period of a minimum of five days were included (Eckhardt 2008). The slope of a straight line on a scatterplot of streamflow $y(k)$ against streamflow $y(k+1)$ that fits through the upper bounds of the scatterplot is the recession value α. Where $y(k)$ is the streamflow value for a given day, and $y(k+1)$ is the streamflow value the following day under the condition that both points are within a period of at least five days of receding streamflow. Eckhardt points out that due to measurement errors, a 2% deviation from the theoretical α value must be accepted (Eckhardt 2008). Therefore, this line must be fitted so that none of the observed values exceed the value predicted by $\alpha$ by more than 2%. (Eckhardt 2008). Figure 4.1 illustrates the streamflow recession for the Neebing River (2008-2017). The estimated recession value α for the Neebing River is 0.975.

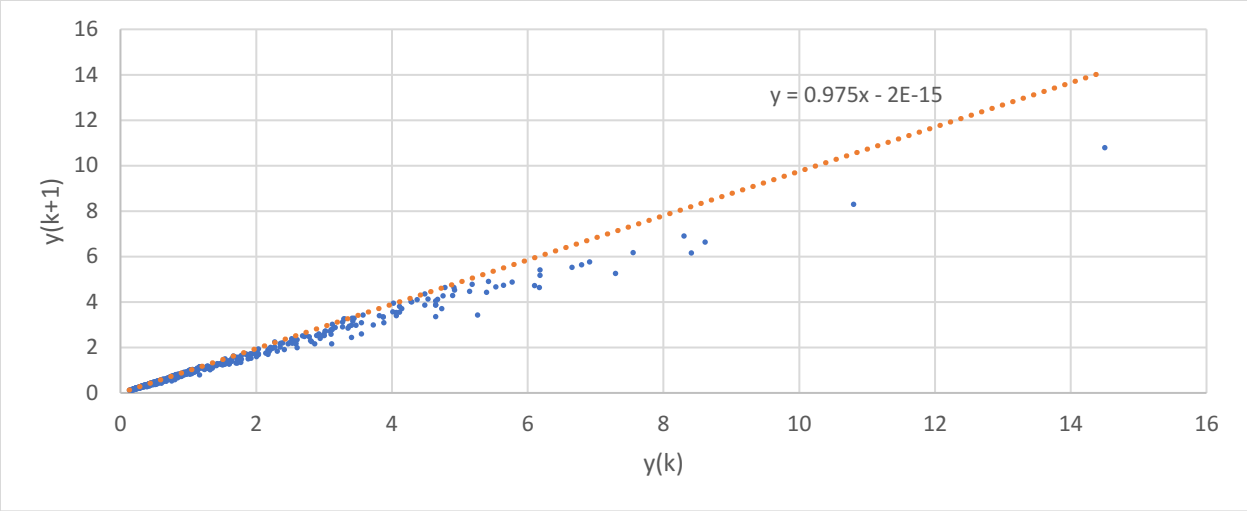


*Figure 4.2. Streamflow recession Neebing River (2008-2017), the slope of the orange line is the recession constant: α = 0.975.*

The streamflow and baseflow values were converted from $m^3/s$ to mm for the entire study area to enable comparison with precipitation data in the double mass balance. The converted variables are distinguished as water yield and baseflow yield. The interannual cumulative values for streamflow, baseflow, and precipitation were plotted in the double-mass balance analysis (Searcy et al. 1960).

The Richards-Baker Flashiness Index was used to describe the day-to-day variability in streamflow, emphasizing the magnitude and frequency of a given flow event (Baker et al. 2004). Watersheds that have a high value for flashiness tend to respond to a flow event with greater magnitude compared to those with a lower flashiness value. The flashiness is influenced by the size of the watershed, the soil characteristics, topography and land cover (Mills and Post 2018). This value was calculated for the annual time scale. The Richards-Baker Flashiness Index is defined as:

*Equation 6. Richard-Baker Flashiness Index*

$q_i$-$q_{i-1}$

$$R - B\ Index = \frac{\sum_{i=1}^{n} |q_i - q_{i-1}|}{\sum_{i=1}^{n} q_i}$$ (Baker et al. 2004)

Where:

$q$ = daily discharge

Here, the sum of absolute values of daily change in discharge for an annual period is divided by the sum of daily discharge for the same period of time (Mills and Post 2018).

Extreme flow events refer to very high and very low discharge levels. The $10^{th}$ and $90^{th}$ percentile of the flow duration curve indicates the extreme high and extreme low flow events (Mills and Post2018). A flow duration curve was created using discharge level data from the hydrometric station. A small ratio of high flow to low flow events indicates long-term storage capacity, limiting the impact of storm events and showing the contributing factor of baseflow during dry periods (Mills and Post 2018).

The groundwater level information was obtained from the Provincial Groundwater Monitoring Network (PGMN). The hourly groundwater level data was converted to daily averages. The annual and seasonal maximum 3-day averaged groundwater level was calculated to cover the high events (Mills and Post 2018). The annual and seasonal minimum 7-day average groundwater level was calculated to cover the low events (Mills and Post 2018).

## 4.3 Stable Isotope Analysis

For the third objective, to determine the water balance of the Neebing River, the variables and indicators used for the second objective were used. The seasonal and annual water balances were determined using Microsoft Excel. The groundwater contribution to streamflow or baseflow was derived from the streamflow data. To further investigate the groundwater contribution to streamflow and the groundwater-surface water interactions, stable isotope samples were collected and analyzed at the Water Research Centre at Nipissing University. During the sampling period, 68 surface water samples were taken from July 2021 to November 2022. Samples were taken during the spring, summer, fall, and winter seasons when different flow conditions were encountered. The highest flow conditions were observed during the spring freshet, and the lowest flow levels at the end of the summer season. Sampling paused while the Neebing River was frozen over during the winter.

Streamflow water sources include precipitation, surface runoff, snowmelt, and groundwater. These interactions between groundwater and surface water are challenging to measure. Still, the isotope analysis of $^{18}O$ and $^{2}H$ was used to better understand this relationship and the seasonal variability (Jung et al. 2021). Groundwater usually contains less $\delta^{2}H$ and $\delta^{18}O$ (Kalbus et al. 2006; Ferronsky and Polyakov 2012). Therefore, seasonal trends could be observable when streamflow contains lower or more significant proportions of groundwater contributions, such as during the winter with ice cover on the stream or during summer, a direct runoff contribution to streamflow. Water samples from the Neebing River were taken for isotope analysis. The sampling methodology followed the guidelines of the IAEA and the Integrative Watershed Research Center at Nipissing University (IAEA - Water Resources Programme 2007; Integrative Watershed Research Center - Nipissing University 2013). Samples were collected in 50 ml bottles for analysis to quantify a ratio of $^{18}O$ and deuterium. The bottles are made of polyethylene material, and samples were taken directly from the Neebing River. The bottles were filled completely, keeping the headspace to a minimum. The water temperature and flow rates were measured at the time of sampling. The samples were labelled and stored in a cool, dark place as per protocol (Integrative Watershed Research Center - Nipissing University 2013). Samples were collected at four sampling sites in the Neebing River watershed. Location one is on the lower Neebing River at the Arthur Street hydrometric station. Location two is located at John Street Road and Thompson Road at the hydrometric station. Sample site three is located at Gratton Rd and the Neebing River crossing. The fourth sample site is located near the 25$^{th}$ Side Road and Neebing crossing. The sample sites cover the three main branches of the Neebing River and parts of the different environments of the watershed, as seen in Figure 4.2.

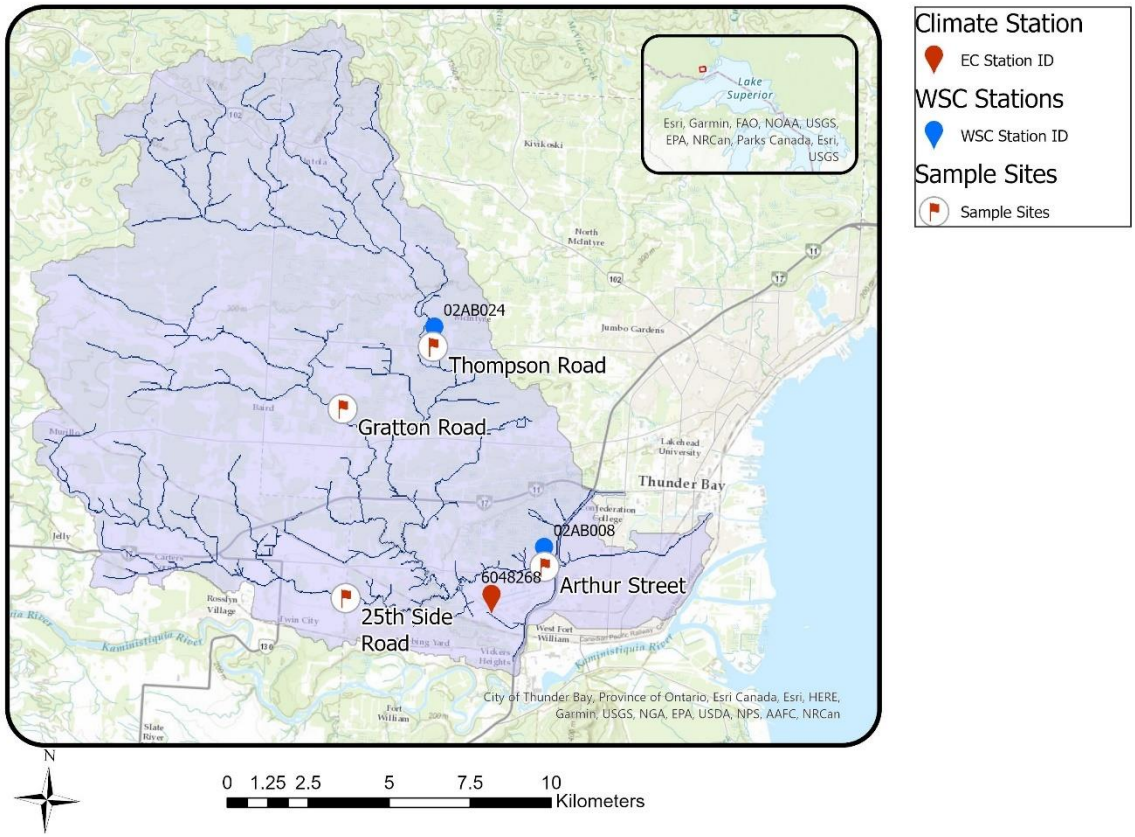


*Figure 4.3. Sampling Sites in the Neebing River study area*

**CHAPTER 5**

# 5 Results

## 5.1 Results: Mapping of Significant Groundwater Recharge Areas

### 5.1.1 Topography

The information from the DEM and the equation 6 was used to generate an infiltration factor grid based on topography with the use of ArcPro GIS software (7.). Highlighted in darker colours are areas with minimal to no slope, and areas with greater slopes are visualized in a lighter colour. The largest area that is highlighted in dark colour, indicating an area of minimal to no slope, is the historic floodplain. This area is mostly covered by built-up impervious surfaces, as will be seen in the next section. This type of landcover makes it less likely to be part of the SGRAs, and due to the positioning of the WSC station, most of the urban area is outside of the study area, even though it is located within the Neebing River drainage basin.

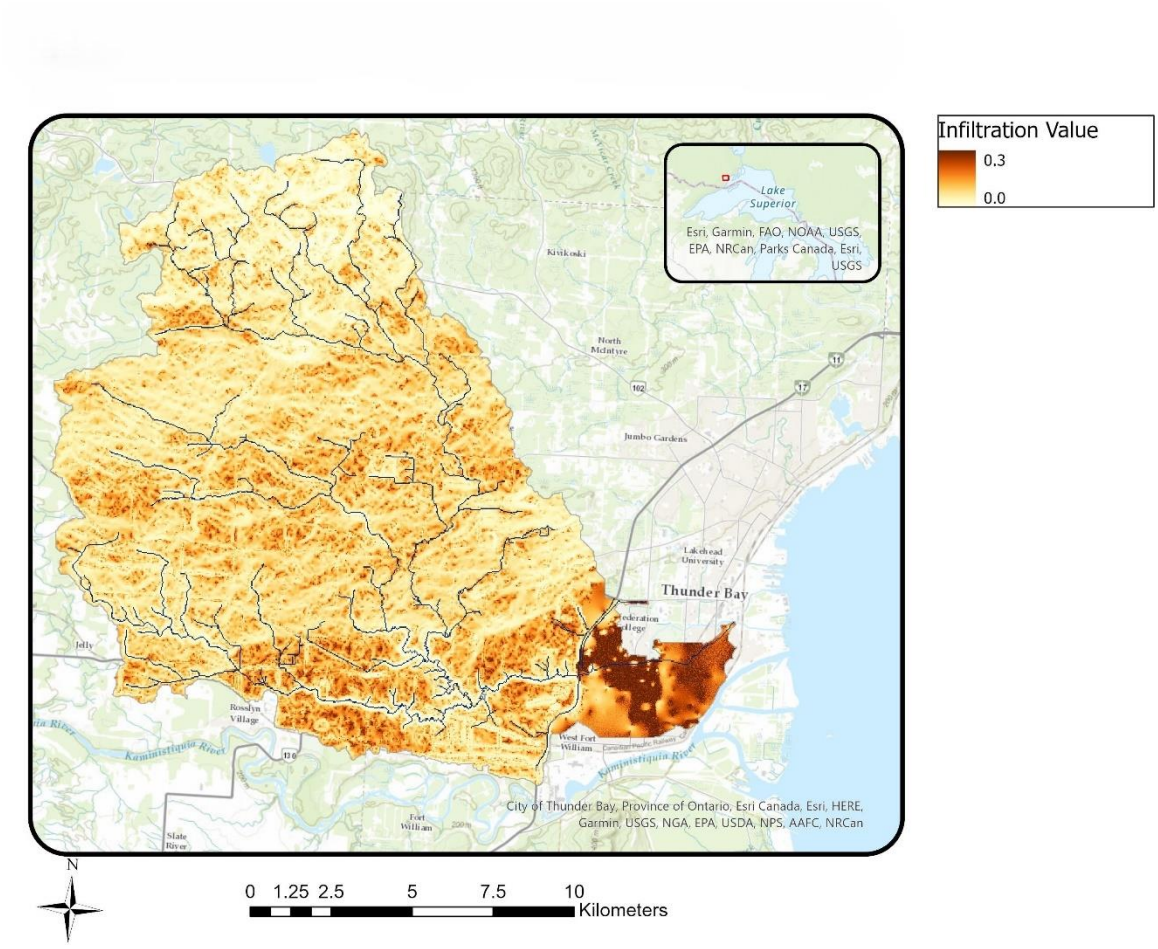


*Figure 5.1. Topography related infiltration grid*

### 5.1.2 Landcover

In addition to topography, land cover influences groundwater recharge. Areas with denser vegetation such as forests, contribute more than built-up areas to groundwater recharge (Niagara Conservation Authority and AquaResource Inc. 2009). Therefore, areas are assigned an infiltration factor based on landcover according to their contribution to groundwater recharge. Infiltration rates for different groundcovers are based on the Ontario Ministry of the Environment 2003 report (Ontario Ministry of the Environment 2003) and the SGRA Delineation Niagara Peninsula Source Protection Area report (Niagara Conservation Authority and AquaResource Inc. 2009). Figure 5.3 below shows the landcover-related infiltration factor grid for the Neebing River basin.

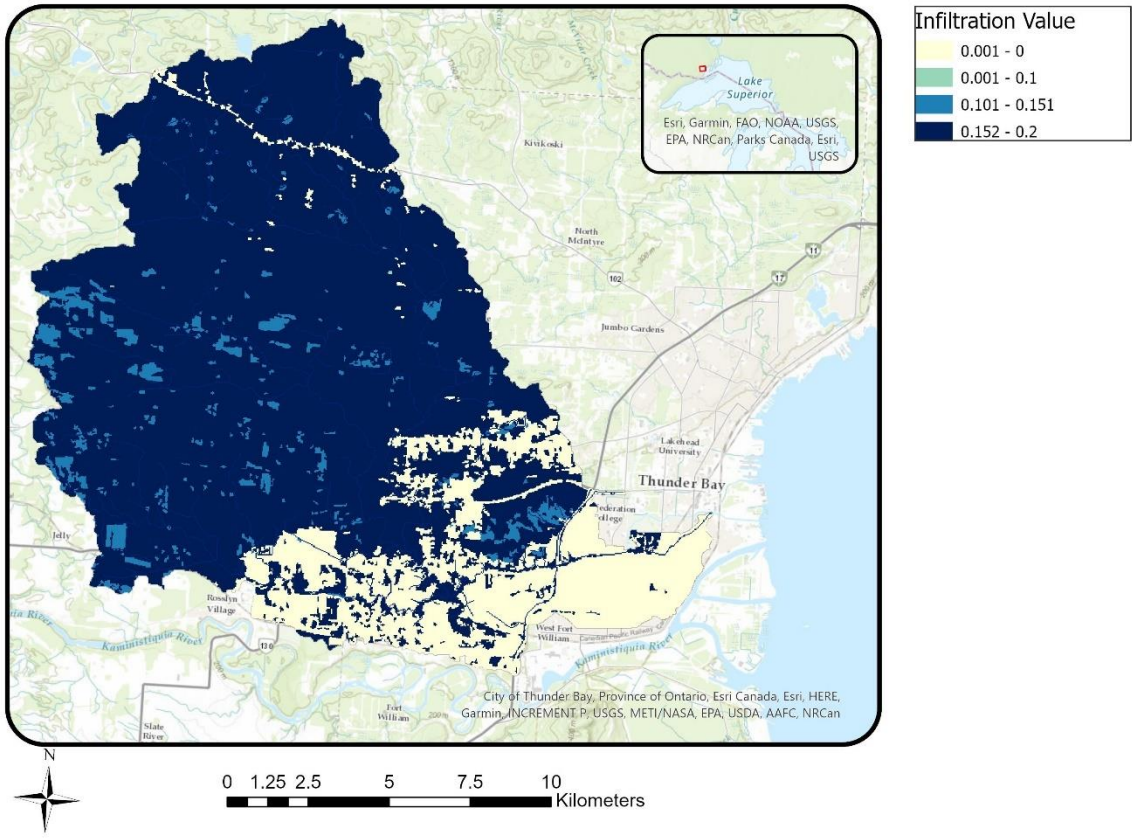


*Figure 5.2. Landcover related infiltration factor grid*

### 5.1.3 Soils

Like slope and landcover, an infiltration factor grid based on soils was created. Soil types consistent of coarser material were assigned a greater infiltration value than finer soil types. Water can infiltrate the ground through the coarser soil types at a higher rate than the finer material. The infiltration rates are based on the Ontario Ministry of the Environment manual (1995). The soil data layer was retrieved from the Ontario GeoHub. This process resulted in a soil related infiltration factor grid (Figure 5.4).

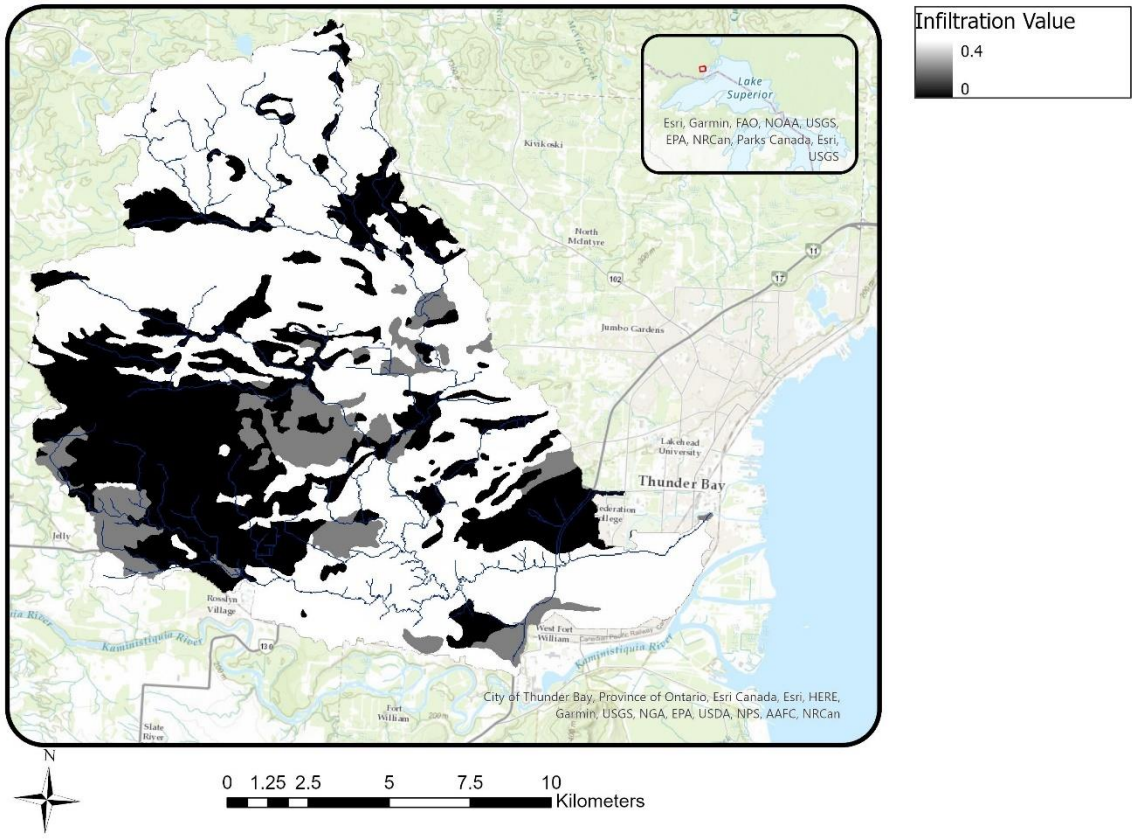


*Figure 5.3. Soil infiltration factor grid*

### 5.1.4 Infiltration Index

The three infiltration grids for slope, landcover, and soil are then combined by adding the infiltration values. The two figures below show (1) the overall infiltration index grid (Figure 5.5) and (2) the infiltration index grid with the areas highlighted that have an above-average contribution to the groundwater recharge and are identified as SGRAs (Figure 5.6).

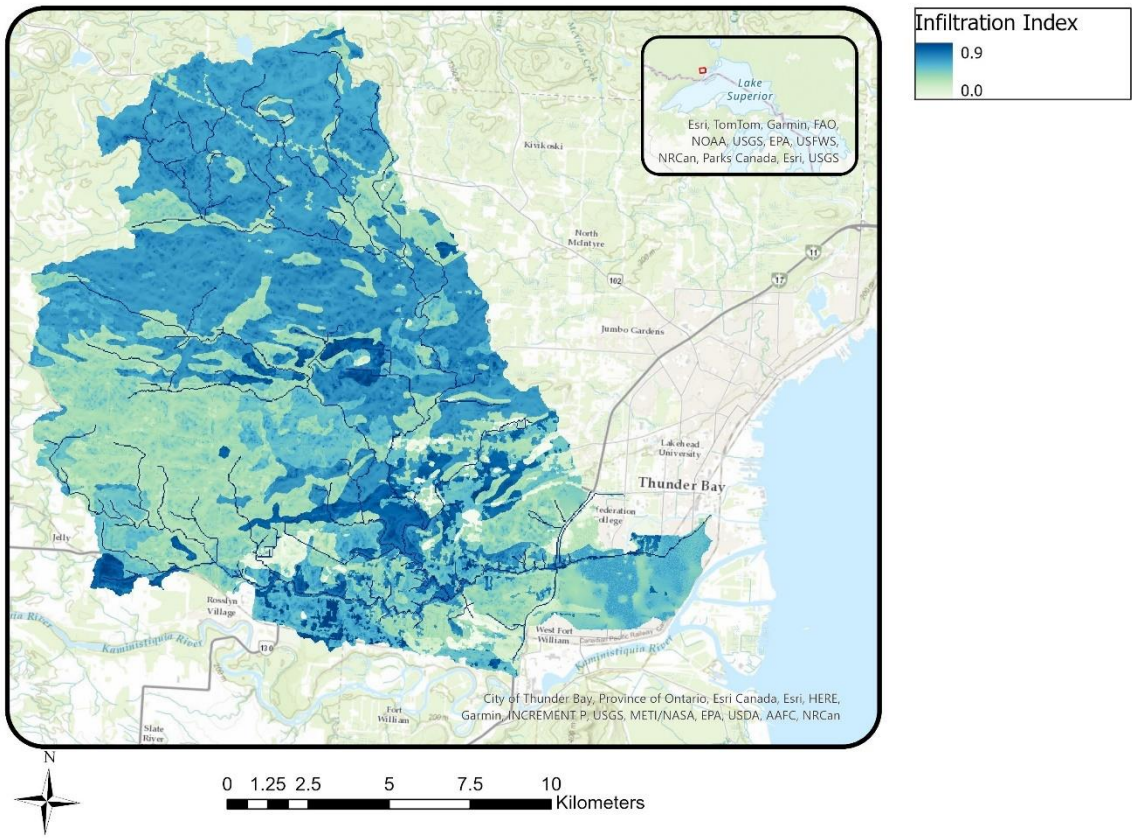


*Figure 5.4. Total Infiltration Index Grid*

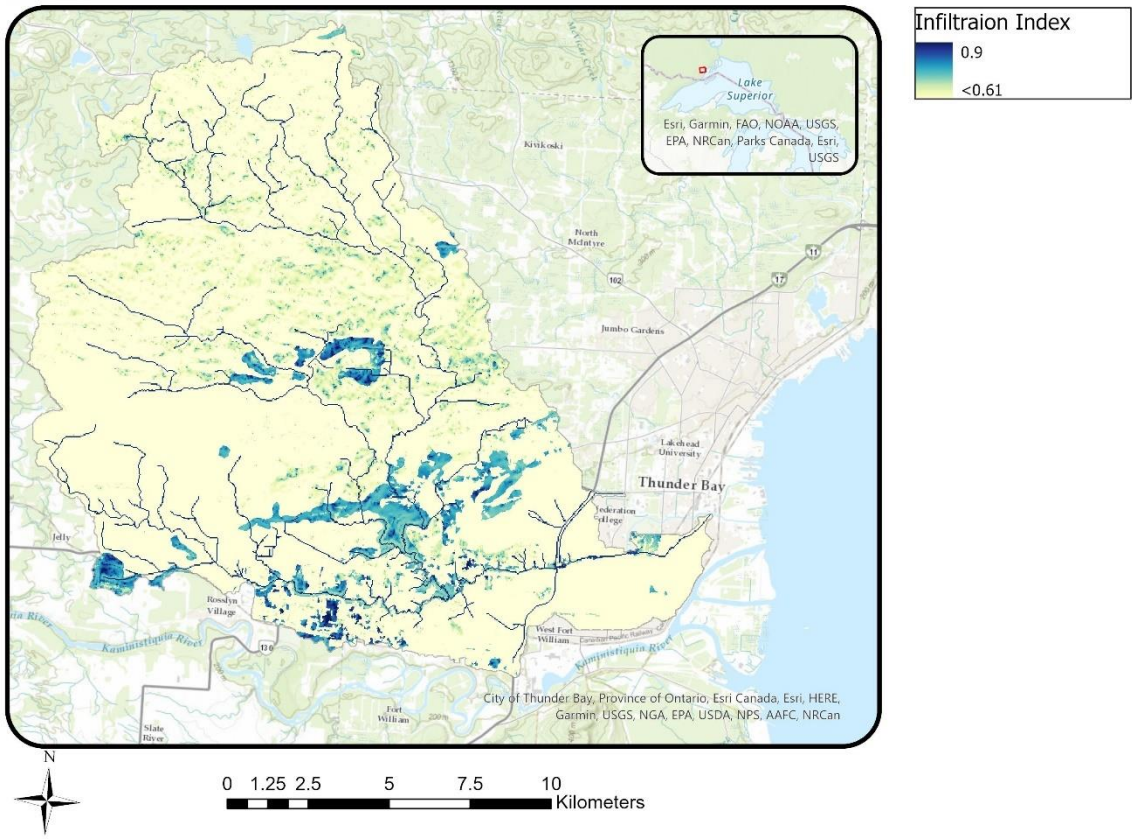


*Figure 5.5. Significant Groundwater Recharge Areas*

## 5.2 Results: Statistical Analysis

### 5.2.1 Flow Duration Curve

A flow duration curve for the Neebling River is presented in Figure 5.7 Based on the historic streamflow data for the Neebing River (2008-2017), this figure gives a probability of occurrence for every given amount of streamflow. Events with extremely high streamflow are rare, whereas events of low streamflow occur often. Streamflow values with 99% exceedance probability are below 0.06 $m^3/s$ for low flow events and with an exceedance probability of 1% above 18.0 $m^3/s$ for high flow events.

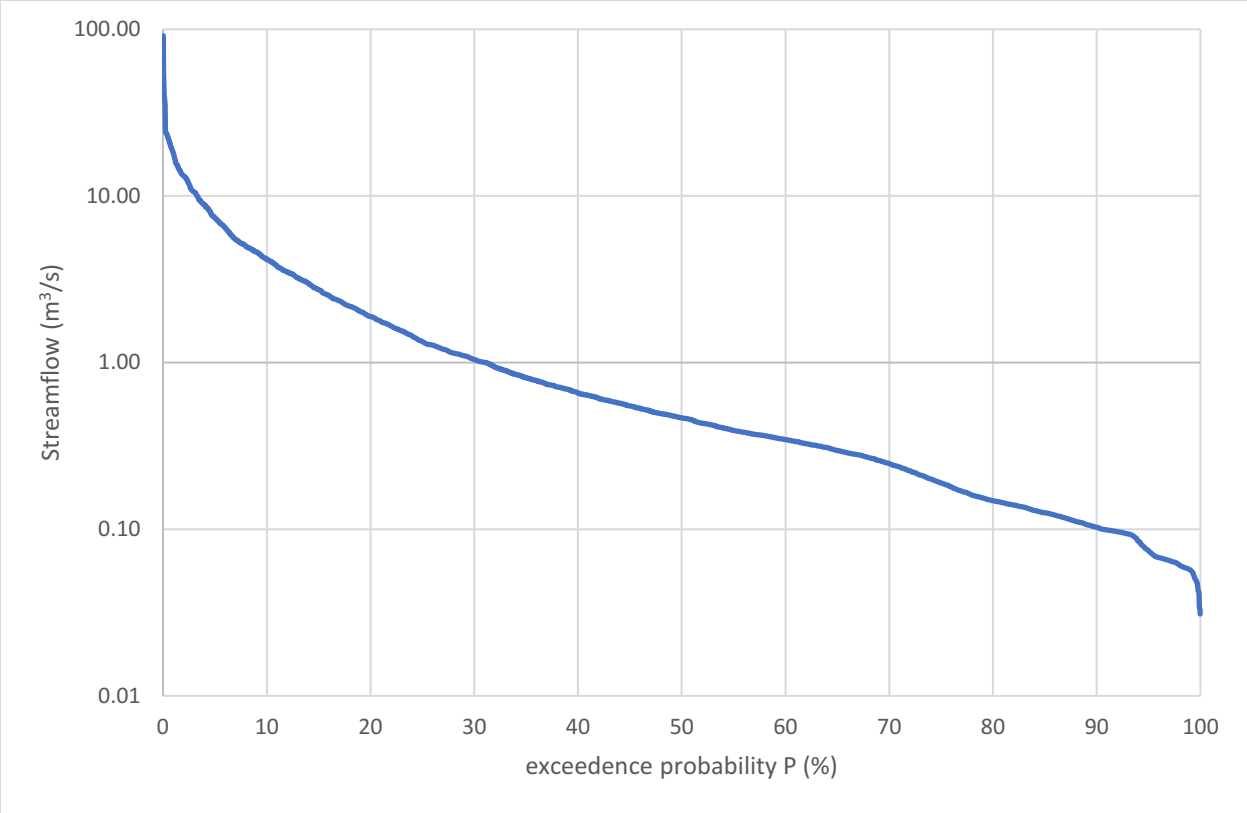


*Figure 5.6. Flow duration curve for the Neebing River (2008-2017)*

### 5.2.2 Correlation Analysis

The correlation analysis indicated significant relationships between the studied parameters. Variables and indicators with correlation coefficients in the three tests greater than ±0.5 and a p-value <0.05 are considered significant. The analysis results show significant correlations for the annual and seasonal timescales, as shown in the tables below. The correlations with a p-value <0.01 are shaded grey to highlight the significance at the 99% level (two-tailed). The complete result tables for Spearman's Rank and Kendall's Rank are included in Appendix C.

Many of the identified correlations on the annual timescale are between related parameters such as temperature and Climate Moisture Index, which is precipitation minus evapotranspiration or streamflow and baseflow. These correlations are also observed in the seasonal analyses. Other correlations that were identified are between hydrologic release and the Richard-Baker Index for flashiness and the Richard-Baker Index and the maximum 3-day average of streamflow.

*Table 5.1. Correlation analysis results for annual timescale, Neebing River (2008-2017)*

| **Annual Correlation** | | **Spearman's Rank** | | **Kendall's Rank** | | **Linear Regression** | | |
|---|---|---|---|---|---|---|---|---|
| **Parameter 1** | **Parameter 2** | **ρ** | **p-value** | **τ** | **p-value** | **$R^2$** | **p-value** | **slope** |
| Mean T | 7d MIN T | 0.661 | 0.038 | 0.511 | 0.040 | 0.677 | 0.003 | + |

| Annual Correlation | | Spearman's Rank | | Kendall's Rank | | Linear Regression | | |
|---|---|---|---|---|---|---|---|---|
| **Parameter 1** | **Parameter 2** | **ρ** | **p-value** | **τ** | **p-value** | **$R^2$** | **p-value** | **slope** |
| Mean T | PET | 0.952 | 0.000 | 0.882 | 0.001 | 0.908 | <0.001 | + |
| Mean T | 10:90 exceed | -0.673 | 0.033 | -0.511 | 0.040 | 0.531 | 0.017 | - |
| 7d MAX T - DOY | 30d MIN R - DOY | -0.863 | 0.001 | -0.719 | 0.004 | 0.720 | 0.002 | - |
| 7d MIN T - DOY | 30d MIN R | 0.695 | 0.026 | 0.535 | 0.036 | 0.599 | 0.009 | + |
| 7d MIN T - DOY | CMI (P-PET) | 0.775 | 0.008 | 0.629 | 0.014 | 0.599 | 0.009 | + |
| 7d MIN T | 3d MAX GW - DOY | 0.829 | 0.042 | 0.733 | 0.039 | 0.773 | 0.021 | + |
| Total P | CMI (P-PET) | 0.867 | 0.001 | 0.689 | 0.006 | 0.888 | <0.001 | + |
| Total R | CMI (P-PET) | 0.794 | 0.006 | 0.600 | 0.016 | 0.798 | <0.001 | + |
| 3d MAX R - DOY | 10:90 exceed | -0.818 | 0.004 | -0.689 | 0.006 | 0.517 | 0.019 | - |
| 3d MAX R - DOY | 3d MAX Q - DOY | -0.842 | 0.002 | -0.644 | 0.009 | 0.833 | <0.001 | - |
| 3d MAX R - DOY | 3d MAX BF - DOY | -0.745 | 0.013 | -0.511 | 0.040 | 0.500 | 0.022 | - |
| 3d MAX R | RBI | 0.879 | 0.001 | 0.733 | 0.003 | 0.848 | <0.001 | + |
| RBI | 3d MAX Q | 0.806 | 0.005 | 0.644 | 0.009 | 0.749 | 0.001 | + |
| RBI | 3d MAX GW - DOY | 0.943 | 0.005 | 0.867 | 0.015 | 0.874 | 0.006 | + |
| 10:90 exceed | 7d MIN BF - DOY | -0.794 | 0.006 | -0.584 | 0.020 | 0.640 | 0.005 | - |
| 10:90 exceed | 7d MIN GW | -0.886 | 0.019 | -0.733 | 0.039 | 0.690 | 0.041 | - |
| Water yield | BF yield | 0.976 | 0.000 | 0.911 | 0.000 | 0.97 | <0.001 | + |
| Water yield | 3d MAX BF - DOY | 0.758 | 0.011 | 0.600 | 0.016 | 0.597 | 0.009 | + |
| 3d MAX Q - DOY | 3d MAX BF - DOY | 0.927 | 0.000 | 0.867 | 0.000 | 0.563 | 0.012 | - |
| 3d MAX Q | 3d MAX BF - DOY | 0.709 | 0.022 | 0.556 | 0.025 | 0.522 | 0.018 | + |
| 3d MAX Q | 3d MAX BF | 0.782 | 0.008 | 0.644 | 0.009 | 0.721 | 0.002 | + |
| 7d MIN Q - DOY | 7d MIN BF -DOY | 0.964 | 0.000 | 0.911 | 0.000 | 0.737 | 0.001 | + |
| 7d MIN Q | 7d MIN BF | 0.985 | 0.000 | 0.944 | 0.000 | 0.987 | <0.001 | + |
| 7d MIN Q | Mean GW | 0.829 | 0.042 | 0.733 | 0.039 | 0.774 | 0.021 | + |
| BF yield | 3d MAX BF -DOY | 0.673 | 0.033 | 0.511 | 0.040 | 0.481 | 0.026 | + |
| 3d MAX BF - DOY | 3d MAX BF | 0.782 | 0.008 | -0.644 | 0.009 | 0.613 | 0.007 | + |
| Mean GW | 7d MIN GW - DOY | -0.821 | 0.023 | -0.619 | 0.051 | 0.595 | 0.042 | - |

*Correlation is significant at 0.01 level (2-tailed)

The winter seasonal analysis (Table 5.2) shows a strong correlation between streamflow and baseflow parameters, and between the day-of-year parameters. There is a relationship between Minimum 7-day Temperature winter day-of-year timing and Minimum 7-day winter baseflow. Similar to the annual analysis, related parameters were found to be correlated in the regression analysis.

*Table 5.2. Correlation analysis results for the winter season, Neebing River (2008-2017)*

| Winter (DJF) Correlation | | Spearman's Rank | | Kendall's Rank | | Linear Regression | | |
|---|---|---|---|---|---|---|---|---|
| **Parameter 1** | **Parameter 2** | **ρ** | **p-value** | **τ** | **p-value** | **$R^2$** | **p-value** | **slope** |
| Mean T - Win | 7d MIN T - Win | 0.764 | 0.006 | 0.636 | 0.006 | 0.756 | <0.001 | + |
| 7d MIN T - Win DOY | 7d MIN BF - Win | 0.621 | 0.041 | 0.519 | 0.032 | 0.623 | 0.004 | + |
| Water yield - Win | 3d MAX Q - Win | 0.945 | 0.000 | 0.855 | 0.000 | 0.784 | <0.001 | + |
| Water yield - Win | 7d MIN Q - Win | 0.800 | 0.003 | 0.600 | 0.010 | 0.526 | 0.012 | + |
| Water yield - Win | BF yield - Win | 0.991 | 0.000 | 0.964 | 0.000 | 0.997 | <0.001 | + |
| Water yield - Win | 3d MAX BF - Win | 0.882 | 0.000 | 0.782 | 0.001 | 0.830 | <0.001 | + |
| Water yield - Win | 7d MIN BF - Win | 0.776 | 0.005 | 0.611 | 0.010 | 0.479 | 0.018 | + |
| 3d MAX Q - Win DOY | 3d MAX BF - Win DOY | 0.962 | 0.000 | 0.915 | 0.000 | 1.000 | <0.001 | + |
| 3d MAX Q - Win DOY | 3d MAX GW - Win DOY | 1.000 | . | 1.000 | . | 0.932 | 0.002 | + |
| 3d MAX Q - Win | BF yield - Win | 0.918 | 0.000 | 0.818 | 0.000 | 0.744 | <0.001 | + |
| 3d MAX Q - Win | 3d MAX BF - Win | 0.955 | 0.000 | 0.855 | 0.000 | 0.994 | <0.001 | + |
| 7d MIN Q - Win DOY | 7d MIN BF - Win DOY | 0.729 | 0.011 | 0.697 | 0.003 | 0.998 | <0.001 | + |
| 7d MIN Q - Win DOY | 7d MIN BF - Win | 0.708 | 0.005 | 0.537 | 0.023 | 0.389 | 0.040 | + |
| 7d MIN Q - Win | BF yield - Win | 0.755 | 0.007 | 0.564 | 0.016 | 0.520 | 0.012 | + |
| 7d MIN Q - Win | 7d MIN BF - Win | 0.986 | 0.000 | 0.945 | 0.000 | 0.983 | <0.001 | + |
| BF yield - Win | 3d MAX BF - Win | 0.855 | 0.001 | 0.745 | 0.001 | 0.794 | <0.001 | + |
| 3d MAX BF - Win DOY | 3d MAX GW - Win DOY | 0.941 | 0.005 | 0.857 | 0.020 | 0.870 | 0.007 | + |
| 7d MIN BF - Win DOY | 7d MIN BF - Win | 0.824 | 0.002 | 0.673 | 0.005 | 0.406 | 0.035 | + |
| 3d MAX GW - Win | 7d MIN GW - Win | 1.000 | . | 1.000 | . | 0.914 | 0.003 | + |

*Correlation is significant at 0.01 level (2-tailed)

The spring seasonal analysis (Table 5.3) shows correlations between total hydrologic release and 3-day max streamflow and baseflow. The 7-day Minimum Temperature Day-of-Year timing and 7-day Minimum Streamflow Day-of-Year timing for the spring season are also correlated. Further correlations are among the streamflow and baseflow parameters.

*Table 5.3. Correlation analysis results for the spring season, Neebing River (2008-2017)*

| Spring (MAM) Correlation | | Spearman's Rank | | Kendall's Rank | | Linear Regression | | |
|---|---|---|---|---|---|---|---|---|
| **Parameter 1** | **Parameter 2** | **ρ** | **p-value** | **τ** | **p-value** | **$R^2$** | **p-value** | **slope** |
| 7d MIN T - Spr DOY | 7d MIN Q - Spr DOY | 0.719 | 0.019 | 0.647 | 0.018 | 0.759 | 0.001 | + |
| Total R - Spr | 3d MAX R - Spr | 0.709 | 0.022 | 0.556 | 0.025 | 0.807 | <0.001 | + |
| Total R - Spr | 3d MAX Q - Spr DOY | 0.952 | 0.000 | 0.867 | 0.000 | 0.802 | <0.001 | + |
| Total R - Spr | 3d MAX BF - Spr DOY | 0.939 | 0.000 | 0.822 | 0.001 | 0.774 | <0.001 | + |
| Total R - Spr | 3d MAX BF - Spr | 0.830 | 0.003 | 0.689 | 0.006 | 0.621 | 0.007 | + |
| Water yield - Spr | 3d MAX Q - Spr DOY | 0.806 | 0.005 | 0.600 | 0.016 | 0.584 | 0.010 | + |
| Water yield - Spr | BF yield - Spr | 0.915 | 0.000 | 0.822 | 0.001 | 0.929 | <0.001 | + |
| Water yield - Spr | 3d MAX BF - Spr DOY | 0.818 | 0.004 | 0.644 | 0.009 | 0.619 | 0.007 | + |
| Water yield - Spr | 3d MAX BF - Spr | 0.855 | 0.002 | 0.689 | 0.006 | 0.698 | 0.003 | + |
| 3d MAX Q - Spr DOY | 3d MAX Q - Spr | 0.648 | 0.043 | 0.556 | 0.025 | 0.691 | 0.003 | + |
| 3d MAX Q - Spr DOY | 3d MAX BF - Spr DOY | 0.988 | 0.000 | 0.956 | 0.000 | 0.997 | <0.001 | + |
| 3d MAX Q - Spr DOY | 3d MAX BF - Spr | 0.879 | 0.001 | 0.733 | 0.003 | 0.792 | <0.001 | + |
| 3d MAX Q - Spr | 3d MAX BF - Spr DOY | 0.721 | 0.019 | 0.600 | 0.016 | 0.679 | 0.003 | + |
| 3d MAX Q - Spr | 3d MAX BF - Spr | 0.855 | 0.002 | 0.733 | 0.003 | 0.753 | 0.001 | + |
| 7d MIN Q - Spr | 7d MIN BF - Spr | 0.991 | 0.000 | 0.966 | 0.000 | 0.997 | <0.001 | + |
| BF yield - Spr | 3d MAX BF - Spr | 0.673 | 0.033 | 0.511 | 0.040 | 0.441 | 0.036 | |
| 3d MAX BF - Spr DOY | 3d MAX BF - Spr | 0.915 | 0.000 | 0.778 | 0.002 | 0.818 | <0.001 | + |
| 3d MAX BF - Spr | 3d MAX GW - Spr | 1.000 | . | 1.000 | . | 0.968 | 0.003 | + |

*Correlation is significant at 0.01 level (2-tailed)

The results for the summer season (Table 5.4) show strong correlations between streamflow and baseflow parameters, and 7-day Maximum Temperature and 3-day Maximum Streamflow Day-of-Year timing and 3-day Maximum Hydrologic Release Day-of-Year timing. Other correlations include hydrologic release and streamflow and baseflow parameters.

*Table 5.4. Correlation analysis results for the summer season, Neebing River (2008-2017)*

| Summer Correlation (JJA) | | Spearman's Rank | | Kendall's Rank | | Linear Regression | | |
|---|---|---|---|---|---|---|---|---|
| **Parameter 1** | **Parameter 2** | **ρ** | **p-value** | **τ** | **p-value** | **$R^2$** | **p-value** | **slope** |
| 7d MAX T - Sum | 3d MAX Q - Sum DOY | 0.815 | 0.004 | 0.584 | 0.020 | 0.580 | 0.010 | + |
| 7d MAX T - Sum | 3d MAX R - Sum DOY | -0.669 | 0.032 | -0.539 | 0.031 | 0.508 | 0.021 | - |
| Total R - Sum | 3d MAX R - Sum | 0.673 | 0.033 | 0.511 | 0.040 | 0.716 | 0.002 | + |
| Total R - Sum | 3d MAX Q - Sum | 0.648 | 0.043 | 0.511 | 0.040 | 0.506 | 0.021 | + |
| 3d MAX R - Sum DOY | 30d MIN R - Sum | -0.818 | 0.004 | -0.644 | 0.009 | 0.696 | 0.003 | - |
| 3d MAX R - Sum DOY | Water yield - Sum | -0.818 | 0.004 | -0.644 | 0.009 | 0.512 | 0.012 | - |
| 3d MAX R - Sum DOY | 3d MAX Q - Sum | -0.842 | 0.002 | -0.644 | 0.009 | 0.595 | 0.009 | - |
| 3d MAX R - Sum DOY | 7d MIN Q - Sum DOY | -0.665 | 0.036 | -0.523 | 0.038 | 0.534 | 0.016 | - |
| 3d MAX R - Sum DOY | BF yield - Sum | -0.721 | 0.019 | -0.556 | 0.025 | 0.566 | 0.012 | - |
| 3d MAX R - Sum DOY | 3d MAX BF - Sum | -0.867 | 0.001 | -0.689 | 0.006 | 0.578 | 0.011 | - |
| 3d MAX R - Sum | 3d MAX Q - Sum | 0.842 | 0.002 | 0.733 | 0.003 | 0.647 | 0.005 | + |
| 3d MAX R - Sum | 3d MAX BF - Sum | 0.830 | 0.003 | 0.689 | 0.006 | 0.539 | 0.016 | + |
| 3d MAX R - Sum | Water yield - Sum | 0.770 | 0.009 | 0.644 | 0.009 | 0.514 | 0.020 | + |
| 3d MAX R - Sum | BF yield - Sum | 0.842 | 0.002 | 0.644 | 0.009 | 0.514 | 0.020 | + |
| Water yield - Sum | 3d MAX Q - Sum | 0.964 | 0.000 | 0.911 | 0.000 | 0.856 | <0.001 | + |
| Water yield - Sum | 7d MIN Q - Sum | 0.636 | 0.048 | 0.511 | 0.040 | 0.510 | 0.020 | + |
| Water yield - Sum | BF yield - Sum | 0.939 | 0.000 | 0.822 | 0.001 | 0.987 | <0.001 | + |
| Water yield - Sum | 3d MAX BF - Sum | 0.855 | 0.002 | 0.778 | 0.002 | 0.546 | 0.015 | + |
| Water yield - Sum | 7d MIN BF - Sum | 0.687 | 0.028 | 0.539 | 0.031 | 0.561 | 0.013 | + |
| 3d MAX Q - Sum | BF yield - Sum | 0.855 | 0.002 | 0.733 | 0.003 | 0.806 | <0.001 | + |
| 3d MAX Q - Sum | 3d MAX BF - Sum | 0.952 | 0.000 | 0.867 | 0.000 | 0.76 | 0.001 | + |
| 7d MIN Q - Sum DOY | 7d MIN BF - Sum DOY | 0.948 | 0.000 | 0.851 | 0.001 | 0.784 | <0.001 | + |
| 7d MIN Q - Sum DOY | 3d MAX GW - Sum | 0.975 | 0.005 | 0.949 | 0.023 | 0.858 | 0.024 | + |
| 7d MIN Q - Sum | BF yield - Sum | 0.648 | 0.043 | 0.511 | 0.040 | 0.557 | 0.013 | + |

| Summer Correlation (JJA) | | Spearman's Rank | | Kendall's Rank | | Linear Regression | | |
|---|---|---|---|---|---|---|---|---|
| **Parameter 1** | **Parameter 2** | **ρ** | **p-value** | **τ** | **p-value** | **$R^2$** | **p-value** | **slope** |
| 7d MIN Q - Sum | 7d MIN BF - Sum | 0.997 | 0.000 | 0.989 | 0.000 | 0.970 | <0.001 | + |
| BF yield - Sum | 3d MAX BF - Sum | 0.733 | 0.016 | 0.600 | 0.016 | 0.532 | 0.017 | + |
| BF yield - Sum | 7d MIN BF - Sum | 0.699 | 0.024 | 0.539 | 0.031 | 0.621 | 0.007 | + |
| 3d MAX BF - Sum DOY | 3d MAX GW - Sum DOY | 0.918 | 0.028 | 0.882 | 0.046 | 0.995 | <0.001 | + |
| 3d MAX BF - Sum DOY | 3d MAX GW - Sum | 1.000 | . | 1.000 | . | 0.964 | 0.003 | + |
| 7d MIN BF - Sum DOY | 3d MAX GW - Sum DOY | 0.918 | 0.028 | 0.882 | 0.046 | 0.348 | 0.265 | + |
| 7d MIN BF - Sum DOY | 3d MAX GW - Sum | 0.975 | 0.005 | 0.949 | 0.023 | 0.913 | 0.011 | + |

*Correlation is significant at 0.01 level (2-tailed)

Similarly, the fall analysis (Table 5.5) shows strong correlations between streamflow and baseflow parameters and between hydrologic release and streamflow and baseflow parameters. There also seems to be a correlation between the 7-day Minimum temperature in fall Day-of-Year timing and both the 30-day Minimum Hydrologic Release in the fall and the 7-day Minimum Groundwater level in the fall. There is also a strong correlation between the 3-day Maximum Baseflow Day-of-Year timing and the 3-day Maximum Groundwater level Day-of-Year timing during the fall.

*Table 5.5. Correlation analysis results for the fall season, Neebing River (2008-2017)*

| Fall (SON) Correlation | | Spearman's Rank | | Kendall's Rank | | Linear Regression | | |
|---|---|---|---|---|---|---|---|---|
| **Parameter 1** | **Parameter 2** | **ρ** | **p-value** | **τ** | **p-value** | **$R^2$** | **p-value** | **slope** |
| 7d MAX T - Fal DOY | 30d MIN R - Fal | 0.706 | 0.023 | 0.552 | 0.029 | 0.515 | 0.020 | + |
| 7d MIN T - Fal DOY | 7d MIN GW - Fal | -0.928 | 0.008 | -0.828 | 0.022 | 0.797 | 0.017 | - |
| Total R - Fal | 3d MAX R - Fal | 0.794 | 0.006 | 0.644 | 0.009 | 0.577 | 0.011 | + |
| Total R - Fal | 30d MIN R - Fal | 0.733 | 0.016 | 0.600 | 0.016 | 0.560 | 0.013 | + |
| 3d MAX R - Fal DOY | 3d MAX Q - Fal DOY | 0.915 | 0.000 | 0.818 | 0.001 | 0.885 | <0.001 | + |
| 3d MAX R - Fal DOY | 3d MAX BF - Fal DOY | 0.875 | 0.001 | 0.719 | 0.004 | 0.576 | 0.011 | + |
| 3d MAX R - Fal DOY | 3d MAX GW - Fal DOY | 0.899 | 0.015 | 0.828 | 0.022 | 0.756 | 0.024 | + |
| 3d MAX R - Fal | 3d MAX Q - Fal | 0.733 | 0.016 | 0.644 | 0.009 | 0.853 | <0.001 | + |
| 3d MAX R - Fal | 3d MAX BF - Fal | 0.721 | 0.019 | 0.600 | 0.016 | 0.861 | <0.001 | + |
| Water yield - Fal | BF yield - Fal | 0.915 | 0.000 | 0.822 | 0.001 | 0.837 | <0.001 | + |

| Fall (SON) Correlation | | Spearman's Rank | | Kendall's Rank | | Linear Regression | | |
|---|---|---|---|---|---|---|---|---|
| Parameter 1 | Parameter 2 | ρ | p-value | τ | p-value | $R^2$ | p-value | slope |
| 3d MAX Q - Fal DOY | 3d MAX BF - Fal DOY | 0.960 | 0.000 | 0.899 | 0.000 | 0.682 | 0.003 | + |
| 3d MAX Q - Fal DOY | 3d MAX GW - Fal DOY | 0.899 | 0.015 | 0.828 | 0.022 | 0.877 | 0.006 | + |
| 3d MAX Q - Fal | 3d MAX BF - Fal | 0.988 | 0.000 | 0.956 | 0.000 | 0.995 | <0.001 | + |
| 7d MIN Q - Fal | 7d MIN BF - Fal | 0.921 | 0.000 | 0.841 | 0.001 | 0.839 | <0.001 | + |
| 3d MAX BF - Fal DOY | 3d MAX GW - Fal DOY | 0.943 | 0.005 | 0.867 | 0.015 | 0.893 | 0.004 | + |
| 3d MAX GW - Fal | 7d MIN GW - Fal | 0.886 | 0.019 | 0.733 | 0.039 | 0.686 | 0.042 | + |

*Correlation is significant at the 0.01 level (2-tailed)

### 5.2.3 Mann-Kendall Trend Test

The Mann-Kendall trend test was conducted to identify trends in the parameters within the study period. The results of this time series analysis are included in Table 5.6. Only results with >90% confidence and a p-value <0.05 are included. The full results are included in Appendix E. The results with p-values <0.025 are considered very certain (VC), p-values <0.05 are probably trending (PT), and p-values <0.1 were flagged as warning (W), indicating that there might be a trend present (Gao et al. 2010).

Only five parameters show a trend that is considered VC: Minimum of 30-day total Hydrologic Release (mm), Minimum of 30-day total Hydrologic Release winter (mm), Minimum of 30-day total Hydrologic Release Spring - Day of Year Timing, Maximum of 3-day averaged Groundwater Elevation winter (masl), and Minimum of 7-day averaged Groundwater Elevation winter (masl). All variables that show trends in Table 5.6 below see a positive or increasing trend except for the Maximum of 3-day averaged Groundwater Elevation Spring - Day of Year Timing, which shows a negative or decreasing trend but only at the warning confidence level.

*Table 5.6Significant Results from the Mann-Kendall Trend Test, Neebing River (2008-2017)*

| Parameter | tau | 2-sided p-value | Confidence | Note |
|---|---|---|---|---|
| 7d MAX T - DOY | 0.514 | 0.035 | PT | |
| 7d MAX T - Win | 0.527 | 0.029 | PT | |
| Total P | 0.511 | 0.049 | PT | |
| Total R | 0.511 | 0.491 | PT | |
| 30d MIN R | 0.733 | 0.004 | VC | |
| 30d MIN R - Win | 0.673 | 0.005 | VC | |
| 30d MIN R – Spr DOY | 0.584 | 0.025 | VC | |

| confidence levels: | Symbol: | p-values |
|---|---|---|
| very certain | VC | <0.025 |
| probably trending | PT | <0.05 |
| warning | W | <0.1 |

| | | | | |
|---|---|---|---|---|
| CMI (P-PET) | 0.467 | 0.074 | W | |
| 7d MIN Q – Sum DOY | 0.477 | 0.071 | W | |
| 3d MAX BF – Win DOY | 0.452 | 0.077 | W | |
| 7d MIN BF – Sum DOY | 0.449 | 0.088 | W | |
| Mean GW | 0.619 | 0.072 | W | <10 years of data |
| 3d MAX GW - Win | 0.867 | 0.024 | VC | <10 years of data |
| 3d MAX GW – Spr DOY | -0.733 | 0.060 | W | <10 years of data |
| 7d MIN GW - Win | 0.867 | 0.024 | VC | <10 years of data |
| 7d MIN GW - Spr | 0.733 | 0.060 | W | <10 years of data |

### 5.2.4 Double-Mass Balance

The double-mass balance analysis estimates the proportion of water yield derived from baseflow (Figure 5.8). This proportion was 58.3% for the Neebing River on the annual scale from 2008 to 2017. The annual double-mass balance result was compared to the seasonal estimates (Figure 5.9). These results vary significantly from 53.5% during the spring season to 82.99% during the winter season (Figure 5.9). Figure 5.10 below shows the estimated precipitation proportion of 35.24% contributing to streamflow/water yield on an annual time scale. The hydrologic release includes the contribution from snowmelt on the seasonal timescale. Noticeable variability occurs from 10.89% and 15.58% in the winter and fall seasons to 24.23% during the summer and 52.48% during the spring. The large proportion of hydrologic release that contributes to streamflow/water yield during springtime is caused by the spring freshet, melting snow and ice. The lower numbers during the summer and fall can be explained by the increased water storage capacity on the land by vegetation cover. The low proportion of hydrologic release contributing to streamflow/water yield during the winter is due to the snow storage and ice cover on the Neebing River (Figure 5.11).

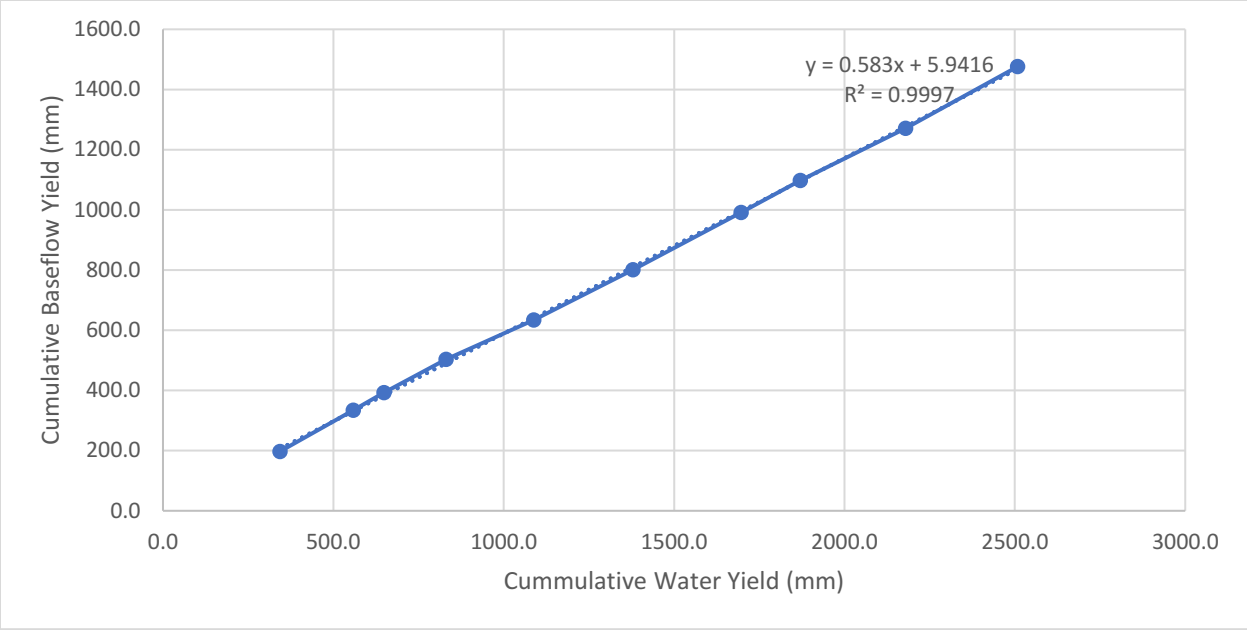


*Figure 5.7. Neebing River cumulative annual baseflow yield to cumulative annual water yield (2008-2017). The equation of the line estimates the proportion of water yield that is derived from baseflow.*

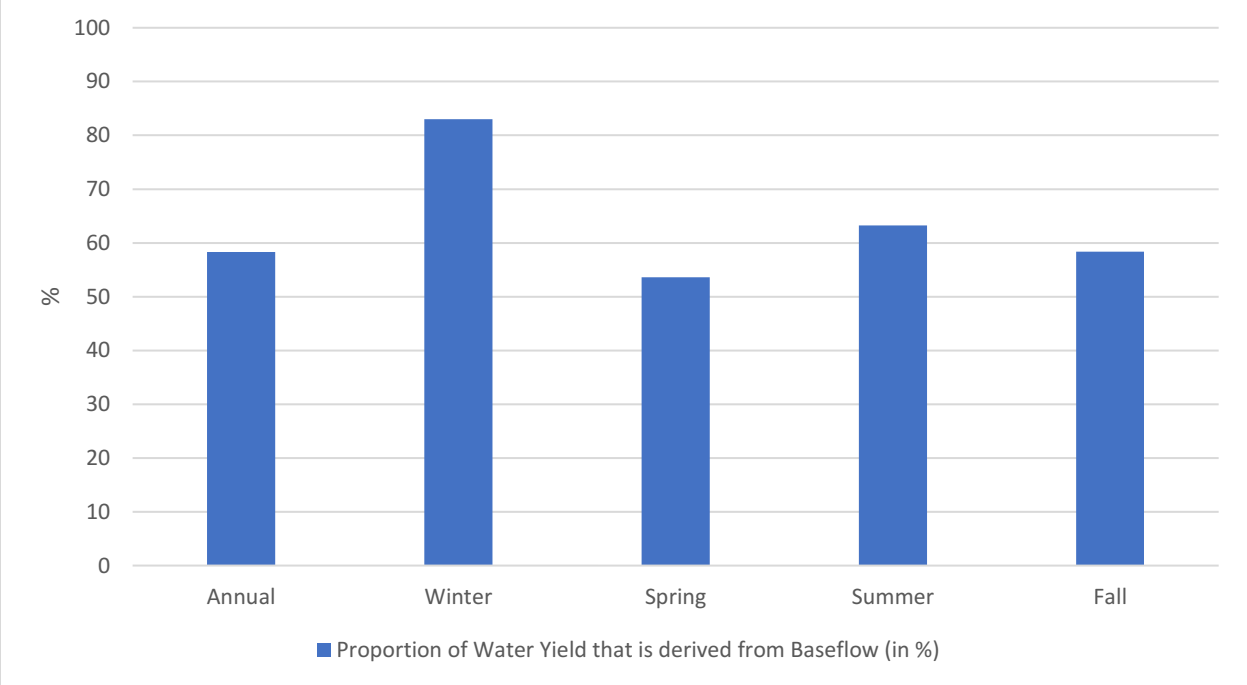


*Figure 5.8. Trends in seasonal double mass balance, the relationship between cumulative water yield and cumulative baseflow yield for the Neebing River (2008-2017)*

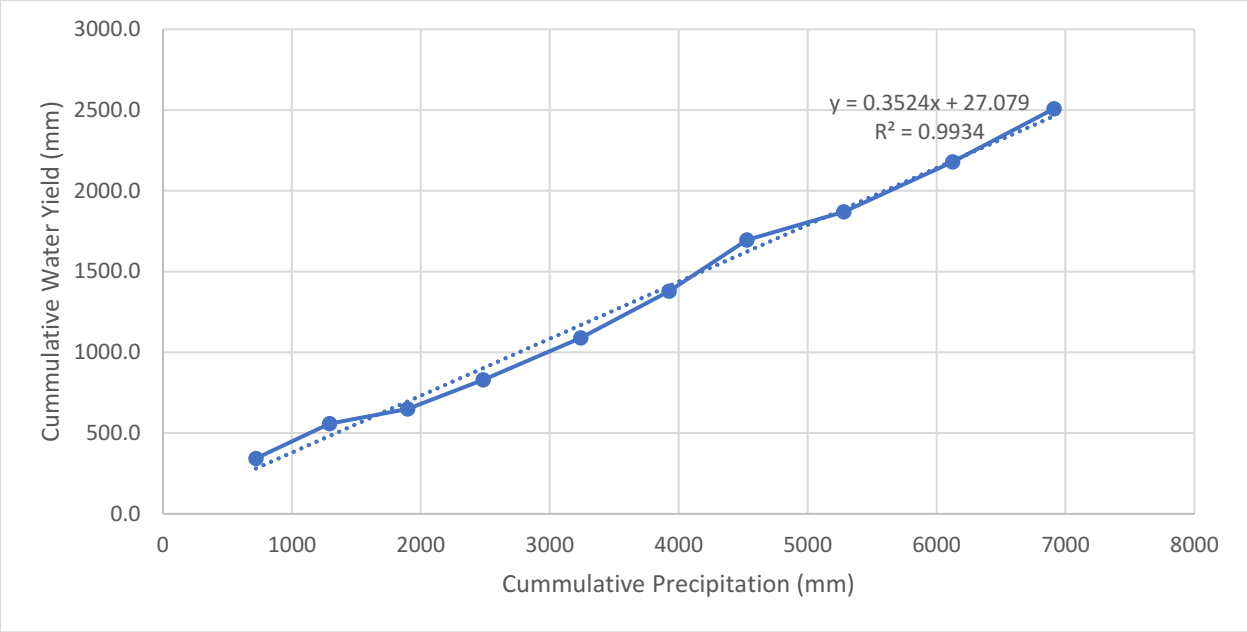


*Figure 5.9. Neebing River cumulative annual water yield to precipitation (2008-2017). The equation of the line estimates the proportion of precipitation that contributes to streamflow/water yield.*

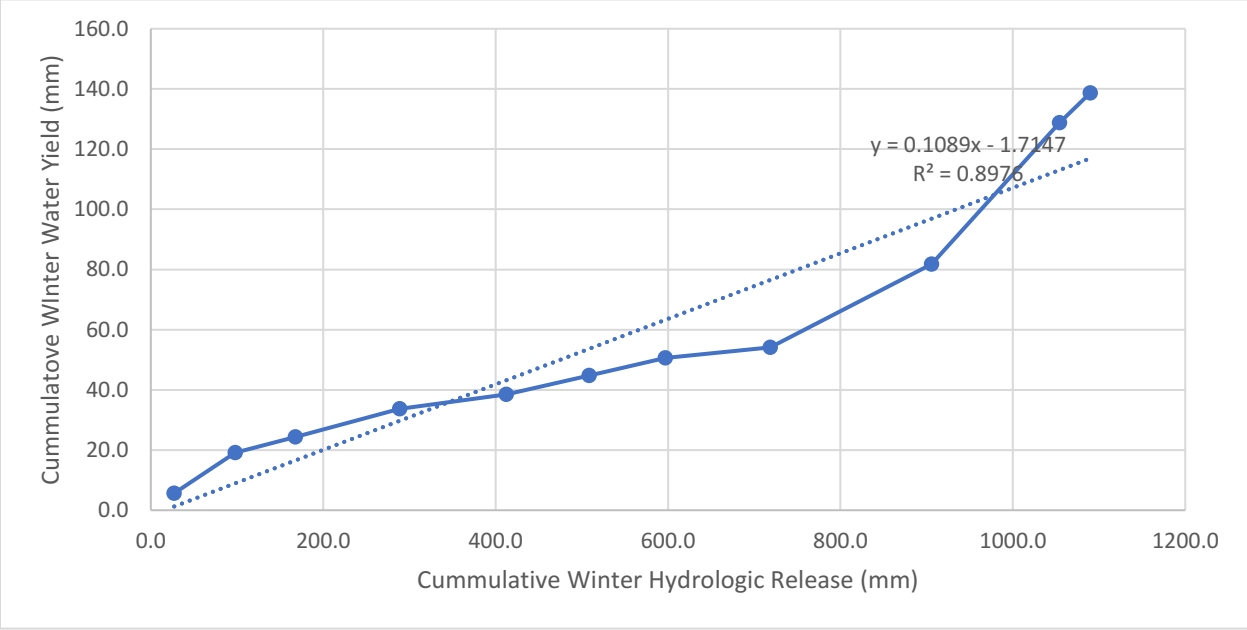


*Figure 5.10. Neebing River cumulative winter water yield to cumulative winter hydrologic release (2008-2017). The equation of the line estimates the proportion of hydrologic release that contributes to streamflow/water yield.*

### 5.2.5 Hydrograph

The streamflow and precipitation information from WSC and ECCC for the study period of 2008-2017 was entered into the online SepHydro tool. The values of $BFI_{max}$ = 0.761 and $\alpha$ = 0.975 were used.

The tool produced a dataset of baseflow separation data where the streamflow was separated into baseflow and runoff components. Furthermore, the tool provided descriptive statistics for the dataset and a hydrograph to visualize the data. The dataset that was produced is continuous and provides an estimate of baseflow and runoff for any given day within the specified time period (2008-2017). The SepHydro tool hydrograph (Figure 5.12) visualizes precipitation, streamflow and baseflow data. Furthermore, the hydrograph shows the positive relationship between precipitation events and streamflow and baseflow. This data can then be combined with additional information to create hydrographs that include extreme flow thresholds for the top and bottom 90$^{th}$ and 10$^{th}$ percentiles (Figure 5.13). Figure 5.13 shows the hydrograph for the Neebing River in 2017 and includes the threshold lines for extreme flow. This visually represents the times when the Neebing River experienced extreme high- or low-flow events. Similar hydrographs for the years 2008-2016 can be found in Appendix D.

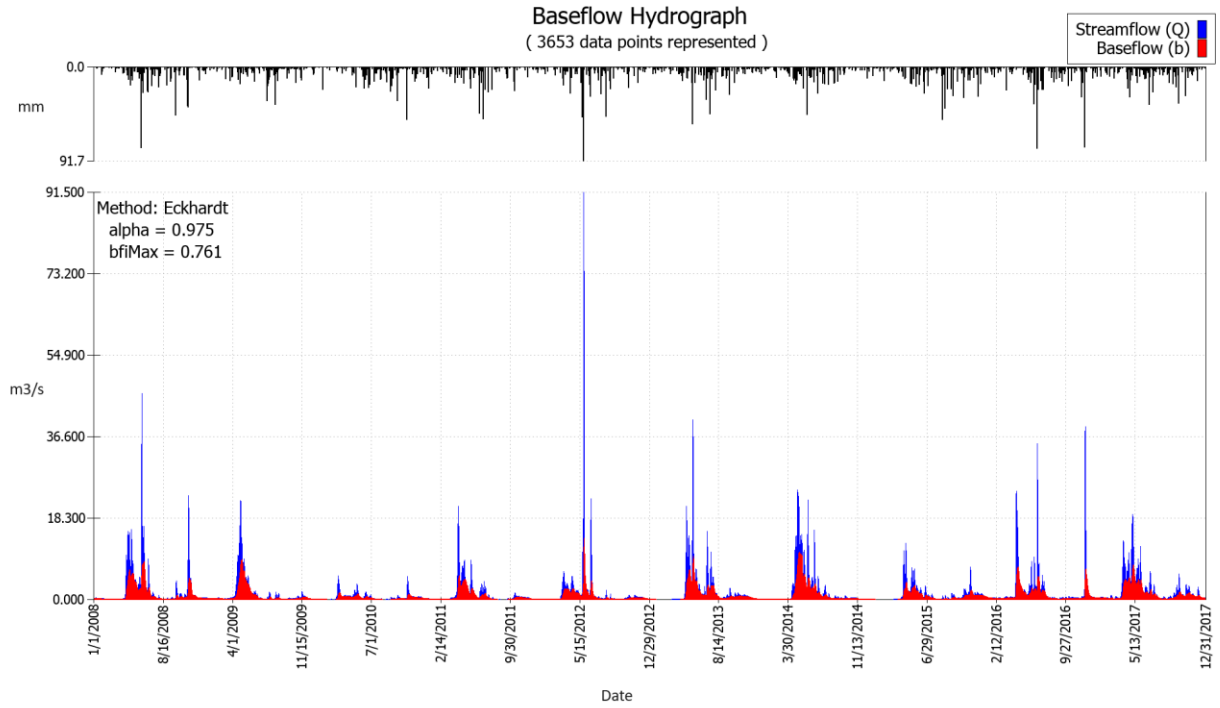


*Figure 5.11. Sephydro Baseflow Hydrograph Eckhardt 2008-2017, Neebing River*

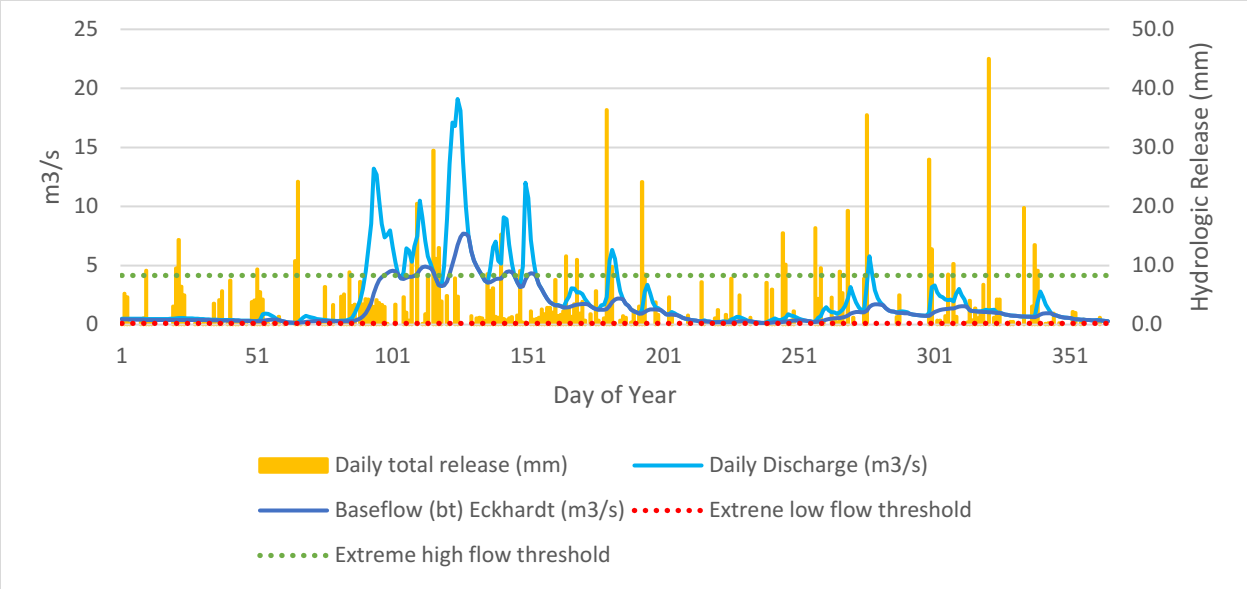


*Figure 5.12. Hydrograph of the Neebing River (2017), with 10% and 90% extreme flow thresholds*

### 5.2.6 Water Balance

The output from the SepHydro tool is daily runoff and baseflow data (in $m^3/s$) for every day in the study period (2008-2017). These daily values were converted to mm/day, accounting for the total area of the Neebing River drainage basin, to be comparable with precipitation data and totalled for annual comparison. Table 5.7 shows the annual water balance and estimates for runoff and baseflow for the Neebing River (2008-2017).

*Table 5.7. Annual total precipitation, water yield, runoff and baseflow for the Neebing River (2008-2017)*

| Year | Precipitation (mm) | Water Yield (mm) | Runoff (mm) | Baseflow Yield (mm) |
|---|---|---|---|---|
| 2008 | 720.20 | 343.13 | 146.04 | 197.08 |
| 2009 | 573.30 | 214.98 | 78.21 | 136.76 |
| 2010 | 604.10 | 90.45 | 31.92 | 58.52 |
| 2011 | 586.90 | 181.93 | 70.91 | 110.98 |
| 2012 | 756.80 | 257.91 | 127.75 | 130.22 |
| 2013 | 684.00 | 290.49 | 123.25 | 167.25 |
| 2014 | 604.20 | 317.41 | 126.57 | 190.85 |
| 2015 | 752.90 | 173.94 | 67.78 | 106.18 |
| 2016 | 842.20 | 309.13 | 136.19 | 172.94 |
| 2017 | 786.60 | 328.92 | 123.55 | 205.39 |
| Average | 691.12 | 250.83 | 103.22 | 147.62 |

### 5.2.7 R-B Index

The annual analysis of the R-B index for flashiness is shown in Figure 5.15. The values range from the smallest value of 0.15 in 2009 to the greatest value of 0.44 in 2012. The slope of the trendline is slightly positive but does not indicate a clear trend.

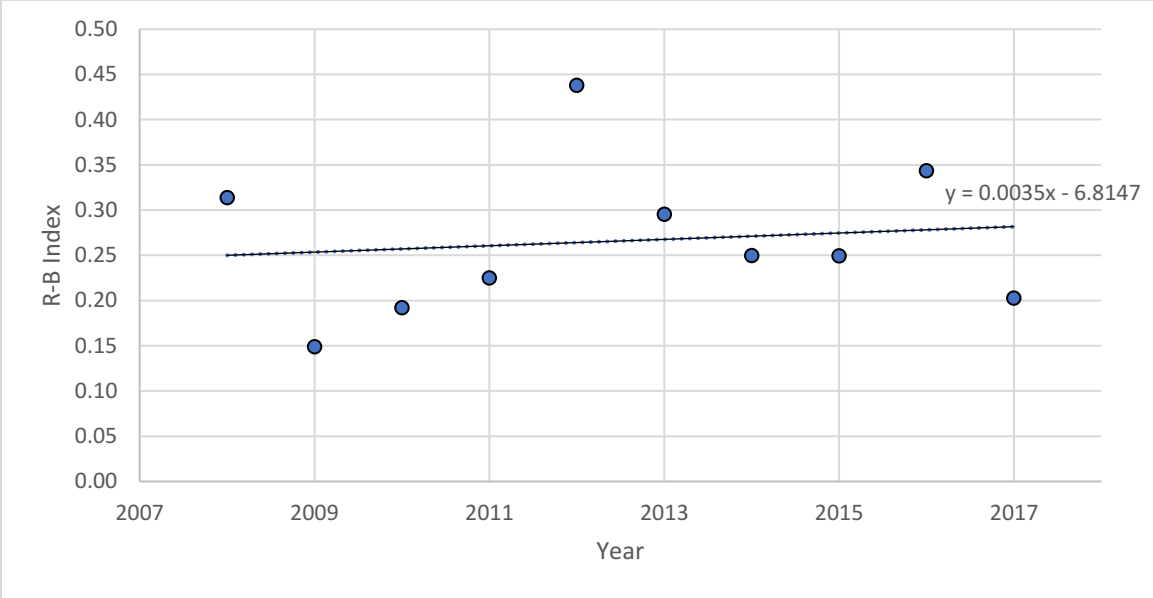


*Figure 5.13. R-B Index for Flashiness Neebing River (2008-2017)*

## 5.3 Results: Stable Isotope Sampling

The results for the stable isotope sampling, show the $\delta^{2}H$ and $\delta^{18}O$ ratios plotted in Figure 5.14. These sampling results are colour-coded and grouped according to sampling location. No clear trend by location is noticeable.

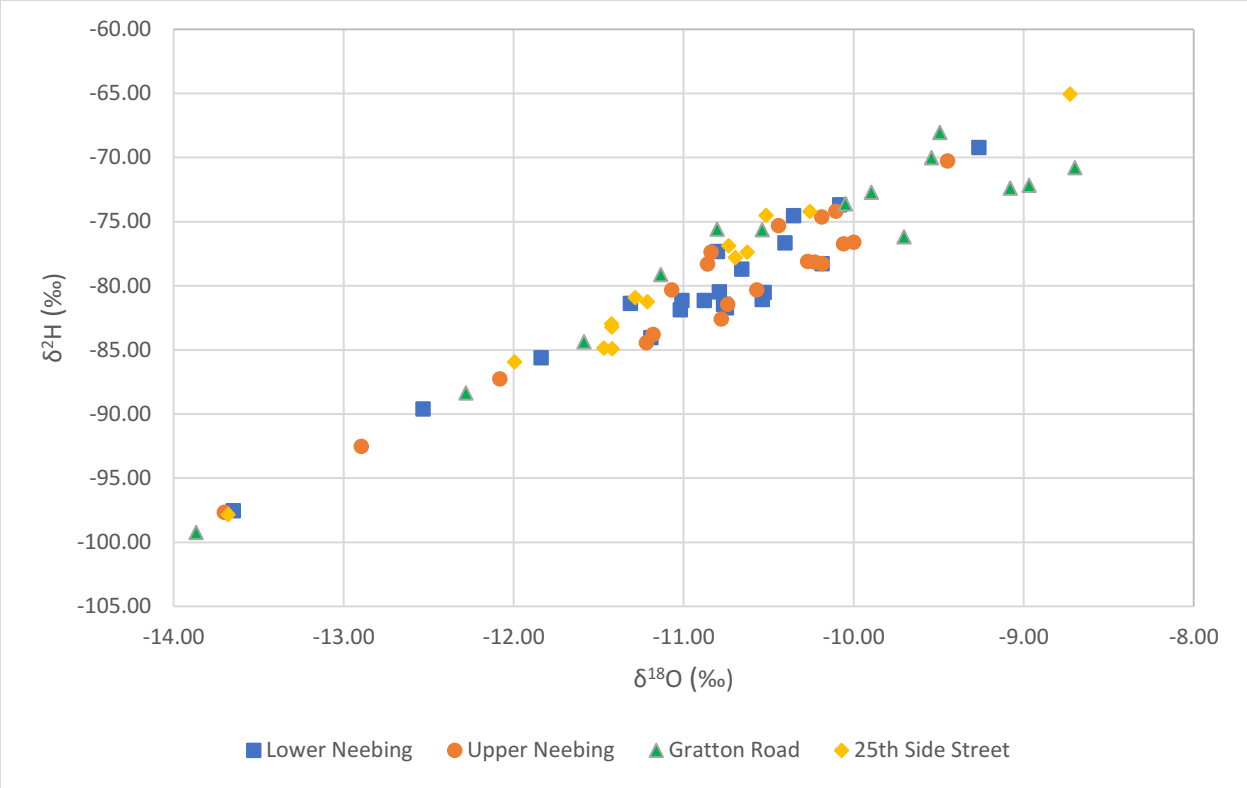


*Figure 5.14. Stable isotope sampling results for the Neebing River (2021-2022) sorted for locations*

Figure 5.15 shows the stable isotope sampling results for all sample sites. The data points are colour-coded for the season in which the sample was collected. It is noteworthy that the winter samples were collected during the first week of December 2021 before the complete freeze-up of the Neebing River. No samples were taken during the middle of winter due to the limiting factor of ice thickness on the Neebing River. The data points are grouped together according to season, with the spring season data points presenting the lowest $\delta^2H$ and $\delta^{18}O$ ratios. The summer and fall data points are close together but with the fall data points trending below most of the summer data points in $\delta^2H$ and $\delta^{18}O$ ratios. The winter data points are clustered in the center of Figure 5.15 above some of the summer and fall data points.

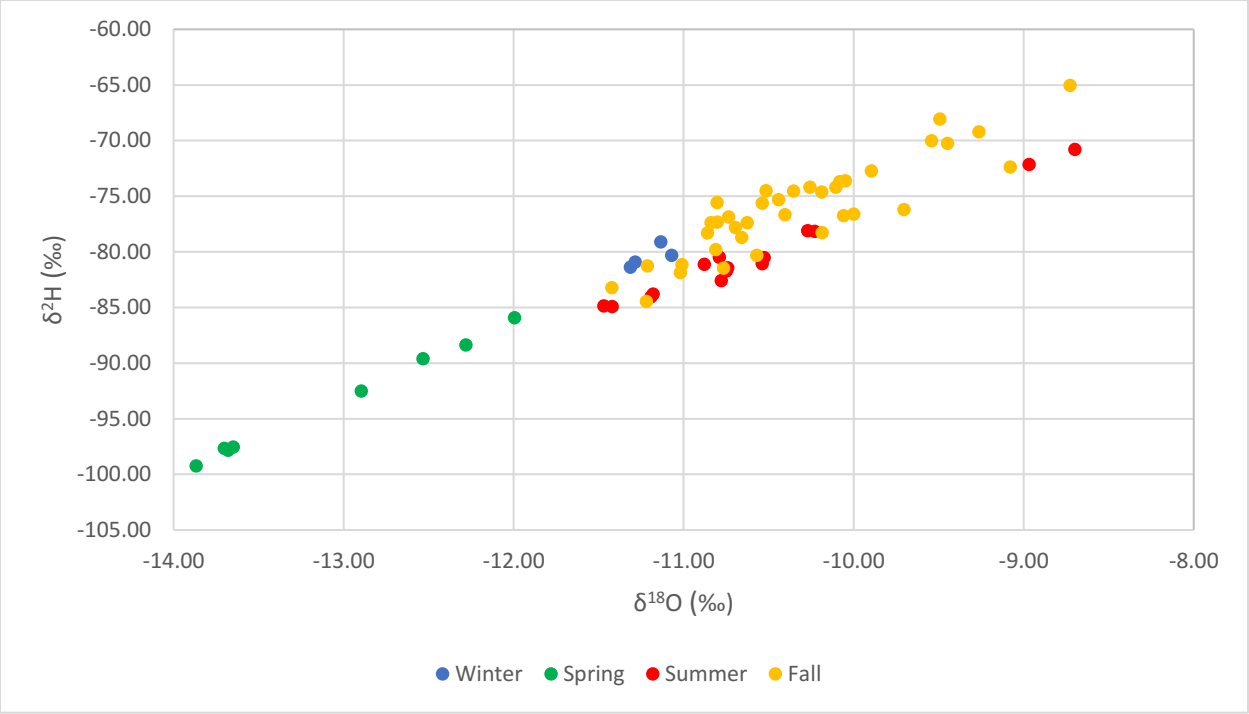


*Figure 5.15. Stable isotope sampling results for the Neebing River (2021-2022) sorted for seasons*

**CHAPTER 6**

# 6 Discussion

## 6.1 Thematic Mapping

The SGRAs that were identified in Figure 5.6 are in different locations in the study area. Areas that were identified to have significant groundwater recharge potential include an area between Highway 11/17, Mapleward Road, Oliver Road and 25$^{th}$ Side Street; the western part of Williams Bog; areas along Pennock Creek and the Ministry of Natural Resources and Forestry tree farm; an area near Jelly at Jelly Road and Blind Line Road; sections of Chapples Park; a forest near Willrod Road and Government Road; and an area around the Thunder Bay Solid Waste and Recycling Facility. These areas share the same characteristics of being relatively flat, vegetation landcover, and more permeable soils. These identified areas are of significance to groundwater recharge and are, therefore, also of relevance for the groundwater contribution to the Neebing River. SGRAs are often only considered by regulatory or governing institutions in Ontario in terms of source water protection. The contribution that SGRAs have on streamflow is not monitored to the same extent as in the source water protection context, even though a reduction in SGRAs might cause noticeable changes in streamflow discharge.

Continuous urbanization and urban sprawl could threaten some of the areas identified as SGRAs. Ongoing housing developments in the Williams Bog area will impact surface water's ability to infiltrate the ground and contribute to groundwater recharge. The proximity of one SGRA to the Thunder Bay Solid Waste and Recycling Facility raises concern for caution for potential groundwater contamination. Pollutants could potentially enter the groundwater and resurface through groundwater, contributing to the Neebing River on the surface. Other areas identified as SGRA are sparsely populated and include forested areas and rural housing. Low slope areas tend to be easily developable, and they are also one of the input variables for SGRAs. This overlap can cause conflicts of different interests and should be addressed in the planning stage of potential developments.

The infiltration index grid (Figure 5.6) can be used in the future to quantify the groundwater infiltration that contributes to streamflow as baseflow (Ontario Ministry of the Environment 2003). The available amount of water could be multiplied by the index to estimate the infiltration at a specific location within the study area. This can be combined with atmospheric data, such as precipitation data from the drainage basin, to estimate specific infiltration volumes based on the infiltration index grid.

## 6.2 Statistical Analysis

### 6.2.1 Flow Duration Curve

The flow duration curve for the Neebing River was expected as it follows the common trend of having low flow events at a greater frequency and high flow events at a lower frequency. Over time, extreme weather events are likely to occur more frequently, and dry areas can become more dry and wet

areas can become more wet due to the changing climate (Rohli and Vega 2018). These shifts in climatic conditions can increase the frequency of high-flow events. Therefore, flow duration curves that are based on historical data have limitations in predicting the potential exceedance probabilities for the future. The general trend of a large number of low-flow events and a low number of high-flow events will remain, but there will likely be shifts in the extreme ends of the flow duration curve.

### 6.2.2 Correlation Analysis

The correlation analysis results show expected relationships between related parameters such as temperature and evapotranspiration or streamflow and baseflow parameters in both the annual and seasonal analyses. The streamflow and baseflow correlations are examples of the surface and subsurface interactions. These relationships were not surprising as one parameter is dependent on the other. For example, temperature is used to calculate evapotranspiration, and baseflow is derived from streamflow data. These relationships were observed on the annual as well as the seasonal scales. The annual correlation analysis contains the most parameters for analysis as some parameters were only analyzed on the annual scale; this includes the precipitation, climate moisture index, Richard-Baker index for flashiness and the 10:90 exceedance percentile ratios. The R-B flashiness index and 10:90 exceedance percentile are also based on streamflow data. Therefore, a correlation between the R-B flashiness index, the 10:90 exceedance percentile and the streamflow and baseflow parameters is not unexpected.

It is noticeable that there are correlations between hydrologic release parameters and other parameters, such as streamflow and baseflow parameters, on the annual scale and all the seasonal scales except for winter. This is likely due to the ice cover on the Neebing River, which limits the direct streamflow contribution pathways through precipitation and runoff. There is a very significant correlation in the spring season between the 3-day Maximum Baseflow and the 3-day Maximum Groundwater level. This indicates that the peak baseflow events are correlated with the highest groundwater levels during the spring season. Whereas during the fall season, it is the 3-day Maximum Baseflow day-of-year timing and the 3-day Maximum Groundwater level day-of-year timing that is strongly correlated. During the summer, there is a strong correlation between the 3-day Maximum Baseflow day-of-year timing and the 3-day Maximum Groundwater level as well as the 3-day Maximum Baseflow day-of-year timing and the 3-day Maximum Groundwater level day-of-year timing. This indicates a strong relationship in the timing of occurrence between 3-day Maximum Groundwater levels and 3-day Maximum Baseflow.

Furthermore, the day-of-year timing (DOY) in some of the streamflow- and baseflow parameters also showed correlations, indicating that the timing of occurrence is correlated between the parameters. These parameters refer to the calendar date on which the parameter was measured/reached. The correlation between the 3-day Maximum in Streamflow- and Baseflow day-of-year timing parameters shows that the timing of the dates of occurrence follows similar temporal trends. This is due to high volumes of baseflow causing increased volumes in streamflow; which is captured through the baseflow separation methodology that derives baseflow from streamflow, dividing streamflow values into the runoff and baseflow components, resulting in increased baseflow values when higher streamflow values are present. This is also observed in the 7-day Minimum Streamflow and Baseflow day-of-year parameters. These correlations were observed during the annual and fall analyses and only for the 7-day Minimum Streamflow and Baseflow during the summer season.

### 6.2.3 Mann-Kendall Trend Test

The results from the Mann-Kendall trend test show an increasing trend in some of the 30-day Minimum Hydrologic Release parameters. On an annual basis and during the winter, the 30-day Minimum Hydrologic Release is increasing. This indicates that there is an increasing trend during the winter in the 30-day Minimum Hydrologic Release, meaning that the minimum amount of hydrologic release has increased over time, and more water was released earlier in the year. There is an increasing trend for the Minimum 30-day total Hydrologic Release Spring – Day of Year Timing, meaning its occurrence is trending to be later in the year. Furthermore, there are increasing trends for the groundwater parameters 3-day Maximum Groundwater and 7-day Minimum Groundwater Winter. This indicates an increasing trend in peak and nadir values for groundwater, meaning the maximum and minimum groundwater levels have become greater over time. Less significant trends in other groundwater parameters, Mean GW and 7d MIN GW – Spr, support this potential trend in increasing groundwater levels. Of note, less than 10 years of groundwater data are considered in this study, which is a requirement for reliable results. Therefore, these results should be interpreted with caution, and the study should be repeated when sufficient data is available.

### 6.2.4 Double Mass Balance

Double mass balance results indicate the reliance of streamflow on the baseflow contribution, especially during the seasons with less precipitation, summer and fall. Of note, during winter, the same relationship between streamflow and baseflow is observed when the ice cover prevents direct streamflow contribution from precipitation. During these times, the Neebing River receives more than half of its streamflow contribution from baseflow. On an annual basis, more than half of Neebing's streamflow is baseflow sourced. The proportion of hydrologic release contributing to streamflow is lowest during winter. An ice layer covers the Neebing River for most of the winter season, making it inaccessible for direct precipitation and runoff contributions. Therefore, potential changes in baseflow contribution to streamflow, such as a reduction in baseflow, could lead to a decrease in overall streamflow, especially during the winter season.

### 6.2.5 Hydrograph

The hydrographs for the Neebing River are a useful tool to identify extreme flow and precipitation events. The hydrographs for the years 2008-2017 show the variability in precipitation and streamflow discharge. High-impact precipitation events, such as those that occurred at the end of May 2012, see Neebing River hydrograph 2012 in Appendix D, and the impact they have on streamflow discharge are easily identifiable. The Neebing River responds with increased streamflow discharge following the high precipitation events before returning to normal streamflow discharge levels. The development of a series of hydrographs enables interannual comparison of the hydrologic conditions in the Neebing River basin.

### 6.2.6 Water balance

The water balance analysis shows that the Neebing River is mostly groundwater-fed. The contribution to the overall water yield is larger from baseflow than from runoff. The streamflow discharge varies on an annual scale and is influenced by the amount of precipitation in any given year. The baseflow contribution ensures constant water flow throughout the year, even during periods of low precipitation. The water balance results established this difference in baseflow and precipitation contribution, demonstrating that the Neebing River's primary source is groundwater. The groundwater contribution is an important hydrologic function that ensures continuous streamflow. The watershed storage capacity ensures this function as it retains and stores water before releasing it as streamflow, evapotranspiration, or groundwater flow.

### 6.2.7 R-B Index

The R-B index analysis for flashiness shows no significant trend during this study period (Figure 5.14). This is supported by the results of the Mann-Kendall trend analysis, which also does not indicate a significant trend for the R-B index. The consistency in R-B values between years suggests that on an annual basis. the stream responds to precipitation events with relatively steady discharge levels. The R-B values generally have an inverse relationship with the drainage area so that the R-B index values increase as the drainage area decreases (Baker et al. 2004). A lower value on the R-B index scale is also associated with a greater stream capacity to respond to a high precipitation event with a lower magnitude of increases in discharge (Baker et al. 2004). The R-B index values for the Neebing River are all between 0.15 and 0.35 for 2008-2018 on a scale from zero to one, with one exception of 0.44 reached in 2012. This exceptional value is also the year of the greatest rain-flood event during the study period (see Appendix D for hydrographs). Overall, there tends to be only small interannual variability in R-B index values, as has been found in other analyses (Baker et al. 2004). The R-B index analysis demonstrates a level of stability in the Neebing River hydrological function to respond to precipitation events, which changes within the catchment could disrupt. Potential developments that cause large-scale increases in impermeable surfaces in the Neebing River catchment could change the stream's hydrologic function. The R-B index is one tool that could continue to be used to monitor the hydrologic function of the Neebing River's ability to respond to high-magnitude precipitation events.

## 6.3 Stable Isotope Analysis

The stable isotope analysis results show a clear seasonal distinction in the $\delta^{18}O$ and the $\delta^{2}H$ ratios. The distinct grouping of results by season could be improved with further sampling, especially during the winter season. The lower $\delta^{2}H$ against $\delta^{18}O$ ratio values measured during the spring season are likely caused by water storage as snow and ice. The spring measurements are significantly different from the other seasons. The winter samples were taken during the first week in December, before the start of the freeze-up. This likely contributes to the similarities seen in the $\delta^{2}H$ against $\delta^{18}O$ ratios calculated for the winter samples and those taken during the summer and fall seasons. The measurements from the summer and fall samples overlap to some extent, with most of the fall samples staying at the lower end of the $\delta^{2}H$ against $\delta^{18}O$ ratios observed during the summer.

**CHAPTER 7**

# 7 Summary and Recommendations

Further study of the groundwater contributions to the Neebing River is recommended. Additional trend analysis is also recommended once subsequent years of groundwater level data become available to have a minimum of ten years of data. The amount of groundwater level data is a study limitation that influences the groundwater level trend analysis, where at least ten years of continuous data is required. Another limitation of the study is the cell size when mapping the SGRAs. The conversion to raster data and a cell size of 15 m by 15 m is a relatively coarse resolution that is reasonably accurate but can lead to some misidentification potentially near the edges of the SGRAs. Additional isotopic sampling of precipitation and groundwater samples within the Neebing River watershed could help validate the quantification of the groundwater contribution. Stable isotope sampling during the winter season could show valuable insight into the changing conditions during the time when the Neebing River is covered by ice. Furthermore, groundwater mapping is recommended as groundwater and surface water do not have identical boundaries and can vary by location (Winter et al. 2003). Groundwater flow can go beyond the boundaries of a catchment area, and groundwater from beyond those boundaries can enter a catchment area (Winter et al. 2003). Groundwater watersheds are dynamic systems that can move in location over time, and groundwater sheds of different scales can be superimposed on one another (Winter et al. 2003). Ongoing study of the Neebing River will provide necessary information to better understand this contributary northern river.

This study provides an essential initial understanding of the trends seen in many important variables that describe the hydrological function of the Neebing River. Additionally, this study demonstrated some of the changes over time in the Neebing River. In particular, the trends in the hydrologic release variables show that the minimum values are increasing on an annual basis and during the winter season. Shifts in climatic conditions can further accelerate these trends, including potentially causing an earlier spring melt. Trends observed in this study may suggest this change as the minimum hydrologic release has begun to occur later in the spring season. These preliminary results provide a knowledge base for future comparisons to describe ongoing changes in the hydrological function of the Neebing River.

One key hydrologic function is the Neebing River's ability to respond to high-magnitude precipitation events. Strong rainfall caused the last flooding events in the catchment during a short time. Monitoring the hydrologic function through variables such as the R-B index for flashiness can help detect trends that could be induced by changing atmospheric conditions through climate change. It is expected that the frequency of the high magnitude events will increase due to climate change. This could be detected through continuous monitoring of Neebing River's hydrologic function.

The Neebing River is very reliant on groundwater contribution to streamflow. This is notable especially during the late summer season, which is associated with low precipitation, and during the winter season when ice cover prevents precipitation and runoff contributions to streamflow. Therefore, the Neebing River streamflow is also heavily dependent on SGRAs. The disruption of these areas through urbanization could impact the groundwater recharge capabilities and potentially decrease the overall

groundwater contribution to the Neebing River. This change in hydrologic function could lead to decreased water levels in the Neebing River, which could negatively impact the fish in the stream. Potential disruptions include the increase of impermeable surfaces, deforestation and urban sprawl. Currently, the headwaters of the Neebing River are not heavily developed, and the present state of limited development allows for adequate SGRAs to contribute enough groundwater for continuous streamflow.

References:


AquaResource Inc. 2012. Delineation of Significant Groundwater Recharge Areas: Supplemental Technical Guide.

Arciniega-Esparza, S., J. A. Breña-Naranjo, A. Pedrozo-Acuña, and C. M. Appendini. 2017. Hydrorecession: A Matlab toolbox for streamflow recession analysis. *Computers and Geosciences* 98. Elsevier Ltd: 87–92. doi: 10.1016/j.cageo.2016.10.005.

Arnold, J. G., and P. M. Allen. 1999. Automated methods for estimating baseflow and ground water recharge from streamflow records. *Journal of the American Water Resources Association* 35(2). American Water Resources Assoc: 411–424. doi: 10.1111/j.1752-1688.1999.tb03599.x.

Azarkhish, A., R. Rudra, P. Daggupati, J. Dhiman, T. Dickinson, and P. Goel. 2021. Investigation of Long-Term Climate and Streamflow Patterns in Ontario. *American Journal of Climate Change* 10(04). Scientific Research Publishing, Inc.: 467–489. doi: 10.4236/ajcc.2021.104024.

Baker, D. B., P. R. Richards, T. T. Loftus, and J. W. Kramer. 2004. A Flashiness Index: Characteristics and Application to Midwestern Rivers and Streams. *Journal of the American Water Resource Association*.

Barbier, E. B., M. Acreman, and D. Knowler. 1997. *Economic Valuation of Wetlands*.

Brinson, M. M. 1993. *Changes in the functioning of wetlands along environmental gradients*. *WETLANDS*. Vol. 13.

Brown, R. D., and R. O. Braaten. 1998. Spatial and temporal variability of Canadian monthly snow depths, 1946–1995. *Atmosphere - Ocean* 36(1): 37–54. doi: 10.1080/07055900.1998.9649605.

Cuddy, S., G. S. Chan, and R. Post. 2013. *Hydrogeological Assessment Submissions - Conservation Authority Guidelines for Development Applications*.

Danielescu, S., K. T. B. MacQuarrie, and A. Popa. 2018. SEPHYDRO: A Customizable Online Tool for Hydrograph Separation. *Groundwater* 56(4). Blackwell Publishing Ltd: 589–593. doi: 10.1111/gwat.12792.

Diro, G. T., W. J. Merryfield, H. Lin, W.-S. Lee, R. Muncaster, V. V Kharin, R. Parent, N. Swart, C. Seinen, D. Akingunola, V. Leung, M. Mansour, M. Chouak, X. Deng, G. Smith, and F. Lemay. 2024. *The Canadian Seasonal to Interannual Prediction System version 3.0 (CanSIPSv3.0)*.

Eckhardt, K. 2005. How to construct recursive digital filters for baseflow separation. *Hydrological Processes* 19: 507–515.

Eckhardt, K. 2008. A comparison of baseflow indices, which were calculated with seven different baseflow separation methods. *Journal of Hydrology* 352(1–2): 168–173. doi: 10.1016/j.jhydrol.2008.01.005.

Ferronsky, V. I., and V. A. Polyakov. 2012. *Isotopes of the Earth's Hydrosphere*. Dordrecht: Springer Netherlands. doi: 10.1007/978-94-007-2856-1.

Fleury, P., B. Ladouche, Y. Conroux, H. Jourde, and N. Dörfliger. 2009. Modelling the hydrologic functions of a karst aquifer under active water management - The Lez spring. *Journal of Hydrology* 365(3–4): 235–243. doi: 10.1016/j.jhydrol.2008.11.037.

Gao, B., K. Mckee, O. Gargiulo, and W. Graham. 2010. *Statistical Evaluation of Hydrologic Data in Northeastern Florida and Southern Georgia*.

Garrett, G. C., V. M. Vulava, T. J. Callahan, and M. L. Jones. 2012. Groundwater-surface water interactions in a lowland watershed: Source contribution to stream flow. *Hydrological Processes* 26(21): 3195–3206. doi: 10.1002/hyp.8257.

Gartner Lee Limited. 2008. *Source Protection Planning Lakehead Source Protection Area – Water Budget and Water Quantity Stress Assessment*.

Hogg, E. H. 1997. Temporal scaling of moisture and the forest-grassland boundary in western Canada. *Agricultural and Forest Meteorology* 84(1–2): 115–122. doi: 10.1016/S0168-1923(96)02380-5.

IAEA - Water Resources Programme. 2007. Sampling Procedures for Isotope Hydrology.

Integrative Watershed Research Center - Nipissing University. 2013. River Water Sampling for Stable Isotopes.

Jung, Y. Y., D. C. Koh, W. J. Shin, H. Il Kwon, Y. H. Oh, and K. S. Lee. 2021. Assessing seasonal variations in water sources of streamflow in a temperate mesoscale catchment with granitic bedrocks using hydrochemistry and stable isotopes. *Journal of Hydrology: Regional Studies* 38. Elsevier B.V. doi: 10.1016/j.ejrh.2021.100940.

Kalbus, E., F. Reinstorf, and M. Schirmer. 2006. Measuring methods for groundwater – surface water interactions: a review. *Hydrology and Earth System Sciences* 10(6): 873–887. doi: 10.5194/hess-10-873-2006.

Lakehead Region Conservation Authority. 2024. Neebing-McIntyre Floodway. https://lakeheadca.com/flood-protection/neebing-mcintyre-floodway. (Accessed August 29, 2024).

Lakehead Region Conservation Authority, and KGS Group. 2018. *Neebing River Floodplain Mapping Update Study General Report*.

Lister, M., B. Lofgren, F. Quinn, L. Wenger, N. Hoffman, L. Mortsch, S. Donner, K. Duncan, R. Kreutzwiser, S. Kulshreshtha, A. Piggott, S. Schellenberg, B. Schertzer, M. Slivitzky, H. Hengeveld, G. Koshida, N. Mayer, B. Mills, J. Smith, and P. Stokoe. 1999. *Climate change impacts on hydrology, water resources management and people of the Great Lakes - St. Lawrence system: a technical survey*.

Macdonald, H. M. 2014. *Lakehead Region Conservation Authority Final Report Neebing McIntyre Floodway Integrity Evaluation Study*.

May, H., S. Rixon, S. Gardner, P. Goel, J. Levison, and A. Binns. 2023. Investigating relationships between climate controls and nutrient flux in surface waters, sediments, and subsurface pathways in an agricultural clay catchment of the Great Lakes Basin. *Science of the Total Environment* 864. Elsevier B.V. doi: 10.1016/j.scitotenv.2022.160979.

McLaughlin, D. L., and M. J. Cohen. 2013. Realizing ecosystem services: Wetland hydrologic function along a gradient of ecosystem condition. *Ecological Applications* 23(7): 1619–1631. doi: 10.1890/12-1489.1.

Merryfield, W. J., W. S. Lee, G. J. Boer, V. V. Kharin, J. F. Scinocca, G. M. Flato, R. S. Ajayamohan, J. C. Fyfe, Y. Tang, and S. Polavarapu. 2013. The Canadian seasonal to interannual prediction system. part I: Models and initialization. *Monthly Weather Review* 141(8): 2910–2945. doi: 10.1175/MWR-D-12-00216.1.

Mills, A., and R. Post. 2018. Hydrologic Function: Framework Considerations and Approach to Subwatershed Baseline Characterization(June).

Montgomery, K. 2023. *Evaluating source water contributions to streamflow in a mixed landuse Precambrian Shield watershed in the Sudbury region*.

Neff, B. P., S. M. Day, A. R. Piggott, and L. M. Fuller. 2005. *Base Flow in the Great Lakes Basin: U.S. Geological Survey Scientific Investigations Report 2005-5217*.

Niagara Conservation Authority, and AquaResource Inc. 2009. *Significant Groundwater Recharge Area Delineation Niagara Peninsula Source Protection Area*. Welland, ON.

Ontario Ministry of Environment and Energy. 1995. *MOEE Hydrological Technical Information Requirements for Land Development Application*.

Ontario Ministry of Natural Resources. 2022. Ontario GeoHub. https://geohub.lio.gov.on.ca/. (Accessed February 2, 2022).

Ontario Ministry of Natural Resources and Forestry - Provincial Mapping Unit. 2023. Ontario Flow Assessment Tool. July 5.

Ontario Ministry of the Environment. 2003. *Stormwater Management Planning and Design Manual*.

Ontario Ministry of the Environment, C. and P. 2013. 2013 Technical rules under the Clean Water Act.

Persaud, E., J. Levison, S. MacRitchie, S. J. Berg, A. R. Erler, B. Parker, and E. Sudicky. 2020. Integrated modelling to assess climate change impacts on groundwater and surface water in the Great Lakes Basin using diverse climate forcing. *Journal of Hydrology* 584. Elsevier B.V. doi: 10.1016/j.jhydrol.2020.124682.

Philip, E., R. P. Rudra, P. K. Goel, and S. I. Ahmed. 2022. Investigation of the Long-Term Trends in the Streamflow Due to Climate Change and Urbanization for a Great Lakes Watershed. *Atmosphere* 13(2). MDPI. doi: 10.3390/atmos13020225.

Piggott, A. R., S. Moin, and C. Southam. 2005. A revised approach to the UKIH method for the calculation of baseflow. *Hydrological Sciences Journal* 50(5): 911–920. doi: 10.1623/hysj.2005.50.5.911.

Rohli, R. V. ;, and A. J. Vega. 2018. *Climatology*. fourth. Burlington, MA: Jones & Bartlett Learning.

Rutledge, A. T. 1998. *Computer programs for describing the recession of ground-water discharge and for estimating mean ground-water recharge and discharge form streamflow data – update: U.S. Geological Survey Water-Resources Investigations Report 98-4148*.

Saunders, G. 2022. Personal correspondence.

Searcy, J. K., C. H. Hardison, and W. B. Langbein. 1960. *Double-Mass Curves With a section Fitting Curves to Cyclic Data Manual of Hydrology: Part 1. General Surface-Water Techniques*.

Sloto, R. A., and M. Y. Crouse. 1996. *HYSEP: A computer program for streamflow hydrograph separation and analysis: U.S. Geological Survey Water-Resources Investigations Report 96-4040*.

Tarigan, S. D. 2016. Modeling effectiveness of management practices for flood mitigation using GIS spatial analysis functions in Upper Cilliwung watershed. In *IOP Conference Series: Earth and Environmental Science*. Vol. 31. Institute of Physics Publishing. doi: 10.1088/1755-1315/31/1/012030.

Taylor, C. H., and D. M. Roth. 1979. Effects of suburban construction on runoff contributing zones in a small southern Ontario drainage basin. *Hydrological Sciences Bulletin* 24(3): 289–301. doi: 10.1080/02626667909491868.

Thornthwaite, C. W. 1948. An approach toward a rational classification of climate. *The Geographical Review* 38: 55–89.

Wagener, T., M. Sivapalan, P. Troch, and R. Woods. 2007. Catchment Classification and Hydrologic Similarity. *Geography Compass* 4: 901–931.

White, W. N. 1932. *A method of estimating ground-water supplies based on discharge by plants and evaporation from soil-results of investigation in Escalante Valley, Utah*. U.S. Geological Survey.

Winter, T. C., D. O. Rosenberry, and J. W. Labaugh. 2003. Where Does the Ground Water in Small Watersheds Come From? *Ground Water* 41(7): 989–1000. doi: 10.1111/j.1745-6584.2003.tb02440.x.

Xie, J., X. Liu, K. Wang, T. Yang, K. Liang, and C. Liu. 2020. Evaluation of typical methods for baseflow separation in the contiguous United States. *Journal of Hydrology* 583. Elsevier B.V. doi: 10.1016/j.jhydrol.2020.124628.

Appendix A – Parameter Codes and Lables

| Parameter Code | Variable |
|---|---|
| Year | Year |
| Mean T | Mean Annual Temperature (°C) |
| 7d MAX T | Maximum of 7-day averaged Temperature (°C) |
| 7d MIN T | Minimum of 7-day averaged Temperature (°C) |
| Total P | Total annual Precipitation (mm) |
| Total R | Total annual Hydrologic Release (mm) |
| 3d MAX R | Maximum of 3-day total Hydrologic Release (mm) |
| 30d MIN R | Minimum of 30-day total Hydrologic Release (mm) |
| PET | Annual Potential Evapotranspiration (mm) |
| CMI (P-PET) | Climate Moisture Index (precipitation minus potential evapotranspiration; mm) |
| RBI | Richards-Baker Flashiness Index |
| 10:90 exceed | 10:90 Exceedance Percentile Ratio |
| Water yield | Water Yield of Streamflow (mm) |
| 3d MAX Q | Maximum of 3-day averaged Streamflow discharge (m3/s) |
| 7d MIN Q | Minimum of 7-day averaged Streamflow discharge (m3/s) |
| BF yield | Water Yield of Baseflow (mm) |
| 3d MAX BF | Maximum of 3-day averaged baseflow discharge (m3/s) |
| 7d MIN BF | Minimum of 7-day averaged baseflow discharge (m3/s) |
| Mean GW | Mean annual Groundwater Elevation (masl) |
| 3d MAX GW | Maximum of 3-day averaged Groundwater Elevation (masl) |
| 7d MIN GW | Minimum of 7-day averaged Groundwater Elevation (masl) |
| - DOY | Suffix: day of year timing |
| - Win | Suffix: Winter seasonal analysis (Dec, Jan Feb) |
| - Spr | Suffix: Spring seasonal analysis (Mar, Apr, May) |
| - Sum | Suffix: Summer seasonal analysis (Jun, Jul, Aug) |
| - Fal | Suffix: Fall seasonal analysis (Sep, Oct, Nov) |

## Appendix B – Spearman's Rank and Kendall's Rank Analysis Results

## Annual Spearman's Rank and Kendall's Rank Analysis Results

The correlation coefficient is above and the p-value below the diagonal.

### Annual Spearman's Rank

| Annual Spearman's rho | MEAN T | 7d MAX T - DOY | 7d MAX T | 7d MIN T - DOY | 7d MIN T | Total P | Total R | 3d MAX R - DOY | 3d MAX R | 30d MIN R - DOY | 30d MIN R | PET | CMI (P-PET) | RBI | 10:90 exceed | water yield | 3d MAX Q - DOY | 3d MAX Q | 7d MIN Q - DOY | 7d MIN Q | BF yield | 3d MAX BF - DOY | 3d MAX BF | 7d MIN BF - DOY | 7d MIN BF | Mean GW | 3d MAX GW - DOY | 3d MAX GW | 7d MIN GW - DOY | 7d MIN GW |
|---|---|---|---|---|---|---|---|---|---|---|---|---|---|---|---|---|---|---|---|---|---|---|---|---|---|---|---|---|---|---|
| **Mean T** | 1.000 | -0.073 | 0.491 | 0.142 | .661* | 0.406 | 0.406 | 0.442 | 0.358 | -0.248 | 0.127 | .952** | 0.018 | 0.103 | -.673* | -0.467 | -0.358 | -0.152 | 0.382 | -0.115 | -0.503 | -0.321 | -0.382 | 0.370 | -0.061 | -0.371 | 0.714 | -.829* | 0.200 | 0.600 |
| | | | | | | | | | | | | | | | | | | | | | | | | | | | | | | |
| **7d MAX T - DOY** | 0.841 | 1.000 | 0.091 | 0.364 | -0.340 | 0.255 | 0.237 | -0.085 | 0.298 | -.863** | 0.292 | -0.049 | 0.292 | 0.024 | 0.243 | -0.036 | 0.012 | -0.249 | -0.492 | -0.231 | -0.049 | -0.049 | -0.401 | -0.444 | -0.256 | 0.143 | -0.314 | 0.200 | -0.314 | -0.086 |
| | | | | | | | | | | | | | | | | | | | | | | | | | | | | | | |
| **7d MAX T** | 0.150 | 0.802 | 1.000 | 0.295 | 0.418 | 0.236 | 0.127 | 0.212 | 0.394 | -0.188 | 0.467 | 0.442 | 0.055 | 0.285 | -0.358 | -0.370 | -0.455 | 0.224 | 0.455 | 0.309 | 0.394 | -0.333 | -0.285 | 0.442 | -0.255 | -0.143 | 0.771 | -0.143 | -0.314 | 0.257 |
| | | | | | | | | | | | | | | | | | | | | | | | | | | | | | | |
| **7d MIN T - DOY** | 0.696 | 0.301 | 0.407 | 1.000 | -0.302 | .665* | .640* | 0.080 | 0.148 | -0.382 | .695* | 0.043 | .775** | 0.166 | -0.135 | 0.258 | 0.006 | -0.062 | -0.098 | 0.302 | 0.295 | 0.098 | -0.302 | 0.092 | 0.296 | 0.429 | -0.371 | -0.371 | -0.429 | 0.714 |
| | | | | | | | | | | | | | | | | | | | | | | | | | | | | | | |
| **7d MIN T** | 0.038 | 0.336 | 0.229 | 0.397 | 1.000 | 0.030 | -0.006 | 0.297 | 0.370 | 0.042 | -0.297 | 0.624 | -0.188 | 0.188 | -0.527 | -0.261 | -0.115 | 0.273 | 0.552 | -0.018 | 0.333 | -0.018 | -0.018 | 0.430 | 0.030 | -0.257 | .829* | -0.486 | -0.029 | 0.486 |
| | | | | | | | | | | | | | | | | | | | | | | | | | | | | | | |
| **Total P** | 0.244 | 0.476 | 0.511 | 0.036 | 0.934 | 1.000 | .964** | -0.055 | .661* | -0.285 | 0.612 | 0.309 | .867** | 0.624 | -0.176 | 0.455 | 0.139 | 0.309 | -0.176 | 0.491 | 0.406 | 0.358 | 0.055 | -0.006 | 0.517 | 0.371 | 0.257 | -0.486 | -0.486 | .943** |
| | | | | | | | | | | | | | | | | | | | | | | | | | | | | | | |
| **Total R** | 0.244 | 0.510 | 0.726 | 0.046 | 0.987 | 0.000 | 1.000 | -0.212 | 0.600 | -0.236 | 0.612 | 0.285 | .794** | 0.564 | -0.091 | 0.455 | 0.309 | 0.273 | -0.261 | 0.455 | 0.406 | 0.455 | 0.139 | -0.067 | 0.444 | 0.200 | 0.086 | -0.714 | -0.143 | .943** |
| | | | | | | | | | | | | | | | | | | | | | | | | | | | | | | |
| **3d MAX R - DOY** | 0.200 | 0.815 | 0.556 | 0.826 | 0.405 | 0.881 | 0.556 | 1.000 | -0.273 | -0.200 | -0.176 | 0.515 | -0.042 | -0.430 | -.818** | -0.418 | -.842** | -0.552 | 0.600 | 0.079 | -0.333 | -.745* | -.745* | 0.515 | 0.176 | 0.429 | -0.143 | -0.143 | -0.429 | 0.486 |
| | | | | | | | | | | | | | | | | | | | | | | | | | | | | | | |
| **3d MAX R** | 0.310 | 0.403 | 0.260 | 0.684 | 0.293 | 0.038 | 0.067 | 0.446 | 1.000 | -0.370 | 0.236 | 0.309 | 0.467 | .879** | 0.164 | 0.176 | 0.248 | .648* | -0.297 | 0.018 | 0.018 | 0.418 | 0.248 | -0.297 | 0.079 | -0.600 | 1.000** | -0.371 | 0.257 | 0.029 |
| | | | | | | | | | | | | | | | | | | | | | | | | | | | | | | |
| **30d MIN R - DOY** | 0.489 | 0.001 | 0.603 | 0.277 | 0.907 | 0.425 | 0.511 | 0.580 | 0.293 | 1.000 | -0.042 | -0.333 | -0.261 | -0.079 | -0.006 | 0.212 | 0.139 | 0.345 | 0.273 | 0.333 | 0.273 | 0.200 | .648* | 0.273 | 0.304 | 0.143 | -0.086 | 0.200 | 0.143 | -0.086 |
| | | | | | | | | | | | | | | | | | | | | | | | | | | | | | | |
| **30d MIN R** | 0.726 | 0.413 | 0.174 | 0.026 | 0.405 | 0.060 | 0.060 | 0.627 | 0.511 | 0.907 | 1.000 | -0.067 | 0.552 | 0.200 | -0.055 | 0.152 | -0.030 | 0.176 | -0.152 | 0.248 | 0.224 | 0.091 | 0.067 | 0.030 | 0.213 | 0.543 | -0.257 | -0.029 | -0.657 | 0.600 |
| | | | | | | | | | | | | | | | | | | | | | | | | | | | | | | |
| **PET** | 0.000 | 0.894 | 0.200 | 0.906 | 0.054 | 0.385 | 0.425 | 0.128 | 0.385 | 0.347 | 0.855 | 1.000 | -0.079 | 0.091 | -.661* | -0.491 | -0.455 | -0.261 | 0.442 | -0.248 | -0.552 | -0.442 | -0.515 | 0.406 | -0.176 | -0.314 | 0.600 | -0.771 | 0.257 | 0.543 |
| | | | | | | | | | | | | | | | | | | | | | | | | | | | | | | |
| **CMI ( P-PET)** | 0.960 | 0.413 | 0.881 | 0.008 | 0.603 | 0.001 | 0.006 | 0.907 | 0.174 | 0.467 | 0.098 | 0.829 | 1.000 | 0.515 | -0.030 | .661* | 0.224 | 0.321 | -0.261 | .673* | .648* | 0.467 | 0.079 | -0.091 | .693* | 0.543 | -0.029 | -0.200 | -0.714 | 0.771 |
| | | | | | | | | | | | | | | | | | | | | | | | | | | | | | | |
| **RBI** | 0.777 | 0.947 | 0.425 | 0.646 | 0.603 | 0.054 | 0.090 | 0.214 | 0.001 | 0.829 | 0.580 | 0.803 | 0.128 | 1.000 | 0.321 | 0.430 | 0.370 | .806** | -0.261 | 0.115 | 0.261 | 0.564 | 0.455 | -0.224 | 0.176 | -0.486 | .943** | -0.143 | 0.200 | -0.086 |
| | | | | | | | | | | | | | | | | | | | | | | | | | | | | | | |
| **10:90 exceed** | 0.033 | 0.498 | 0.310 | 0.709 | 0.117 | 0.627 | 0.803 | 0.004 | 0.651 | 0.987 | 0.887 | 0.038 | 0.934 | 0.365 | 1.000 | 0.248 | .661* | 0.370 | -.794** | -0.261 | 0.164 | 0.527 | 0.539 | -.794** | -0.304 | -0.429 | -0.143 | 0.429 | 0.429 | -.886* |
| | | | | | | | | | | | | | | | | | | | | | | | | | | | | | | |
| **Water yield** | 0.174 | 0.920 | 0.293 | 0.471 | 0.467 | 0.187 | 0.187 | 0.229 | 0.627 | 0.556 | 0.676 | 0.150 | 0.038 | 0.214 | 0.489 | 1.000 | 0.576 | 0.479 | -0.200 | .733* | .976** | .758* | 0.515 | -0.042 | .687* | .886* | -0.600 | 0.543 | -0.657 | 0.257 |

| | | | | | | | | | | | | | | | | | | | | | | | | | | | | | | |
|---|---|---|---|---|---|---|---|---|---|---|---|---|---|---|---|---|---|---|---|---|---|---|---|---|---|---|---|---|---|---|
| **3d MAX Q - DOY** | 0.310 | 0.973 | 0.187 | 0.987 | 0.751 | 0.701 | 0.385 | 0.002 | 0.489 | 0.701 | 0.934 | 0.187 | 0.533 | 0.293 | 0.038 | 0.082 | 1.000 | 0.503 | -0.576 | 0.224 | 0.491 | .927** | .709* | -0.491 | 0.128 | -0.429 | 0.200 | -0.257 | 0.486 | -0.086 |
| **3d MAX Q** | 0.676 | 0.487 | 0.533 | 0.866 | 0.446 | 0.385 | 0.446 | 0.098 | 0.043 | 0.328 | 0.627 | 0.467 | 0.365 | 0.005 | 0.293 | 0.162 | 0.138 | 1.000 | -0.164 | 0.273 | 0.370 | .709* | .782** | -0.164 | 0.292 | -0.371 | 0.771 | -0.029 | 0.143 | -0.086 |
| **7d MIN Q - DOY** | 0.276 | 0.148 | 0.187 | 0.787 | 0.098 | 0.627 | 0.467 | 0.067 | 0.405 | 0.446 | 0.676 | 0.200 | 0.467 | 0.467 | 0.006 | 0.580 | 0.082 | 0.651 | 1.000 | 0.030 | -0.152 | -0.479 | -0.370 | .964** | 0.061 | 0.600 | 0.143 | -0.029 | -0.600 | 0.714 |
| **7d MIN Q** | 0.751 | 0.521 | 0.385 | 0.397 | 0.960 | 0.150 | 0.187 | 0.829 | 0.960 | 0.347 | 0.489 | 0.489 | 0.033 | 0.751 | 0.467 | 0.016 | 0.533 | 0.446 | 0.934 | 1.000 | .806** | 0.479 | 0.345 | 0.152 | .985** | .829* | -0.314 | 0.200 | -0.657 | 0.600 |
| **BF yield** | 0.138 | 0.894 | 0.260 | 0.407 | 0.347 | 0.244 | 0.244 | 0.347 | 0.960 | 0.446 | 0.533 | 0.098 | 0.043 | 0.467 | 0.651 | 0.000 | 0.150 | 0.293 | 0.676 | 0.005 | 1.000 | .673* | 0.467 | 0.018 | .748* | .886* | -0.600 | 0.543 | -0.657 | 0.257 |
| **3d MAX BF - DOY** | 0.365 | 0.894 | 0.347 | 0.787 | 0.960 | 0.310 | 0.187 | 0.013 | 0.229 | 0.580 | 0.803 | 0.200 | 0.174 | 0.090 | 0.117 | 0.011 | 0.000 | 0.022 | 0.162 | 0.162 | 0.033 | 1.000 | .782** | -0.382 | 0.413 | -0.257 | 0.314 | -0.143 | 0.257 | 0.029 |
| **3d MAX BF** | 0.276 | 0.250 | 0.425 | 0.397 | 0.960 | 0.881 | 0.701 | 0.013 | 0.489 | 0.043 | 0.855 | 0.128 | 0.829 | 0.187 | 0.108 | 0.128 | 0.022 | 0.008 | 0.293 | 0.328 | 0.174 | 0.008 | 1.000 | -0.345 | 0.298 | -0.314 | 0.257 | 0.086 | 0.429 | -0.314 |
| **7d MIN BF - DOY** | 0.293 | 0.199 | 0.200 | 0.800 | 0.214 | 0.987 | 0.855 | 0.128 | 0.405 | 0.446 | 0.934 | 0.244 | 0.803 | 0.533 | 0.006 | 0.907 | 0.150 | 0.651 | 0.000 | 0.676 | 0.960 | 0.276 | 0.328 | 1.000 | 0.158 | 0.600 | 0.143 | -0.029 | -0.600 | 0.714 |
| **7d MIN BF** | 0.868 | 0.475 | 0.476 | 0.406 | 0.934 | 0.126 | 0.199 | 0.626 | 0.828 | 0.393 | 0.555 | 0.626 | 0.026 | 0.626 | 0.393 | 0.028 | 0.725 | 0.413 | 0.868 | 0.000 | 0.013 | 0.235 | 0.403 | 0.663 | 1.000 | 0.754 | -0.116 | 0.174 | -0.667 | 0.580 |
| **Mean GW** | 0.468 | 0.787 | 0.787 | 0.397 | 0.623 | 0.468 | 0.704 | 0.397 | 0.208 | 0.787 | 0.266 | 0.544 | 0.266 | 0.329 | 0.397 | 0.019 | 0.397 | 0.468 | 0.208 | 0.042 | 0.019 | 0.623 | 0.544 | 0.208 | 0.084 | 1.000 | -0.607 | 0.321 | -.821* | 0.607 |
| **3d MAX GW - DOY** | 0.111 | 0.544 | 0.072 | 0.468 | 0.042 | 0.623 | 0.872 | 0.787 | | 0.872 | 0.623 | 0.208 | 0.957 | 0.005 | 0.787 | 0.208 | 0.704 | 0.072 | 0.787 | 0.544 | 0.208 | 0.544 | 0.623 | 0.787 | 0.827 | 0.148 | 1.000 | -0.143 | 0.214 | -0.357 |
| **3d MAX GW** | 0.042 | 0.704 | 0.787 | 0.468 | 0.329 | 0.329 | 0.111 | 0.787 | 0.468 | 0.704 | 0.957 | 0.072 | 0.704 | 0.787 | 0.397 | 0.266 | 0.623 | 0.957 | 0.957 | 0.704 | 0.266 | 0.787 | 0.872 | 0.957 | 0.742 | 0.482 | 0.760 | 1.000 | -0.643 | -0.536 |
| **7d MIN GW - DOY** | 0.704 | 0.544 | 0.544 | 0.397 | 0.957 | 0.329 | 0.787 | 0.397 | 0.623 | 0.787 | 0.156 | 0.623 | 0.111 | 0.704 | 0.397 | 0.156 | 0.329 | 0.787 | 0.208 | 0.156 | 0.156 | 0.623 | 0.397 | 0.208 | 0.148 | 0.023 | 0.645 | 0.119 | 1.000 | -0.250 |
| **7d MIN GW** | 0.208 | 0.872 | 0.623 | 0.111 | 0.329 | 0.005 | 0.005 | 0.329 | 0.957 | 0.872 | 0.208 | 0.266 | 0.072 | 0.872 | 0.019 | 0.623 | 0.872 | 0.872 | 0.111 | 0.208 | 0.623 | 0.957 | 0.544 | 0.111 | 0.228 | 0.148 | 0.432 | 0.215 | 0.589 | 1.000 |

*. Correlation is significant at the 0.05 level (2-tailed).

**. Correlation is significant at the 0.01 level (2-tailed).

## Annual Kendall's Rank

| Annual Kendall's tau_b | MEAN T | 7d MAX T - DOY | 7d MAX T | 7d MIN T - DOY | 7d MIN T | Total P | Total R | 3d MAX R - DOY | 3d MAX R | 30d MIN R - DOY | 30d MIN R | PET | CMI (P-PET) | RBI | 10:90 exceed | water yield | 3d MAX Q - DOY | 3d MAX Q | 7d MIN Q - DOY | 7d MIN Q | BF yield | 3d MAX BF - DOY | 3d MAX BF | 7d MIN BF - DOY | 7d MIN BF | Mean GW | 3d MAX GW - DOY | 3d MAX GW | 7d MIN GW - DOY | 7d MIN GW |
|---|---|---|---|---|---|---|---|---|---|---|---|---|---|---|---|---|---|---|---|---|---|---|---|---|---|---|---|---|---|---|
| **Mean T** | 1.000 | -0.045 | 0.467 | 0.116 | .511* | 0.333 | 0.333 | 0.378 | 0.289 | -0.200 | 0.111 | .822** | 0.022 | 0.111 | -.511* | -0.378 | -0.289 | -0.244 | 0.244 | -0.022 | -0.378 | -0.244 | -0.422 | 0.244 | 0.045 | -0.333 | 0.600 | -.733* | 0.067 | 0.467 |
| **7d MAX T - DOY** | 0.857 | 1.000 | 0.135 | 0.283 | -0.225 | 0.180 | 0.180 | -0.045 | 0.270 | -.719** | 0.225 | -0.045 | 0.135 | 0.000 | 0.180 | 0.045 | 0.045 | -0.180 | -0.360 | -0.090 | 0.000 | 0.000 | -0.270 | -0.360 | -0.159 | 0.200 | -0.200 | 0.067 | -0.200 | -0.067 |
| **7d MAX T** | 0.060 | 0.590 | 1.000 | 0.256 | 0.333 | 0.156 | 0.067 | 0.200 | 0.289 | -0.111 | 0.289 | 0.378 | 0.022 | 0.200 | -0.333 | -0.200 | -0.378 | 0.022 | 0.333 | -0.200 | -0.200 | -0.244 | -0.244 | 0.333 | -0.180 | -0.067 | 0.600 | -0.200 | -0.200 | 0.200 |
| **7d MIN T - DOY** | 0.649 | 0.272 | 0.316 | 1.000 | -0.256 | 0.489 | 0.489 | 0.023 | 0.070 | -0.303 | .535* | 0.023 | .629* | 0.070 | -0.070 | 0.210 | 0.023 | -0.070 | -0.116 | 0.210 | 0.210 | 0.070 | -0.256 | -0.023 | 0.188 | 0.333 | -0.333 | -0.333 | -0.333 | 0.600 |
| **7d MIN T** | 0.040 | 0.369 | 0.180 | 0.316 | 1.000 | 0.022 | 0.022 | 0.244 | 0.244 | -0.200 | 0.022 | 0.422 | -0.111 | 0.156 | -0.378 | -0.156 | -0.067 | -0.244 | 0.378 | -0.022 | -0.244 | -0.022 | -0.022 | 0.289 | 0.045 | -0.200 | .733* | -0.333 | -0.067 | 0.333 |

| | | | | | | | | | | | | | | | | | | | | | | | | | | | | | | |
|---|---|---|---|---|---|---|---|---|---|---|---|---|---|---|---|---|---|---|---|---|---|---|---|---|---|---|---|---|---|---|
| **Total P** | 0.180 | 0.472 | 0.531 | 0.056 | 0.929 | 1.000 | .911** | -0.022 | .511* | -0.244 | 0.422 | 0.244 | .689** | .511* | -0.200 | 0.289 | 0.111 | 0.244 | -0.067 | 0.378 | 0.289 | 0.244 | -0.022 | 0.022 | 0.449 | 0.067 | 0.200 | -0.333 | -0.333 | .867* |
| **Total R** | 0.180 | 0.472 | 0.788 | 0.056 | 0.929 | 0.000 | 1.000 | -0.111 | .511* | -0.156 | 0.422 | 0.244 | .600* | .511* | -0.111 | 0.289 | 0.200 | 0.244 | -0.156 | 0.378 | 0.289 | 0.333 | 0.067 | -0.067 | 0.360 | 0.067 | 0.200 | -0.600 | -0.067 | .867* |
| **3d MAX R - DOY** | 0.128 | 0.857 | 0.421 | 0.927 | 0.325 | 0.929 | 0.655 | 1.000 | -0.244 | -0.111 | -0.156 | 0.467 | -0.067 | -0.333 | -.689** | -0.289 | -.644** | -0.422 | .511* | 0.156 | -0.200 | -.511* | -.600* | 0.422 | 0.225 | 0.333 | -0.067 | -0.067 | -0.333 | 0.333 |
| **3d MAX R** | 0.245 | 0.281 | 0.245 | 0.784 | 0.325 | 0.040 | 0.040 | 0.325 | 1.000 | -0.200 | 0.111 | 0.200 | 0.289 | .733** | 0.111 | 0.067 | 0.156 | 0.467 | -0.200 | 0.067 | -0.022 | 0.289 | 0.200 | -0.200 | 0.090 | -0.467 | 1.000** | -0.333 | 0.200 | 0.067 |
| **30d MIN R - DOY** | 0.421 | 0.004 | 0.655 | 0.236 | 0.929 | 0.325 | 0.531 | 0.655 | 0.421 | 1.000 | -0.111 | -0.200 | -0.200 | -0.022 | 0.067 | 0.111 | 0.022 | 0.244 | 0.200 | 0.289 | 0.200 | 0.067 | 0.422 | 0.200 | 0.225 | 0.200 | 0.067 | 0.067 | 0.067 | -0.067 |
| **30d MIN R** | 0.655 | 0.369 | 0.245 | 0.036 | 0.421 | 0.089 | 0.089 | 0.531 | 0.655 | 0.655 | 1.000 | -0.067 | 0.467 | 0.111 | 0.022 | 0.156 | -0.022 | 0.111 | -0.111 | 0.156 | 0.156 | 0.111 | 0.111 | -0.022 | 0.090 | 0.467 | -0.200 | 0.067 | -0.467 | 0.467 |
| **PET** | 0.001 | 0.857 | 0.128 | 0.927 | 0.089 | 0.325 | 0.325 | 0.060 | 0.421 | 0.421 | 0.788 | 1.000 | -0.067 | 0.111 | -.511* | -0.378 | -0.378 | -0.244 | 0.333 | -0.111 | 0.378 | -0.333 | -.511* | 0.333 | -0.045 | -0.200 | 0.467 | -0.600 | 0.200 | 0.333 |
| **CMI ( P-PET)** | 0.929 | 0.590 | 0.929 | 0.014 | 0.655 | 0.006 | 0.016 | 0.788 | 0.245 | 0.421 | 0.060 | 0.788 | 1.000 | 0.378 | 0.022 | .511* | 0.244 | 0.289 | -0.200 | 0.422 | .511* | 0.378 | 0.022 | -0.111 | .494* | 0.333 | -0.067 | -0.067 | -0.600 | 0.600 |
| **RBI** | 0.655 | 1.000 | 0.421 | 0.784 | 0.531 | 0.040 | 0.040 | 0.180 | 0.003 | 0.929 | 0.655 | 0.655 | 0.128 | 1.000 | 0.289 | 0.244 | 0.333 | .644** | -0.111 | 0.156 | 0.156 | 0.467 | 0.289 | -0.022 | 0.180 | -0.333 | .867* | -0.200 | 0.067 | -0.067 |
| **10:90 exceed** | 0.040 | 0.472 | 0.180 | 0.784 | 0.128 | 0.421 | 0.655 | 0.006 | 0.655 | 0.788 | 0.929 | 0.040 | 0.929 | 0.245 | 1.000 | 0.156 | .511* | 0.289 | -.644** | -0.200 | 0.067 | 0.378 | 0.378 | -.644** | -0.270 | -0.200 | -0.067 | 0.200 | 0.200 | -.733* |
| **Water yield** | 0.128 | 0.857 | 0.421 | 0.412 | 0.531 | 0.245 | 0.245 | 0.245 | 0.788 | 0.655 | 0.531 | 0.128 | 0.040 | 0.325 | 0.531 | 1.000 | 0.467 | 0.333 | -0.156 | .556* | .911** | .600* | 0.422 | -0.067 | .494* | .733* | -0.467 | 0.333 | -0.467 | 0.200 |
| **3d MAX Q - DOY** | 0.245 | 0.857 | 0.128 | 0.927 | 0.784 | 0.655 | 0.421 | 0.009 | 0.531 | 0.929 | 0.929 | 0.128 | 0.325 | 0.180 | 0.040 | 0.060 | 1.000 | 0.422 | -0.422 | 0.200 | 0.378 | .867** | .511* | -0.333 | 0.135 | -0.333 | 0.067 | -0.200 | 0.333 | -0.067 |
| **3d MAX Q** | 0.325 | 0.472 | 0.929 | 0.784 | 0.325 | 0.325 | 0.325 | 0.089 | 0.060 | 0.325 | 0.655 | 0.325 | 0.245 | 0.009 | 0.245 | 0.180 | 0.089 | 1.000 | -0.111 | 0.156 | 0.244 | .556* | .644** | -0.111 | 0.180 | -0.333 | 0.600 | 0.067 | 0.067 | -0.067 |
| **7d MIN Q - DOY** | 0.325 | 0.151 | 0.180 | 0.649 | 0.128 | 0.788 | 0.531 | 0.040 | 0.421 | 0.421 | 0.655 | 0.180 | 0.421 | 0.655 | 0.009 | 0.531 | 0.089 | 0.655 | 1.000 | 0.111 | -0.067 | -0.378 | -0.289 | .911** | 0.135 | 0.467 | 0.067 | 0.067 | -0.467 | 0.467 |
| **7d MIN Q** | -0.022 | -0.090 | -0.200 | 0.210 | 0.022 | 0.378 | 0.378 | 0.156 | 0.067 | 0.289 | 0.156 | -0.111 | 0.422 | 0.156 | -0.200 | .556* | 0.200 | 0.156 | 0.111 | 1.000 | .644** | 0.333 | 0.156 | 0.200 | .944** | .733* | -0.200 | 0.067 | -0.467 | 0.467 |
| **BF yield** | 0.128 | 1.000 | 0.421 | 0.412 | 0.325 | 0.245 | 0.245 | 0.421 | 0.929 | 0.421 | 0.531 | 0.128 | 0.040 | 0.531 | 0.788 | 0.000 | 0.128 | 0.325 | 0.788 | 0.009 | 1.000 | .511* | 0.333 | 0.022 | .584* | .733* | -0.467 | 0.333 | -0.467 | 0.200 |
| **3d MAX BF - DOY** | 0.325 | 1.000 | 0.325 | 0.784 | 0.929 | 0.325 | 0.180 | 0.040 | 0.245 | 0.788 | 0.655 | 0.180 | 0.128 | 0.060 | 0.128 | 0.016 | 0.000 | 0.025 | 0.128 | 0.180 | 0.040 | 1.000 | .644** | -0.289 | 0.270 | -0.200 | 0.200 | -0.067 | 0.200 | 0.067 |
| **3d MAX BF** | 0.089 | 0.281 | 0.325 | 0.316 | 0.929 | 0.929 | 0.788 | 0.016 | 0.421 | 0.089 | 0.655 | 0.040 | 0.929 | 0.245 | 0.128 | 0.089 | 0.040 | 0.009 | 0.245 | 0.531 | 0.180 | 0.009 | 1.000 | -0.289 | 0.090 | -0.200 | 0.200 | 0.200 | 0.467 | -0.200 |
| **7d MIN BF - DOY** | 0.325 | 0.151 | 0.180 | 0.927 | 0.245 | 0.929 | 0.788 | 0.089 | 0.421 | 0.421 | 0.929 | 0.180 | 0.655 | 0.929 | 0.009 | 0.788 | 0.180 | 0.655 | 0.000 | 0.421 | 0.929 | 0.245 | 0.245 | 1.000 | 0.225 | 0.467 | 0.067 | 0.067 | -0.467 | 0.467 |
| **7d MIN BF** | 0.857 | 0.528 | 0.472 | 0.464 | 0.857 | 0.072 | 0.151 | 0.369 | 0.719 | 0.369 | 0.719 | 0.857 | 0.048 | 0.472 | 0.281 | 0.048 | 0.590 | 0.472 | 0.590 | 0.000 | 0.020 | 0.281 | 0.719 | 0.369 | 1.000 | 0.552 | -0.138 | 0.138 | -0.552 | 0.414 |
| **Mean GW** | 0.348 | 0.573 | 0.851 | 0.348 | 0.573 | 0.851 | 0.851 | 0.348 | 0.188 | 0.573 | 0.188 | 0.573 | 0.348 | 0.348 | 0.573 | 0.039 | 0.348 | 0.348 | 0.188 | 0.039 | 0.039 | 0.573 | 0.573 | 0.188 | 0.126 | 1.000 | -0.524 | 0.238 | -0.619 | 0.333 |
| **3d MAX GW - DOY** | 0.091 | 0.573 | 0.091 | 0.348 | 0.039 | 0.573 | 0.573 | 0.851 | | 0.851 | 0.573 | 0.188 | 0.851 | 0.015 | 0.851 | 0.188 | 0.851 | 0.091 | 0.851 | 0.573 | 0.188 | 0.573 | 0.573 | 0.851 | 0.702 | 0.099 | 1.000 | -0.143 | 0.143 | -0.238 |
| **3d MAX GW** | 0.039 | 0.851 | 0.573 | 0.348 | 0.348 | 0.348 | 0.091 | 0.851 | 0.348 | 0.851 | 0.851 | 0.091 | 0.851 | 0.573 | 0.573 | 0.348 | 0.573 | 0.851 | 0.851 | 0.851 | 0.348 | 0.851 | 0.573 | 0.851 | 0.702 | 0.453 | 0.652 | 1.000 | -0.429 | -0.429 |

| | | | | | | | | | | | | | | | | | | | | | | | | | | | | | | | |
|---|---|---|---|---|---|---|---|---|---|---|---|---|---|---|---|---|---|---|---|---|---|---|---|---|---|---|---|---|---|---|---|
| **7d MIN GW - DOY** | 0.851 | 0.573 | 0.573 | 0.348 | 0.851 | 0.348 | 0.851 | 0.348 | 0.573 | 0.851 | 0.188 | 0.573 | 0.091 | 0.851 | 0.573 | 0.188 | 0.348 | 0.851 | 0.188 | 0.188 | 0.188 | 0.573 | 0.188 | 0.188 | 0.126 | 0.051 | 0.652 | 0.176 | 1.000 | -0.143 |
| **7d MIN GW** | 0.188 | 0.851 | 0.573 | 0.091 | 0.348 | 0.015 | 0.015 | 0.348 | 0.851 | 0.851 | 0.188 | 0.348 | 0.091 | 0.851 | 0.039 | 0.573 | 0.851 | 0.851 | 0.188 | 0.188 | 0.573 | 0.851 | 0.573 | 0.188 | 0.251 | 0.293 | 0.453 | 0.176 | 0.652 | 1.000 |

*. Correlation is significant at the 0.05 level (2-tailed).

**. Correlation is significant at the 0.01 level (2-tailed).

## Winter Spearman's Rank and Kendall's Rank Analysis

The correlation coefficient is above, and the p-value is below the diagonal.

### Winter Spearman's Rank Analysis

| Winter Spearman's rho | Mean T - Win | 7d MAX T - Win DOY | 7d MAX T - Win | 7d MIN T - Win DOY | 7d MIN T - Win | Total R - Win | 3d MAX R -Win DOY | 3d MAX R -Win | 30d MIN R - Win DOY | 30d MIN R - Win | Water yield - Win | 3d MAX R - Win DOY | 3d MAX R - Win | 7d MIN Q - Win DOY | 7d MIN Q - Win | BF yield - Win | 3d MAX BF - Win DOY | 3d MAX BF - Win | 7d MIN BF - Win DOY | 7d MIN BF - Win | 3d MAX GW - Win DOY | 3d MAX GW - Win | 7d MIN GW - Win DOY | 7d MIN GW - Win |
|---|---|---|---|---|---|---|---|---|---|---|---|---|---|---|---|---|---|---|---|---|---|---|---|---|
| **Mean T - Win** | 1.000 | -0.118 | 0.491 | -0.156 | .764** | 0.527 | -0.251 | 0.373 | -0.200 | 0.491 | 0.100 | 0.178 | 0.127 | 0.027 | 0.055 | 0.109 | 0.196 | 0.236 | -0.228 | 0.068 | 0.754 | 0.429 | 0.334 | 0.429 |
| **7d MAX T - Win DOY** | 0.729 | 1.000 | 0.519 | 0.187 | -0.519 | 0.419 | 0.315 | 0.396 | -0.260 | 0.360 | 0.100 | 0.445 | 0.109 | -.647* | -0.150 | 0.077 | 0.389 | 0.105 | -0.409 | -0.206 | -0.058 | -0.543 | 0.698 | -0.543 |
| **7d MAX T - Win** | 0.125 | 0.102 | 1.000 | 0.547 | 0.264 | 0.455 | 0.301 | 0.555 | -0.082 | .618* | 0.373 | 0.519 | 0.473 | -0.100 | 0.300 | 0.309 | 0.575 | 0.536 | -0.009 | 0.315 | 0.667 | 0.771 | 0.334 | 0.771 |
| **7d MIN T - Win DOY** | 0.646 | 0.583 | 0.082 | 1.000 | -0.074 | 0.055 | 0.383 | 0.064 | 0.267 | 0.285 | 0.570 | 0.506 | 0.584 | 0.409 | 0.579 | 0.515 | 0.582 | 0.464 | 0.548 | .621* | 0.290 | .829* | -0.030 | .829* |
| **7d MIN T - Win** | 0.006 | 0.102 | 0.433 | 0.830 | 1.000 | 0.345 | -0.150 | 0.282 | -0.137 | 0.127 | 0.182 | -0.042 | 0.200 | 0.336 | 0.191 | 0.200 | 0.070 | 0.373 | 0.059 | 0.247 | 0.580 | 0.543 | 0.030 | 0.543 |
| **Total R - Win** | 0.096 | 0.199 | 0.160 | 0.872 | 0.298 | 1.000 | 0.091 | 0.509 | -0.442 | 0.482 | 0.227 | 0.327 | 0.127 | -0.255 | -0.027 | 0.273 | 0.402 | 0.218 | -0.478 | -0.009 | 0.203 | 0.257 | 0.213 | 0.257 |
| **3d MAX R - Win DOY** | 0.457 | 0.345 | 0.369 | 0.246 | 0.659 | 0.790 | 1.000 | 0.041 | 0.265 | -0.059 | 0.036 | 0.089 | -0.041 | 0.068 | 0.278 | -0.027 | 0.108 | 0.041 | 0.032 | 0.236 | 0.261 | 0.257 | 0.638 | 0.257 |
| **3d MAX R - Win** | 0.259 | 0.228 | 0.077 | 0.851 | 0.401 | 0.110 | 0.905 | 1.000 | -0.323 | 0.345 | 0.136 | 0.458 | 0.273 | -0.155 | 0.036 | 0.164 | 0.514 | 0.418 | -0.155 | 0.032 | 0.377 | 0.486 | 0.516 | 0.486 |
| **30d MIN R - Win DOY** | 0.555 | 0.440 | 0.811 | 0.427 | 0.689 | 0.174 | 0.431 | 0.332 | 1.000 | -0.123 | -0.410 | -0.115 | -0.305 | 0.442 | -0.123 | -0.474 | -0.218 | -0.360 | 0.068 | -0.094 | -0.029 | -0.257 | 0.334 | -0.257 |
| **30d MIN R - Win** | 0.125 | 0.277 | 0.043 | 0.395 | 0.709 | 0.133 | 0.863 | 0.298 | 0.719 | 1.000 | 0.427 | .626* | 0.527 | 0.173 | 0.427 | 0.382 | .683* | 0.500 | 0.027 | 0.438 | 0.696 | 0.714 | -0.030 | 0.714 |
| **Water yield - Win** | 0.770 | 0.769 | 0.259 | 0.067 | 0.593 | 0.502 | 0.915 | 0.689 | 0.210 | 0.190 | 1.000 | .720* | .945** | 0.364 | .800** | .991** | .813** | .882** | .647* | .776** | 0.638 | 0.714 | -0.091 | 0.714 |
| **3d MAX R - Win DOY** | 0.601 | 0.170 | 0.102 | 0.112 | 0.902 | 0.326 | 0.795 | 0.156 | 0.737 | 0.039 | 0.012 | 1.000 | .767** | 0.229 | 0.514 | .706* | .962** | .706* | 0.319 | 0.451 | 1.000** | 0.290 | 0.647 | 0.290 |
| **3d MAX R - Win** | 0.709 | 0.749 | 0.142 | 0.059 | 0.555 | 0.709 | 0.905 | 0.417 | 0.361 | 0.096 | 0.000 | 0.006 | 1.000 | 0.409 | .782** | .918** | .860** | .955** | .674* | .772** | 0.580 | 0.771 | -0.213 | 0.771 |
| **7d MIN Q - Win DOY** | 0.937 | 0.031 | 0.770 | 0.211 | 0.312 | 0.450 | 0.842 | 0.650 | 0.174 | 0.612 | 0.272 | 0.498 | 0.212 | 1.000 | .673* | 0.336 | 0.304 | 0.355 | .729* | .708* | 0.551 | 0.771 | -0.152 | 0.771 |
| **7d MIN Q - Win** | 0.873 | 0.659 | 0.370 | 0.062 | 0.574 | 0.937 | 0.408 | 0.915 | 0.719 | 0.190 | 0.003 | 0.106 | 0.004 | 0.023 | 1.000 | .755** | .645* | .727* | .825** | .986** | 0.725 | 0.657 | 0.152 | 0.657 |
| **BF yield - Win** | 0.750 | 0.821 | 0.355 | 0.105 | 0.555 | 0.417 | 0.936 | 0.631 | 0.141 | 0.247 | 0.000 | 0.015 | 0.000 | 0.312 | 0.007 | 1.000 | .799** | .855** | .615* | .731* | 0.638 | 0.714 | -0.091 | 0.714 |
| **3d MAX BF - Win DOY** | 0.563 | 0.237 | 0.064 | 0.061 | 0.838 | 0.220 | 0.752 | 0.106 | 0.520 | 0.021 | 0.002 | 0.000 | 0.001 | 0.364 | 0.032 | 0.003 | 1.000 | .818** | 0.403 | .610* | .941** | 0.580 | 0.462 | 0.580 |
| **3d MAX BF - Win** | 0.484 | 0.759 | 0.089 | 0.150 | 0.259 | 0.519 | 0.905 | 0.201 | 0.277 | 0.117 | 0.000 | 0.015 | 0.000 | 0.285 | 0.011 | 0.001 | 0.002 | 1.000 | 0.560 | .717* | 0.638 | 0.714 | -0.091 | 0.714 |
| **7d MIN BF - Win DOY** | 0.501 | 0.212 | 0.979 | 0.081 | 0.863 | 0.137 | 0.926 | 0.649 | 0.841 | 0.936 | 0.031 | 0.340 | 0.023 | 0.011 | 0.002 | 0.044 | 0.219 | 0.073 | 1.000 | .824** | 0.551 | 0.771 | -0.152 | 0.771 |
| **7d MIN BF - Win** | 0.841 | 0.543 | 0.345 | 0.041 | 0.465 | 0.979 | 0.485 | 0.926 | 0.784 | 0.177 | 0.005 | 0.164 | 0.005 | 0.015 | 0.000 | 0.011 | 0.046 | 0.013 | 0.002 | 1.000 | 0.485 | .841* | -0.154 | .841* |
| **3d MAX GW - Win DOY** | 0.084 | 0.913 | 0.148 | 0.577 | 0.228 | 0.700 | 0.618 | 0.461 | 0.957 | 0.125 | 0.173 | | 0.228 | 0.257 | 0.103 | 0.173 | 0.005 | 0.173 | 0.257 | 0.329 | 1.000 | 0.290 | 0.647 | 0.290 |

| | | | | | | | | | | | | | | | | | | | | | | | | |
|---|---|---|---|---|---|---|---|---|---|---|---|---|---|---|---|---|---|---|---|---|---|---|---|---|
| **3d MAX GW - Win** | 0.397 | 0.266 | 0.072 | 0.042 | 0.266 | 0.623 | 0.623 | 0.329 | 0.623 | 0.111 | 0.111 | 0.577 | 0.072 | 0.072 | 0.156 | 0.111 | 0.228 | 0.111 | 0.072 | 0.036 | 0.577 | 1.000 | -0.213 | 1.000** |
| **7d MIN GW - Win DOY** | 0.518 | 0.123 | 0.518 | 0.954 | 0.954 | 0.686 | 0.173 | 0.295 | 0.518 | 0.954 | 0.864 | 0.165 | 0.686 | 0.774 | 0.774 | 0.864 | 0.356 | 0.864 | 0.774 | 0.771 | 0.165 | 0.686 | 1.000 | -0.213 |
| **7d MIN GW - Win** | 0.397 | 0.266 | 0.072 | 0.042 | 0.266 | 0.623 | 0.623 | 0.329 | 0.623 | 0.111 | 0.111 | 0.577 | 0.072 | 0.072 | 0.156 | 0.111 | 0.228 | 0.111 | 0.072 | 0.036 | 0.577 | | 0.686 | 1.000 |

**. Correlation is significant at the 0.01 level (2-tailed).

*. Correlation is significant at the 0.05 level (2-tailed).

## Winter Kendall's Rank Analysis

| **Winter Kendall's tau_b** | **Mean T - Win** | **7d MAX T - Win DOY** | **7d MAX T - Win** | **7d MIN T - Win DOY** | **7d MIN T - Win** | **Total R - Win** | **3d MAX R -Win DOY** | **3d MAX R -Win** | **30d MIN R - Win DOY** | **30d MIN R - Win** | **Water yield - Win** | **3d MAX R - Win DOY** | **3d MAX R - Win** | **7d MIN Q - Win DOY** | **7d MIN Q - Win** | **BF yield - Win** | **3d MAX BF - Win DOY** | **3d MAX BF - Win** | **7d MIN BF - Win DOY** | **7d MIN BF - Win** | **3d MAX GW - Win DOY** | **3d MAX GW - Win** | **7d MIN GW - Win DOY** | **7d MIN GW - Win** |
|---|---|---|---|---|---|---|---|---|---|---|---|---|---|---|---|---|---|---|---|---|---|---|---|---|
| **Mean T - Win** | 1.000 | -0.073 | 0.418 | -0.132 | .636** | 0.345 | -0.183 | 0.309 | -0.147 | 0.345 | 0.018 | 0.138 | 0.091 | -0.018 | 0.055 | 0.055 | 0.177 | 0.164 | -0.220 | 0.019 | 0.552 | 0.333 | 0.298 | 0.333 |
| **7d MAX T - Win DOY** | 0.755 | 1.000 | 0.367 | 0.152 | -0.367 | 0.330 | 0.204 | 0.257 | -0.204 | 0.257 | 0.073 | 0.397 | 0.073 | -.477* | -0.110 | 0.037 | 0.357 | 0.110 | -0.315 | -0.150 | 0.000 | -0.467 | 0.596 | -0.467 |
| **7d MAX T - Win** | 0.073 | 0.118 | 1.000 | 0.397 | 0.200 | 0.345 | 0.183 | 0.455 | 0.073 | 0.418 | 0.236 | 0.413 | 0.309 | -0.091 | 0.127 | 0.200 | 0.452 | 0.382 | 0.000 | 0.130 | 0.552 | 0.600 | 0.298 | 0.600 |
| **7d MIN T - Win DOY** | 0.580 | 0.526 | 0.097 | 1.000 | -0.057 | 0.057 | 0.191 | -0.019 | 0.210 | 0.245 | 0.397 | 0.388 | 0.434 | 0.283 | 0.434 | 0.359 | 0.449 | 0.283 | 0.419 | .519* | 0.276 | 0.600 | 0.000 | 0.600 |
| **7d MIN T - Win** | 0.006 | 0.118 | 0.392 | 0.813 | 1.000 | 0.200 | -0.073 | 0.164 | -0.110 | 0.055 | 0.164 | -0.059 | 0.164 | 0.200 | 0.200 | 0.200 | 0.059 | 0.309 | 0.000 | 0.241 | 0.414 | 0.467 | 0.149 | 0.467 |
| **Total R - Win** | 0.139 | 0.160 | 0.139 | 0.813 | 0.392 | 1.000 | 0.037 | 0.382 | -0.294 | 0.418 | 0.164 | 0.256 | 0.091 | -0.236 | -0.018 | 0.200 | 0.334 | 0.091 | -0.367 | -0.019 | 0.138 | 0.200 | 0.149 | 0.200 |
| **3d MAX R - Win DOY** | 0.435 | 0.389 | 0.435 | 0.428 | 0.755 | 0.876 | 1.000 | 0.073 | 0.204 | -0.037 | 0.037 | 0.040 | -0.110 | 0.073 | 0.220 | 0.000 | 0.079 | 0.037 | 0.019 | 0.187 | 0.138 | 0.200 | 0.596 | 0.200 |
| **3d MAX R - Win** | 0.186 | 0.274 | 0.052 | 0.937 | 0.484 | 0.102 | 0.755 | 1.000 | -0.183 | 0.236 | 0.127 | 0.374 | 0.200 | -0.127 | 0.018 | 0.164 | 0.413 | 0.345 | -0.147 | 0.019 | 0.276 | 0.333 | 0.447 | 0.333 |
| **30d MIN R - Win DOY** | 0.532 | 0.389 | 0.755 | 0.384 | 0.639 | 0.212 | 0.389 | 0.435 | 1.000 | -0.147 | -0.330 | -0.079 | -0.257 | 0.257 | -0.110 | -0.367 | -0.159 | -0.257 | 0.019 | -0.112 | 0.000 | -0.200 | 0.298 | -0.200 |
| **30d MIN R - Win** | 0.139 | 0.274 | 0.073 | 0.305 | 0.815 | 0.073 | 0.876 | 0.312 | 0.532 | 1.000 | 0.309 | .492* | 0.382 | 0.127 | 0.273 | 0.273 | .531* | 0.309 | 0.000 | 0.315 | 0.552 | 0.467 | 0.000 | 0.467 |
| **Water yield - Win** | 0.938 | 0.755 | 0.312 | 0.097 | 0.484 | 0.484 | 0.876 | 0.586 | 0.160 | 0.186 | 1.000 | .531* | .855** | 0.236 | .600* | .964** | .649** | .782** | .477* | .611** | 0.552 | 0.467 | 0.000 | 0.467 |
| **3d MAX R - Win DOY** | 0.573 | 0.106 | 0.091 | 0.121 | 0.809 | 0.295 | 0.872 | 0.126 | 0.747 | 0.044 | 0.030 | 1.000 | .570* | 0.177 | 0.374 | .492* | .915** | .570* | 0.238 | 0.321 | 1.000** | 0.138 | 0.540 | 0.138 |
| **3d MAX R - Win** | 0.697 | 0.755 | 0.186 | 0.069 | 0.484 | 0.697 | 0.639 | 0.392 | 0.274 | 0.102 | 0.000 | 0.020 | 1.000 | 0.309 | .600* | .818** | .688** | .855** | .550* | .611** | 0.414 | 0.600 | -0.149 | 0.600 |
| **7d MIN Q - Win DOY** | 0.938 | 0.042 | 0.697 | 0.236 | 0.392 | 0.312 | 0.755 | 0.586 | 0.274 | 0.586 | 0.312 | 0.469 | 0.186 | 1.000 | .491* | 0.200 | 0.216 | 0.309 | .697** | .537* | 0.414 | 0.600 | -0.149 | 0.600 |
| **7d MIN Q - Win** | 0.815 | 0.639 | 0.586 | 0.069 | 0.392 | 0.938 | 0.349 | 0.938 | 0.639 | 0.243 | 0.010 | 0.126 | 0.010 | 0.036 | 1.000 | .564* | .492* | .527* | .661** | .945** | 0.552 | 0.467 | 0.000 | 0.467 |
| **BF yield - Win** | 0.815 | 0.876 | 0.392 | 0.133 | 0.392 | 0.392 | 1.000 | 0.484 | 0.118 | 0.243 | 0.000 | 0.044 | 0.000 | 0.392 | 0.016 | 1.000 | .610* | .745** | 0.440 | .574* | 0.552 | 0.467 | 0.000 | 0.467 |
| **3d MAX BF - Win DOY** | 0.469 | 0.146 | 0.064 | 0.073 | 0.809 | 0.171 | 0.747 | 0.091 | 0.518 | 0.030 | 0.008 | 0.000 | 0.005 | 0.376 | 0.044 | 0.013 | 1.000 | .688** | 0.298 | 0.441 | .857* | 0.276 | 0.386 | 0.276 |
| **3d MAX BF - Win** | 0.484 | 0.639 | 0.102 | 0.236 | 0.186 | 0.697 | 0.876 | 0.139 | 0.274 | 0.186 | 0.001 | 0.020 | 0.000 | 0.186 | 0.024 | 0.001 | 0.005 | 1.000 | .477* | .537* | 0.552 | 0.467 | 0.000 | 0.467 |
| **7d MIN BF - Win DOY** | 0.349 | 0.183 | 1.000 | 0.081 | 1.000 | 0.118 | 0.938 | 0.532 | 0.938 | 1.000 | 0.042 | 0.333 | 0.019 | 0.003 | 0.005 | 0.061 | 0.226 | 0.042 | 1.000 | .673** | 0.414 | 0.600 | -0.149 | 0.600 |
| **7d MIN BF - Win** | 0.938 | 0.530 | 0.583 | 0.032 | 0.309 | 0.938 | 0.432 | 0.938 | 0.637 | 0.183 | 0.010 | 0.195 | 0.010 | 0.023 | 0.000 | 0.015 | 0.075 | 0.023 | 0.005 | 1.000 | 0.357 | 0.690 | -0.154 | 0.690 |
| **3d MAX GW - Win DOY** | 0.126 | 1.000 | 0.126 | 0.444 | 0.251 | 0.702 | 0.702 | 0.444 | 1.000 | 0.126 | 0.126 | | 0.251 | 0.251 | 0.126 | 0.126 | 0.020 | 0.126 | 0.251 | 0.330 | 1.000 | 0.138 | 0.540 | 0.138 |
| **3d MAX GW - Win** | 0.348 | 0.188 | 0.091 | 0.091 | 0.188 | 0.573 | 0.573 | 0.348 | 0.573 | 0.188 | 0.188 | 0.702 | 0.091 | 0.091 | 0.188 | 0.188 | 0.444 | 0.188 | 0.091 | 0.056 | 0.702 | 1.000 | -0.149 | 1.000** |
| **7d MIN GW - Win DOY** | 0.421 | 0.107 | 0.421 | 1.000 | 0.687 | 0.687 | 0.107 | 0.227 | 0.421 | 1.000 | 1.000 | 0.152 | 0.687 | 0.687 | 1.000 | 1.000 | 0.306 | 1.000 | 0.687 | 0.682 | 0.152 | 0.687 | 1.000 | -0.149 |

| | | | | | | | | | | | | | | | | | | | | | | | | |
|---|---|---|---|---|---|---|---|---|---|---|---|---|---|---|---|---|---|---|---|---|---|---|---|---|
| **7d MIN GW - Win** | 0.348 | 0.188 | 0.091 | 0.091 | 0.188 | 0.573 | 0.573 | 0.348 | 0.573 | 0.188 | 0.188 | 0.702 | 0.091 | 0.091 | 0.188 | 0.188 | 0.444 | 0.188 | 0.091 | 0.056 | 0.702 | | 0.687 | 1.000 |

**. Correlation is significant at the 0.01 level (2-tailed).

*. Correlation is significant at the 0.05 level (2-tailed).

## Spring Spearman's Rank and Kendall's Rank Analysis

The correlation coefficient is above, and the p-value is below the diagonal.

## Spring Spearman's Rank Analysis

| Spring Spearman's rho | Mean T - Spr | 7d MAX T - Spr DOY | 7d MAX T - Spr | 7d MIN T - Spr DOY | 7d MIN T - Spr | Total R | 3d MAX R - Spr DOY | 3d MAX R - Spr | 30d MIN R - Spr DOY | 30d MIN R - Spr | Water yield | 3d MAX Q - Spr DOY | 3d MAX Q - Spr | 7d MIN Q - Spr DOY | 7d MIN Q - Spr | BF Yield | 3d MAX BF - Spr DOY | 3d MAX BF - Spr | 7d MIN BF - Spr DOY | 7d MIN BF - Spr | 3d MAX GW - Spr DOY | 3d MAX GW - Spr | 7d MIN GW - Spr DOY | 7d MIN GW - Spr |
|---|---|---|---|---|---|---|---|---|---|---|---|---|---|---|---|---|---|---|---|---|---|---|---|---|
| **Mean T - Spr** | 1.000 | -0.427 | 0.479 | -0.335 | 0.600 | -0.418 | -0.127 | -0.006 | -0.231 | 0.079 | -0.527 | -0.345 | -0.212 | 0.085 | -0.042 | -.733* | -0.333 | -0.394 | 0.130 | -0.012 | -0.300 | -.900* | -1.000** | 0.700 |
| **7d MAX T - Spr DOY** | 0.219 | 1.000 | -0.250 | 0.500 | -0.140 | 0.122 | -0.207 | 0.091 | 0.315 | -0.329 | 0.067 | 0.098 | -0.366 | 0.185 | -0.189 | 0.311 | 0.085 | -0.140 | -0.150 | -0.129 | 0.103 | 0.564 | 0.667 | -0.051 |
| **7d MAX T - Spr** | 0.162 | 0.486 | 1.000 | -0.549 | 0.115 | -0.455 | -0.345 | -0.261 | 0.182 | 0.091 | -0.285 | -0.382 | -0.103 | -0.518 | -0.236 | -0.455 | -0.370 | -0.200 | -0.493 | -0.226 | -0.300 | 0.100 | 0.000 | -0.300 |
| **7d MIN T - Spr DOY** | 0.343 | 0.141 | 0.100 | 1.000 | 0.201 | .665* | 0.116 | 0.561 | 0.437 | 0.085 | 0.567 | 0.628 | 0.390 | .719* | 0.323 | 0.598 | .689* | 0.506 | 0.486 | 0.360 | -0.400 | 0.300 | 0.100 | 0.500 |
| **7d MIN T - Spr** | 0.067 | 0.699 | 0.751 | 0.577 | 1.000 | 0.152 | 0.152 | .661* | -0.286 | 0.018 | -0.188 | 0.127 | 0.297 | 0.111 | -0.103 | -0.418 | 0.188 | 0.079 | 0.104 | -0.128 | 0.200 | -0.100 | -0.300 | 0.300 |
| **Total R** | 0.229 | 0.737 | 0.187 | 0.036 | 0.676 | 1.000 | 0.600 | .709* | 0.146 | 0.394 | .818** | .952** | 0.612 | 0.295 | -0.127 | .661* | .939** | .830** | 0.305 | -0.135 | 0.300 | 0.600 | 0.700 | -0.200 |
| **3d MAX R - Spr DOY** | 0.726 | 0.565 | 0.328 | 0.750 | 0.676 | 0.067 | 1.000 | 0.612 | -0.292 | 0.539 | 0.200 | 0.442 | 0.273 | -0.138 | -0.455 | 0.018 | 0.370 | 0.248 | -0.156 | -0.471 | 0.700 | 0.000 | 0.300 | -0.200 |
| **3d MAX R - Spr** | 0.987 | 0.802 | 0.467 | 0.092 | 0.038 | 0.022 | 0.060 | 1.000 | -0.213 | 0.370 | 0.382 | 0.539 | 0.418 | 0.190 | -0.139 | 0.188 | 0.564 | 0.418 | 0.078 | -0.159 | 0.100 | 0.700 | 0.600 | -0.100 |
| **30d MIN R - Spr DOY** | 0.521 | 0.375 | 0.614 | 0.206 | 0.424 | 0.688 | 0.413 | 0.555 | 1.000 | 0.158 | 0.304 | 0.292 | 0.274 | 0.217 | 0.164 | 0.316 | 0.328 | 0.310 | 0.052 | 0.224 | -0.700 | 0.000 | -0.300 | 0.200 |
| **30d MIN R - Spr** | 0.829 | 0.353 | 0.803 | 0.815 | 0.960 | 0.260 | 0.108 | 0.293 | 0.663 | 1.000 | 0.382 | 0.333 | 0.224 | -0.020 | -0.018 | 0.152 | 0.297 | 0.236 | 0.013 | -0.012 | -0.300 | -0.100 | 0.200 | 0.300 |
| **Water yield** | 0.117 | 0.854 | 0.425 | 0.087 | 0.603 | 0.004 | 0.580 | 0.276 | 0.393 | 0.276 | 1.000 | .806** | 0.527 | 0.361 | 0.236 | .915** | .818** | .855** | 0.435 | 0.232 | -0.300 | .900* | 0.800 | -0.300 |
| **3d MAX Q - Spr DOY** | 0.328 | 0.789 | 0.276 | 0.052 | 0.726 | 0.000 | 0.200 | 0.108 | 0.413 | 0.347 | 0.005 | 1.000 | .648* | 0.321 | -0.127 | .636* | .988** | .879** | 0.396 | -0.128 | 0.300 | 0.600 | 0.700 | -0.200 |
| **3d MAX Q - Spr** | 0.556 | 0.298 | 0.777 | 0.265 | 0.405 | 0.060 | 0.446 | 0.229 | 0.444 | 0.533 | 0.117 | 0.043 | 1.000 | 0.059 | 0.176 | 0.309 | .721* | .855** | 0.221 | 0.110 | 0.300 | 0.500 | 0.200 | -0.300 |
| **7d MIN Q - Spr DOY** | 0.815 | 0.609 | 0.125 | 0.019 | 0.759 | 0.408 | 0.704 | 0.599 | 0.547 | 0.957 | 0.306 | 0.365 | 0.871 | 1.000 | 0.610 | 0.413 | 0.374 | 0.216 | .877** | .675* | -.894* | -0.224 | -0.447 | .894* |
| **7d MIN Q - Spr** | 0.907 | 0.601 | 0.511 | 0.362 | 0.777 | 0.726 | 0.187 | 0.701 | 0.650 | 0.960 | 0.511 | 0.726 | 0.627 | 0.061 | 1.000 | 0.345 | -0.018 | 0.115 | .642* | .991** | -0.800 | 0.100 | -0.300 | 0.500 |
| **BF yield** | 0.016 | 0.382 | 0.187 | 0.068 | 0.229 | 0.038 | 0.960 | 0.603 | 0.374 | 0.676 | 0.000 | 0.048 | 0.385 | 0.235 | 0.328 | 1.000 | .648* | .673* | 0.422 | 0.349 | -0.300 | .900* | 0.800 | -0.300 |
| **3d MAX BF - Spr DOY** | 0.347 | 0.815 | 0.293 | 0.028 | 0.603 | 0.000 | 0.293 | 0.090 | 0.354 | 0.405 | 0.004 | 0.000 | 0.019 | 0.287 | 0.960 | 0.043 | 1.000 | .915** | 0.441 | -0.024 | 0.100 | 0.700 | 0.600 | -0.100 |
| **3d MAX BF - Spr** | 0.260 | 0.699 | 0.580 | 0.136 | 0.829 | 0.003 | 0.489 | 0.229 | 0.383 | 0.511 | 0.002 | 0.001 | 0.002 | 0.548 | 0.751 | 0.033 | 0.000 | 1.000 | 0.376 | 0.080 | 0.100 | 1.000** | .900* | -0.600 |
| **7d MIN BF - Spr DOY** | 0.721 | 0.679 | 0.148 | 0.154 | 0.775 | 0.392 | 0.668 | 0.831 | 0.886 | 0.972 | 0.209 | 0.258 | 0.540 | 0.001 | 0.045 | 0.225 | 0.202 | 0.284 | 1.000 | .665* | -.894* | -0.224 | -0.447 | .894* |
| **7d MIN BF - Spr** | 0.973 | 0.722 | 0.530 | 0.307 | 0.724 | 0.711 | 0.169 | 0.661 | 0.534 | 0.973 | 0.518 | 0.724 | 0.762 | 0.032 | 0.000 | 0.323 | 0.947 | 0.827 | 0.036 | 1.000 | -0.872 | -0.051 | -0.410 | 0.564 |
| **3d MAX GW - Spr DOY** | 0.624 | 0.870 | 0.624 | 0.505 | 0.747 | 0.624 | 0.188 | 0.873 | 0.188 | 0.624 | 0.624 | 0.624 | 0.624 | 0.041 | 0.104 | 0.624 | 0.873 | 0.873 | 0.041 | 0.054 | 1.000 | 0.314 | -0.086 | -.829* |
| **3d MAX GW - Spr** | 0.037 | 0.322 | 0.873 | 0.624 | 0.873 | 0.285 | 1.000 | 0.188 | 1.000 | 0.873 | 0.037 | 0.285 | 0.391 | 0.718 | 0.873 | 0.037 | 0.188 | | 0.718 | 0.935 | 0.544 | 1.000 | 0.086 | -0.600 |

| | | | | | | | | | | | | | | | | | | | | | | | | |
|---|---|---|---|---|---|---|---|---|---|---|---|---|---|---|---|---|---|---|---|---|---|---|---|---|
| **7d MIN GW - Spr DOY** | | 0.219 | 1.000 | 0.873 | 0.624 | 0.188 | 0.624 | 0.285 | 0.624 | 0.747 | 0.104 | 0.188 | 0.747 | 0.450 | 0.624 | 0.104 | 0.285 | 0.037 | 0.450 | 0.493 | 0.872 | 0.872 | 1.000 | -0.143 |
| **7d MIN GW - Spr** | 0.188 | 0.935 | 0.624 | 0.391 | 0.624 | 0.747 | 0.747 | 0.873 | 0.747 | 0.624 | 0.624 | 0.747 | 0.624 | 0.041 | 0.391 | 0.624 | 0.873 | 0.285 | 0.041 | 0.322 | 0.042 | 0.208 | 0.787 | 1.000 |

*. Correlation is significant at the 0.05 level (2-tailed).
**. Correlation is significant at the 0.01 level (2-tailed).

## Spring Kendall's Rank Analysis

| Spring Kendall's tau_b | Mean T - Spr | 7d MAX T - Spr DOY | 7d MAX T - Spr | 7d MIN T - Spr DOY | 7d MIN T - Spr | Total R | 3d MAX R - Spr DOY | 3d MAX R - Spr | 30d MIN R - Spr DOY | 30d MIN R - Spr | Water yield | 3d MAX Q - Spr DOY | 3d MAX Q - Spr | 7d MIN Q - Spr DOY | 7d MIN Q - Spr | BF yield | 3d MAX BF - Spr DOY | 3d MAX BF - Spr | 7d MIN BF - Spr DOY | 7d MIN BF - Spr | 3d MAX GW - Spr DOY | 3d MAX GW - Spr | 7d MIN GW - Spr DOY | 7d MIN GW - Spr |
|---|---|---|---|---|---|---|---|---|---|---|---|---|---|---|---|---|---|---|---|---|---|---|---|---|
| **Mean T - Spr** | 1.000 | -0.296 | 0.422 | -0.250 | 0.467 | -0.422 | -0.067 | 0.022 | -0.225 | 0.022 | -0.422 | -0.289 | -0.200 | 0.053 | 0.022 | -.511* | -0.244 | -0.378 | 0.102 | 0.046 | -0.200 | -0.800 | -1.000* | 0.600 |
| **7d MAX T - Spr DOY** | 0.241 | 1.000 | -0.159 | 0.349 | -0.159 | 0.068 | -0.114 | 0.114 | 0.138 | -0.250 | -0.068 | 0.114 | -0.250 | 0.081 | -0.068 | 0.114 | 0.068 | -0.159 | -0.131 | -0.047 | 0.105 | 0.316 | 0.527 | -0.105 |
| **7d MAX T - Spr** | 0.089 | 0.528 | 1.000 | -0.432 | 0.067 | -0.378 | -0.200 | -0.111 | 0.180 | -0.022 | -0.200 | -0.244 | -0.067 | -0.422 | -0.200 | -0.378 | -0.200 | -0.156 | -0.409 | -0.184 | -0.200 | 0.000 | -0.200 | -0.200 |
| **7d MIN T - Spr DOY** | 0.321 | 0.173 | 0.087 | 1.000 | 0.114 | .523* | 0.068 | 0.386 | 0.368 | 0.068 | 0.432 | 0.477 | 0.386 | .647* | 0.250 | .523* | .523* | 0.386 | 0.392 | 0.282 | -0.400 | 0.200 | 0.000 | 0.400 |
| **7d MIN T - Spr** | 0.060 | 0.528 | 0.788 | 0.652 | 1.000 | 0.111 | 0.111 | .556* | -0.225 | 0.022 | -0.156 | 0.067 | 0.244 | 0.105 | 0.022 | -0.333 | 0.111 | 0.067 | 0.051 | 0.000 | 0.200 | 0.000 | -0.200 | 0.200 |
| **Total R** | 0.089 | 0.787 | 0.128 | 0.038 | 0.655 | 1.000 | 0.467 | .556* | 0.090 | 0.289 | .644** | .867** | .511* | 0.264 | -0.156 | 0.467 | .822** | .689** | 0.205 | -0.138 | 0.200 | 0.400 | 0.600 | -0.200 |
| **3d MAX R - Spr DOY** | 0.788 | 0.652 | 0.421 | 0.787 | 0.655 | 0.060 | 1.000 | 0.467 | -0.270 | 0.378 | 0.111 | 0.333 | 0.156 | -0.105 | -0.333 | -0.067 | 0.289 | 0.156 | -0.153 | -0.368 | 0.600 | 0.000 | 0.200 | -0.200 |
| **3d MAX R - Spr** | 0.929 | 0.652 | 0.655 | 0.125 | 0.025 | 0.025 | 0.060 | 1.000 | -0.180 | 0.200 | 0.289 | 0.422 | 0.333 | 0.158 | -0.067 | 0.111 | 0.467 | 0.333 | 0.051 | -0.092 | 0.000 | 0.600 | 0.400 | 0.000 |
| **30d MIN R - Spr DOY** | 0.369 | 0.587 | 0.472 | 0.148 | 0.369 | 0.719 | 0.281 | 0.472 | 1.000 | 0.090 | 0.270 | 0.135 | 0.225 | 0.213 | 0.090 | 0.270 | 0.180 | 0.225 | 0.000 | 0.163 | -0.600 | 0.000 | -0.200 | 0.200 |
| **30d MIN R - Spr** | 0.929 | 0.321 | 0.929 | 0.787 | 0.929 | 0.245 | 0.128 | 0.421 | 0.719 | 1.000 | 0.289 | 0.244 | 0.156 | -0.053 | 0.022 | 0.111 | 0.200 | 0.244 | 0.000 | 0.046 | -0.200 | 0.000 | 0.200 | 0.200 |
| **Water yield** | 0.089 | 0.787 | 0.421 | 0.087 | 0.531 | 0.009 | 0.655 | 0.245 | 0.281 | 0.245 | 1.000 | .600* | 0.422 | 0.316 | 0.111 | .822** | .644** | .689** | 0.358 | 0.138 | -0.200 | 0.800 | 0.600 | -0.200 |
| **3d MAX Q - Spr DOY** | 0.245 | 0.652 | 0.325 | 0.058 | 0.788 | 0.000 | 0.180 | 0.089 | 0.590 | 0.325 | 0.016 | 1.000 | .556* | 0.264 | -0.111 | 0.422 | .956** | .733** | 0.307 | -0.092 | 0.200 | 0.400 | 0.600 | -0.200 |
| **3d MAX Q - Spr** | 0.421 | 0.321 | 0.788 | 0.125 | 0.325 | 0.040 | 0.531 | 0.180 | 0.369 | 0.531 | 0.089 | 0.025 | 1.000 | 0.053 | 0.156 | 0.244 | .600* | .733** | 0.205 | 0.092 | 0.200 | 0.400 | 0.200 | -0.200 |
| **7d MIN Q - Spr DOY** | 0.845 | 0.768 | 0.118 | 0.018 | 0.696 | 0.328 | 0.696 | 0.558 | 0.433 | 0.845 | 0.241 | 0.328 | 0.845 | 1.000 | 0.474 | 0.369 | 0.316 | 0.158 | .758** | .546* | -0.837 | -0.120 | -0.359 | 0.837 |
| **7d MIN Q - Spr** | 0.929 | 0.787 | 0.421 | 0.321 | 0.929 | 0.531 | 0.180 | 0.788 | 0.719 | 0.929 | 0.655 | 0.655 | 0.531 | 0.079 | 1.000 | 0.200 | -0.067 | 0.067 | 0.511 | .966** | -0.600 | 0.000 | -0.200 | 0.200 |
| **BF yield** | 0.040 | 0.652 | 0.128 | 0.038 | 0.180 | 0.060 | 0.788 | 0.655 | 0.281 | 0.655 | 0.001 | 0.089 | 0.325 | 0.171 | 0.421 | 1.000 | 0.467 | .511* | 0.358 | 0.230 | -0.200 | 0.800 | 0.600 | -0.200 |
| **3d MAX BF - Spr DOY** | 0.325 | 0.787 | 0.421 | 0.038 | 0.655 | 0.001 | 0.245 | 0.060 | 0.472 | 0.421 | 0.009 | 0.000 | 0.016 | 0.241 | 0.788 | 0.060 | 1.000 | .778** | 0.358 | -0.046 | 0.000 | 0.600 | 0.400 | 0.000 |
| **3d MAX BF - Spr** | 0.128 | 0.528 | 0.531 | 0.125 | 0.788 | 0.006 | 0.531 | 0.180 | 0.369 | 0.325 | 0.006 | 0.003 | 0.003 | 0.558 | 0.788 | 0.040 | 0.002 | 1.000 | 0.358 | 0.046 | 0.000 | 1.000* | 0.800 | -0.400 |
| **7d MIN BF - Spr DOY** | 0.699 | 0.627 | 0.122 | 0.145 | 0.847 | 0.440 | 0.562 | 0.847 | 1.000 | 1.000 | 0.177 | 0.247 | 0.440 | 0.009 | 0.054 | 0.177 | 0.177 | 0.177 | 1.000 | 0.529 | -0.837 | -0.120 | -0.359 | 0.837 |
| **7d MIN BF - Spr** | 0.856 | 0.855 | 0.469 | 0.274 | 1.000 | 0.587 | 0.147 | 0.717 | 0.525 | 0.856 | 0.587 | 0.717 | 0.717 | 0.048 | 0.000 | 0.365 | 0.856 | 0.856 | 0.051 | 1.000 | -0.738 | -0.105 | -0.316 | 0.316 |
| **3d MAX GW - Spr DOY** | 0.624 | 0.801 | 0.624 | 0.327 | 0.624 | 0.624 | 0.142 | 1.000 | 0.142 | 0.624 | 0.624 | 0.624 | 0.624 | 0.052 | 0.142 | 0.624 | 1.000 | 1.000 | 0.052 | 0.077 | 1.000 | 0.200 | -0.067 | -.733* |
| **3d MAX GW - Spr** | 0.050 | 0.448 | 1.000 | 0.624 | 1.000 | 0.327 | 1.000 | 0.142 | 1.000 | 1.000 | 0.050 | 0.327 | 0.327 | 0.782 | 1.000 | 0.050 | 0.142 | | 0.782 | 0.801 | 0.573 | 1.000 | 0.200 | -0.467 |
| **7d MIN GW - Spr DOY** | | 0.207 | 0.624 | 1.000 | 0.624 | 0.142 | 0.624 | 0.327 | 0.624 | 0.624 | 0.142 | 0.142 | 0.624 | 0.405 | 0.624 | 0.142 | 0.327 | 0.050 | 0.405 | 0.448 | 0.851 | 0.573 | 1.000 | -0.200 |
| **7d MIN GW - Spr** | 0.142 | 0.801 | 0.624 | 0.327 | 0.624 | 0.624 | 0.624 | 1.000 | 0.624 | 0.624 | 0.624 | 0.624 | 0.624 | 0.052 | 0.624 | 0.624 | 1.000 | 0.327 | 0.052 | 0.448 | 0.039 | 0.188 | 0.573 | 1.000 |

*. Correlation is significant at the 0.05 level (2-tailed).

**. Correlation is significant at the 0.01 level (2-tailed).

## Summer Spearman's Rank and Kendall's Rank Analysis

The correlation coefficient is above, and the p-value is below the diagonal.

## Summer Spearman's Rank Analysis

| Summer Spearman's rho | Mean T - Sum | 7d MAX T - Sum DOY | 7d MAX T - Sum | 7d MIN T - Sum DOY | 7d MIN T - Sum | Total R | 3d MAX R - Sum DOY | 3d MAX R - Sum | 30d MIN R - Sum DOY | 30d MIN R - Sum DOY | Water yield - Sum | 3d MAX Q - Sum DOY | 3d MAX Q - Sum | 7d MIN Q - Sum DOY | 7d MIN Q - Sum | BF yield | 3d MAX BF - Sum DOY | 3d MAX BF - Sum | 7d MIN BF - Sum DOY | 7d MIN BF - Sum | 3d MAX GW - Sum DOY | 3d MAX GW - Sum | 7d MIN GW - Sum DOY | 7d MIN GW - Sum |
|---|---|---|---|---|---|---|---|---|---|---|---|---|---|---|---|---|---|---|---|---|---|---|---|---|
| **Mean T - Sum** | 1.000 | 0.067 | .648* | -0.255 | 0.097 | -0.067 | -0.091 | 0.236 | 0.018 | -0.115 | -0.055 | 0.529 | 0.115 | -0.110 | -0.345 | -0.236 | 0.401 | 0.188 | -0.122 | -0.322 | 0.224 | 0.000 | 0.300 | -0.200 |
| **7d MAX T - Sum DOY** | 0.854 | 1.000 | 0.091 | 0.186 | 0.027 | -0.401 | 0.195 | -0.061 | 0.347 | 0.055 | 0.036 | 0.351 | -0.085 | 0.141 | -0.091 | 0.213 | 0.179 | -0.219 | 0.265 | -0.058 | -0.783 | -0.800 | -0.200 | -0.500 |
| **7d MAX T - Sum** | 0.043 | 0.802 | 1.000 | -0.109 | -0.109 | -0.091 | 0.200 | -0.042 | 0.394 | -0.212 | -0.042 | .815** | 0.018 | 0.183 | -0.067 | -0.127 | 0.119 | -0.006 | 0.201 | -0.073 | 0.224 | 0.100 | 0.600 | -0.100 |
| **7d MIN T - Sum DOY** | 0.476 | 0.607 | 0.763 | 1.000 | 0.390 | 0.055 | -0.049 | -0.225 | -0.413 | -0.067 | 0.103 | -0.146 | -0.043 | 0.376 | 0.511 | 0.085 | 0.525 | -0.146 | 0.500 | 0.491 | 0.783 | 0.800 | 0.700 | 0.300 |
| **7d MIN T - Sum** | 0.789 | 0.940 | 0.763 | 0.265 | 1.000 | -0.140 | -.669* | 0.249 | -0.280 | 0.322 | 0.383 | -0.305 | 0.371 | 0.627 | 0.304 | 0.316 | 0.462 | 0.426 | .652* | 0.332 | 0.224 | 0.600 | 0.100 | .900* |
| **Total R** | 0.855 | 0.250 | 0.803 | 0.881 | 0.700 | 1.000 | -0.345 | .673* | 0.212 | 0.152 | 0.600 | -0.055 | .648* | 0.189 | 0.394 | 0.394 | 0.326 | 0.564 | 0.006 | 0.401 | .894* | 0.600 | 0.500 | -0.100 |
| **3d MAX R - Sum DOY** | 0.803 | 0.590 | 0.580 | 0.894 | 0.035 | 0.328 | 1.000 | -.673* | -0.091 | -.818** | -.818** | 0.097 | -.842** | -.665* | -0.503 | -.721* | -0.470 | -.867** | -0.517 | -0.553 | -0.783 | -.900* | -0.500 | -0.600 |
| **3d MAX R - Sum** | 0.511 | 0.868 | 0.907 | 0.532 | 0.487 | 0.033 | 0.033 | 1.000 | 0.370 | 0.455 | .758* | 0.073 | .842** | 0.433 | 0.273 | 0.576 | 0.301 | .830** | 0.225 | 0.322 | 0.671 | 0.400 | 0.100 | 0.000 |
| **30d MIN R - Sum DOY** | 0.960 | 0.327 | 0.260 | 0.235 | 0.434 | 0.556 | 0.803 | 0.293 | 1.000 | 0.370 | 0.515 | 0.614 | 0.467 | 0.372 | 0.091 | 0.600 | -0.069 | 0.309 | 0.292 | 0.128 | -0.112 | -0.200 | 0.500 | -0.300 |
| **30d MIN R - Sum** | 0.751 | 0.881 | 0.556 | 0.854 | 0.364 | 0.676 | 0.004 | 0.187 | 0.293 | 1.000 | .770** | 0.140 | .721* | 0.604 | 0.539 | .842** | 0.220 | .697* | 0.462 | 0.590 | 0.112 | 0.300 | 0.300 | 0.200 |
| **Water yield** | 0.881 | 0.920 | 0.907 | 0.776 | 0.275 | 0.067 | 0.004 | 0.011 | 0.128 | 0.009 | 1.000 | 0.146 | .964** | .774** | .636* | .939** | 0.489 | .855** | 0.614 | .687* | .894* | .900* | .900* | 0.400 |
| **3d MAX R - Sum DOY** | 0.116 | 0.321 | 0.004 | 0.687 | 0.392 | 0.881 | 0.789 | 0.841 | 0.059 | 0.700 | 0.688 | 1.000 | 0.134 | 0.229 | 0.000 | 0.140 | 0.138 | 0.030 | 0.235 | 0.015 | 0.112 | -0.100 | 0.600 | -0.500 |
| **3d MAX R - Sum** | 0.751 | 0.815 | 0.960 | 0.907 | 0.291 | 0.043 | 0.002 | 0.002 | 0.174 | 0.019 | 0.000 | 0.713 | 1.000 | .671* | 0.576 | .855** | 0.470 | .952** | 0.462 | 0.626 | .894* | .900* | .900* | 0.400 |
| **7d MIN Q - Sum DOY** | 0.763 | 0.698 | 0.613 | 0.284 | 0.052 | 0.601 | 0.036 | 0.211 | 0.290 | 0.065 | 0.009 | 0.524 | 0.034 | 1.000 | .695* | .756* | 0.357 | 0.579 | .948** | .725* | .918* | .975** | 0.821 | 0.564 |
| **7d MIN Q - Sum** | 0.328 | 0.802 | 0.855 | 0.132 | 0.393 | 0.260 | 0.138 | 0.446 | 0.803 | 0.108 | 0.048 | 1.000 | 0.082 | 0.026 | 1.000 | .648* | 0.207 | 0.564 | 0.535 | .997** | 0.447 | 0.500 | 0.600 | 0.100 |
| **BF yield - Sum** | 0.511 | 0.555 | 0.726 | 0.815 | 0.374 | 0.260 | 0.019 | 0.082 | 0.067 | 0.002 | 0.000 | 0.700 | 0.002 | 0.011 | 0.043 | 1.000 | 0.339 | .733* | 0.620 | .699* | 0.224 | 0.300 | 0.700 | 0.000 |
| **3d MAX BF - Sum DOY** | 0.250 | 0.620 | 0.743 | 0.119 | 0.178 | 0.358 | 0.170 | 0.398 | 0.850 | 0.542 | 0.151 | 0.703 | 0.170 | 0.312 | 0.566 | 0.338 | 1.000 | 0.345 | 0.409 | 0.242 | .918* | 0.821 | 0.872 | 0.205 |
| **3d MAX BF - Sum** | 0.603 | 0.544 | 0.987 | 0.688 | 0.220 | 0.090 | 0.001 | 0.003 | 0.385 | 0.025 | 0.002 | 0.934 | 0.000 | 0.079 | 0.090 | 0.016 | 0.329 | 1.000 | 0.328 | 0.608 | .894* | 1.000** | 0.700 | 0.700 |
| **7d MIN BF - Sum DOY** | 0.738 | 0.459 | 0.578 | 0.141 | 0.041 | 0.987 | 0.126 | 0.532 | 0.413 | 0.179 | 0.059 | 0.514 | 0.179 | 0.000 | 0.111 | 0.056 | 0.241 | 0.354 | 1.000 | 0.561 | .918* | .975** | 0.821 | 0.564 |
| **7d MIN BF - Sum** | 0.364 | 0.874 | 0.841 | 0.150 | 0.348 | 0.250 | 0.097 | 0.364 | 0.725 | 0.073 | 0.028 | 0.967 | 0.053 | 0.018 | 0.000 | 0.024 | 0.500 | 0.062 | 0.092 | 1.000 | 0.447 | 0.500 | 0.600 | 0.100 |
| **3d MAX GW - Sum DOY** | 0.718 | 0.118 | 0.718 | 0.118 | 0.718 | 0.041 | 0.118 | 0.215 | 0.858 | 0.858 | 0.041 | 0.858 | 0.041 | 0.028 | 0.450 | 0.718 | 0.028 | 0.041 | 0.028 | 0.450 | 1.000 | .894* | 0.671 | 0.335 |
| **3d MAX GW - Sum** | 1.000 | 0.104 | 0.873 | 0.104 | 0.285 | 0.285 | 0.037 | 0.505 | 0.747 | 0.624 | 0.037 | 0.873 | 0.037 | 0.005 | 0.391 | 0.624 | 0.089 |  | 0.005 | 0.391 | 0.041 | 1.000 | 0.700 | 0.700 |
| **7d MIN GW - Sum DOY** | 0.624 | 0.747 | 0.285 | 0.188 | 0.873 | 0.391 | 0.391 | 0.873 | 0.391 | 0.624 | 0.037 | 0.285 | 0.037 | 0.089 | 0.285 | 0.188 | 0.054 | 0.188 | 0.089 | 0.285 | 0.215 | 0.188 | 1.000 | 0.300 |
| **7d MIN GW - Sum** | 0.747 | 0.391 | 0.873 | 0.624 | 0.037 | 0.873 | 0.285 | 1.000 | 0.624 | 0.747 | 0.505 | 0.391 | 0.505 | 0.322 | 0.873 | 1.000 | 0.741 | 0.188 | 0.322 | 0.873 | 0.581 | 0.188 | 0.624 | 1.000 |

*. Correlation is significant at the 0.05 level (2-tailed).

**. Correlation is significant at the 0.01 level (2-tailed).

## Summer Kendall's Rank Analysis

| Summer Kendall's tau_b | Mean T - Sum | 7d MAX T - Sum DOY | 7d MAX T - Sum | 7d MIN T - Sum DOY | 7d MIN T - Sum | Total R - Sum | 3d MAX R - Sum DOY | 3d MAX R - Sum | 30d MIN R - Sum DOY | 30d MIN R - Sum DOY | Water yield - Sum | 3d MAX Q - Sum DOY | 3d MAX Q - Sum | 7d MIN Q - Sum DOY | 7d MIN Q - Sum | BF yield - Sum | 3d MAX BF - Sum DOY | 3d MAX BF - Sum | 7d MIN BF - Sum DOY | 7d MIN BF - Sum | 3d MAX GW - Sum DOY | 3d MAX GW - Sum | 7d MIN GW - Sum DOY | 7d MIN GW - Sum |
|---|---|---|---|---|---|---|---|---|---|---|---|---|---|---|---|---|---|---|---|---|---|---|---|---|
| **Mean T - Sum** | 1.000 | 0.045 | .511* | -0.225 | 0.090 | -0.067 | -0.067 | 0.156 | -0.022 | -0.111 | -0.022 | 0.360 | 0.067 | -0.159 | -0.333 | -0.111 | 0.290 | 0.111 | -0.180 | -0.315 | 0.120 | -0.200 | 0.200 | -0.200 |
| **7d MAX T - Sum DOY** | 0.857 | 1.000 | 0.135 | 0.068 | 0.023 | -0.315 | 0.180 | 0.000 | 0.270 | 0.000 | 0.090 | 0.295 | 0.000 | 0.138 | -0.090 | 0.180 | 0.171 | -0.135 | 0.159 | -0.068 | -0.598 | -0.600 | -0.200 | -0.200 |
| **7d MAX T - Sum** | 0.040 | 0.590 | 1.000 | -0.090 | -0.045 | -0.111 | 0.067 | 0.022 | 0.289 | -0.156 | 0.022 | .584* | 0.022 | 0.159 | -0.022 | -0.067 | 0.097 | -0.022 | 0.135 | -0.045 | 0.120 | 0.000 | 0.400 | 0.000 |
| **7d MIN T - Sum DOY** | 0.369 | 0.787 | 0.719 | 1.000 | 0.318 | 0.000 | -0.045 | -0.225 | -0.315 | -0.045 | 0.045 | -0.114 | -0.045 | 0.230 | 0.405 | 0.045 | 0.416 | -0.135 | 0.341 | 0.386 | 0.598 | 0.600 | 0.600 | 0.200 |
| **7d MIN T - Sum** | 0.719 | 0.928 | 0.857 | 0.207 | 1.000 | -0.135 | -.539* | 0.180 | -0.180 | 0.270 | 0.270 | -0.295 | 0.270 | 0.414 | 0.180 | 0.270 | 0.416 | 0.270 | 0.432 | 0.205 | 0.120 | 0.400 | 0.000 | 0.800 |
| **Total R - Sum** | 0.788 | 0.209 | 0.655 | 1.000 | 0.590 | 1.000 | -0.156 | .511* | 0.156 | 0.156 | 0.422 | -0.045 | .511* | 0.159 | 0.289 | 0.244 | 0.290 | 0.378 | 0.000 | 0.315 | 0.837 | 0.400 | 0.400 | 0.000 |
| **3d MAX R - Sum DOY** | 0.788 | 0.472 | 0.788 | 0.857 | 0.031 | 0.531 | 1.000 | -.556* | -0.022 | -.644** | -.644** | 0.135 | -.644** | -.523* | -0.333 | -.556* | -0.339 | -.689** | -0.449 | -0.360 | -0.598 | -0.800 | -0.400 | -0.400 |
| **3d MAX R - Sum** | 0.531 | 1.000 | 0.929 | 0.369 | 0.472 | 0.040 | 0.025 | 1.000 | 0.289 | 0.289 | .644** | 0.045 | .733** | 0.341 | 0.244 | 0.467 | 0.242 | .689** | 0.180 | 0.270 | 0.598 | 0.400 | 0.000 | 0.000 |
| **30d MIN R - Sum DOY** | 0.929 | 0.281 | 0.245 | 0.209 | 0.472 | 0.531 | 0.929 | 0.245 | 1.000 | 0.289 | 0.378 | .494* | 0.378 | 0.296 | 0.067 | 0.467 | -0.097 | 0.244 | 0.225 | 0.090 | -0.120 | -0.200 | 0.200 | -0.200 |
| **30d MIN R - Sum** | 0.655 | 1.000 | 0.531 | 0.857 | 0.281 | 0.531 | 0.009 | 0.245 | 0.245 | 1.000 | .644** | 0.135 | .556* | 0.477 | 0.422 | .644** | 0.242 | .511* | 0.315 | 0.449 | 0.120 | 0.200 | 0.200 | 0.200 |
| **Water yield - Sum** | 0.929 | 0.719 | 0.929 | 0.857 | 0.281 | 0.089 | 0.009 | 0.009 | 0.128 | 0.009 | 1.000 | 0.135 | .911** | .659** | .511* | .822** | 0.484 | .778** | .494* | .539* | 0.837 | 0.800 | 0.800 | 0.400 |
| **3d MAX R - Sum DOY** | 0.151 | 0.241 | 0.020 | 0.652 | 0.241 | 0.857 | 0.590 | 0.857 | 0.048 | 0.590 | 0.590 | 1.000 | 0.135 | 0.184 | 0.000 | 0.135 | 0.147 | 0.090 | 0.159 | 0.023 | 0.120 | 0.000 | 0.400 | -0.400 |
| **3d MAX R - Sum** | 0.788 | 1.000 | 0.929 | 0.857 | 0.281 | 0.040 | 0.009 | 0.003 | 0.128 | 0.025 | 0.000 | 0.590 | 1.000 | .568* | 0.422 | .733** | 0.435 | .867** | 0.405 | 0.449 | 0.837 | 0.800 | 0.800 | 0.400 |
| **7d MIN Q - Sum DOY** | 0.528 | 0.587 | 0.528 | 0.365 | 0.103 | 0.528 | 0.038 | 0.176 | 0.241 | 0.058 | 0.009 | 0.469 | 0.024 | 1.000 | .523* | .568* | 0.297 | 0.477 | .851** | .552* | .882* | .949* | 0.738 | 0.527 |
| **7d MIN Q - Sum** | 0.180 | 0.719 | 0.929 | 0.106 | 0.472 | 0.245 | 0.180 | 0.325 | 0.788 | 0.089 | 0.040 | 1.000 | 0.089 | 0.038 | 1.000 | .511* | 0.193 | 0.378 | 0.360 | .989** | 0.359 | 0.400 | 0.400 | 0.000 |
| **BF yield - Sum** | 0.655 | 0.472 | 0.788 | 0.857 | 0.281 | 0.325 | 0.025 | 0.060 | 0.060 | 0.009 | 0.001 | 0.590 | 0.003 | 0.024 | 0.040 | 1.000 | 0.290 | .600* | 0.405 | .539* | 0.120 | 0.200 | 0.600 | -0.200 |
| **3d MAX BF - Sum DOY** | 0.264 | 0.513 | 0.710 | 0.112 | 0.112 | 0.264 | 0.192 | 0.352 | 0.710 | 0.352 | 0.063 | 0.575 | 0.094 | 0.260 | 0.456 | 0.264 | 1.000 | 0.290 | 0.318 | 0.220 | .882* | 0.738 | 0.738 | 0.316 |
| **3d MAX BF - Sum** | 0.655 | 0.590 | 0.929 | 0.590 | 0.281 | 0.128 | 0.006 | 0.006 | 0.325 | 0.040 | 0.002 | 0.719 | 0.000 | 0.058 | 0.128 | 0.016 | 0.264 | 1.000 | 0.315 | 0.405 | 0.837 | 1.000* | 0.600 | 0.600 |
| **7d MIN BF - Sum DOY** | 0.472 | 0.528 | 0.590 | 0.176 | 0.087 | 1.000 | 0.072 | 0.472 | 0.369 | 0.209 | 0.048 | 0.528 | 0.106 | 0.001 | 0.151 | 0.106 | 0.224 | 0.209 | 1.000 | 0.386 | .882* | .949* | 0.738 | 0.527 |
| **7d MIN BF - Sum** | 0.209 | 0.787 | 0.857 | 0.125 | 0.417 | 0.209 | 0.151 | 0.281 | 0.719 | 0.072 | 0.031 | 0.928 | 0.072 | 0.030 | 0.000 | 0.031 | 0.400 | 0.106 | 0.125 | 1.000 | 0.359 | 0.400 | 0.400 | 0.000 |
| **3d MAX GW - Sum DOY** | 0.782 | 0.166 | 0.782 | 0.166 | 0.782 | 0.052 | 0.166 | 0.166 | 0.782 | 0.782 | 0.052 | 0.782 | 0.052 | 0.046 | 0.405 | 0.782 | 0.046 | 0.052 | 0.046 | 0.405 | 1.000 | 0.837 | 0.598 | 0.359 |
| **3d MAX GW - Sum** | 0.624 | 0.142 | 1.000 | 0.142 | 0.327 | 0.327 | 0.050 | 0.327 | 0.624 | 0.624 | 0.050 | 1.000 | 0.050 | 0.023 | 0.327 | 0.624 | 0.077 |  | 0.023 | 0.327 | 0.052 | 1.000 | 0.600 | 0.600 |
| **7d MIN GW - Sum DOY** | 0.624 | 0.624 | 0.327 | 0.142 | 1.000 | 0.327 | 0.327 | 1.000 | 0.624 | 0.624 | 0.050 | 0.327 | 0.050 | 0.077 | 0.327 | 0.142 | 0.077 | 0.142 | 0.077 | 0.327 | 0.166 | 0.142 | 1.000 | 0.200 |
| **7d MIN GW - Sum** | 0.624 | 0.624 | 1.000 | 0.624 | 0.050 | 1.000 | 0.327 | 1.000 | 0.624 | 0.624 | 0.327 | 0.327 | 0.327 | 0.207 | 1.000 | 0.624 | 0.448 | 0.142 | 0.207 | 1.000 | 0.405 | 0.142 | 0.624 | 1.000 |

*. Correlation is significant at the 0.05 level (2-tailed).

**. Correlation is significant at the 0.01 level (2-tailed).

## Fall Spearman's Rank and Kendall's Rank Analysis

The correlation coefficient is above, and the p-value is below the diagonal.

### Fall Spearman's Rank Analysis

| Fall Spearman's rho | Mean T | 7d MAX T - Fal DOY | 7d MAX T - Fal | 7d MIN T - Fal DOY | 7d MIN T - Fal | Total R -Fal | 3d MAX R - Fal DOY | 3d MAX R - Fal | 30d MIN R - Fal DOY | 30d MIN R - Fal | Water yield | 3d MAX Q - Fal DOY | 3d MAX Q - Fal | 7d MIN Q - Fal DOY | 7d MIN Q - Fal | BF yield | 3d MAX BF - Fal DOY | 3d MAX BF - Fal | 7d MIN BF - Fal DOY | 7d MIN BF - Fal | 3d MAX GW - Fal DOY | 3d MAX GW - Fal | 7d MIN GW - Fal DOY | 7d MIN GW - Fal |
|---|---|---|---|---|---|---|---|---|---|---|---|---|---|---|---|---|---|---|---|---|---|---|---|---|
| **Mean T** | 1.000 | 0.448 | 0.006 | 0.283 | .867** | 0.418 | 0.456 | 0.139 | 0.309 | 0.576 | 0.164 | 0.565 | 0.370 | -0.231 | -0.127 | 0.006 | 0.588 | 0.382 | 0.018 | -0.079 | .829* | 0.429 | -0.638 | 0.143 |
| **7d MAX T - Fal DOY** | 0.194 | 1.000 | -0.436 | 0.081 | 0.509 | 0.215 | 0.357 | -0.018 | -0.043 | .706* | 0.178 | 0.443 | 0.153 | -0.006 | 0.117 | 0.006 | 0.337 | 0.252 | 0.237 | 0.321 | 0.600 | 0.486 | -0.725 | 0.486 |
| **7d MAX T - Fal** | 0.987 | 0.208 | 1.000 | .720* | 0.006 | -0.042 | 0.000 | -0.091 | 0.297 | -0.055 | -0.006 | 0.061 | 0.152 | -0.018 | -0.127 | 0.139 | 0.273 | 0.067 | -0.339 | -0.189 | 0.257 | -0.543 | 0.203 | -0.657 |
| **7d MIN T - Fal DOY** | 0.428 | 0.824 | 0.019 | 1.000 | 0.320 | -0.271 | 0.407 | -0.252 | 0.474 | 0.080 | -0.222 | 0.574 | 0.062 | 0.068 | -0.369 | -0.246 | .702* | 0.006 | 0.238 | -0.229 | 0.406 | -.812* | 0.191 | -.928** |
| **7d MIN T - Fal** | 0.001 | 0.133 | 0.987 | 0.367 | 1.000 | 0.358 | .669* | 0.188 | 0.030 | .636* | 0.248 | .681* | 0.418 | -0.122 | -0.358 | 0.127 | .673* | 0.430 | 0.092 | -0.250 | .886* | 0.086 | -0.754 | -0.143 |
| **Total R - Fal** | 0.229 | 0.551 | 0.907 | 0.449 | 0.310 | 1.000 | 0.207 | .794** | -0.333 | .733* | .794** | 0.182 | .770** | -0.474 | 0.333 | .673* | 0.200 | .794** | -.732* | 0.189 | 0.543 | 0.543 | -0.638 | 0.486 |
| **3d MAX R - Fal DOY** | 0.185 | 0.311 | 1.000 | 0.243 | 0.035 | 0.567 | 1.000 | 0.432 | 0.116 | 0.474 | 0.249 | .915** | 0.584 | -0.113 | -0.310 | 0.024 | .875** | 0.541 | 0.198 | -0.229 | .899* | 0.116 | -0.471 | -0.145 |
| **3d MAX R - Fal** | 0.701 | 0.960 | 0.803 | 0.482 | 0.603 | 0.006 | 0.213 | 1.000 | -0.394 | 0.455 | .697* | 0.310 | .733* | -0.535 | 0.115 | 0.467 | 0.321 | .721* | -0.585 | -0.006 | 0.771 | 0.429 | -0.319 | 0.429 |
| **30d MIN R - Fal DOY** | 0.385 | 0.906 | 0.405 | 0.166 | 0.934 | 0.347 | 0.751 | 0.260 | 1.000 | -0.067 | -0.285 | 0.152 | 0.006 | -0.079 | 0.285 | -0.321 | 0.261 | -0.042 | 0.185 | 0.305 | -0.086 | 0.200 | 0.377 | -0.086 |
| **30d MIN R - Fal** | 0.082 | 0.023 | 0.881 | 0.826 | 0.048 | 0.016 | 0.166 | 0.187 | 0.855 | 1.000 | .733* | 0.450 | .745* | -0.407 | 0.345 | 0.588 | 0.467 | .806** | -0.412 | 0.409 | 0.543 | 0.543 | -0.638 | 0.486 |
| **Water yield** | 0.651 | 0.623 | 0.987 | 0.538 | 0.489 | 0.006 | 0.487 | 0.025 | 0.425 | 0.016 | 1.000 | 0.128 | .867** | -.717* | 0.479 | .915** | 0.200 | .915** | -.714* | 0.476 | 0.543 | 0.543 | -0.638 | 0.486 |
| **3d MAX Q - Fal DOY** | 0.089 | 0.200 | 0.868 | 0.083 | 0.030 | 0.614 | 0.000 | 0.383 | 0.675 | 0.192 | 0.725 | 1.000 | 0.474 | -0.076 | -0.407 | -0.109 | .960** | 0.444 | 0.321 | -0.284 | .899* | 0.116 | -0.471 | -0.145 |
| **3d MAX Q - Fal** | 0.293 | 0.672 | 0.676 | 0.866 | 0.229 | 0.009 | 0.077 | 0.016 | 0.987 | 0.013 | 0.001 | 0.166 | 1.000 | -0.584 | 0.345 | .733* | 0.539 | .988** | -0.579 | 0.287 | .829* | 0.429 | -0.638 | 0.143 |
| **7d MIN Q - Fal DOY** | 0.521 | 0.987 | 0.960 | 0.852 | 0.738 | 0.166 | 0.756 | 0.111 | 0.828 | 0.243 | 0.020 | 0.834 | 0.077 | 1.000 | -0.419 | -0.511 | -0.237 | -.638* | 0.515 | -0.526 | -0.486 | -0.543 | 0.116 | -0.371 |
| **7d MIN Q - Fal** | 0.726 | 0.748 | 0.726 | 0.294 | 0.310 | 0.347 | 0.383 | 0.751 | 0.425 | 0.328 | 0.162 | 0.243 | 0.328 | 0.228 | 1.000 | 0.479 | -0.345 | 0.394 | -0.554 | .921** | -0.314 | 0.600 | 0.058 | 0.600 |
| **BF yield** | 0.987 | 0.987 | 0.701 | 0.493 | 0.726 | 0.033 | 0.947 | 0.174 | 0.365 | 0.074 | 0.000 | 0.763 | 0.016 | 0.132 | 0.162 | 1.000 | -0.030 | .770** | -.745* | 0.427 | 0.086 | 0.314 | -0.696 | 0.257 |
| **3d MAX BF - Fal DOY** | 0.074 | 0.340 | 0.446 | 0.024 | 0.033 | 0.580 | 0.001 | 0.365 | 0.467 | 0.174 | 0.580 | 0.000 | 0.108 | 0.510 | 0.328 | 0.934 | 1.000 | 0.503 | 0.172 | -0.213 | .943** | -0.029 | -0.232 | -0.314 |
| **3d MAX BF - Fal** | 0.276 | 0.483 | 0.855 | 0.987 | 0.214 | 0.006 | 0.106 | 0.019 | 0.907 | 0.005 | 0.000 | 0.199 | 0.000 | 0.047 | 0.260 | 0.009 | 0.138 | 1.000 | -0.579 | 0.372 | .829* | 0.429 | -0.638 | 0.143 |
| **7d MIN BF - Fal DOY** | 0.960 | 0.510 | 0.339 | 0.509 | 0.800 | 0.016 | 0.584 | 0.076 | 0.610 | 0.236 | 0.020 | 0.366 | 0.080 | 0.127 | 0.097 | 0.013 | 0.634 | 0.080 | 1.000 | -0.362 | -0.116 | -0.377 | 0.132 | -0.406 |
| **7d MIN BF - Fal** | 0.828 | 0.366 | 0.601 | 0.524 | 0.486 | 0.601 | 0.524 | 0.987 | 0.392 | 0.241 | 0.165 | 0.426 | 0.422 | 0.118 | 0.000 | 0.219 | 0.554 | 0.290 | 0.304 | 1.000 | -0.314 | 0.600 | 0.058 | 0.600 |
| **3d MAX GW - Fal DOY** | 0.042 | 0.208 | 0.623 | 0.425 | 0.019 | 0.266 | 0.015 | 0.072 | 0.872 | 0.266 | 0.266 | 0.015 | 0.042 | 0.329 | 0.544 | 0.872 | 0.005 | 0.042 | 0.827 | 0.544 | 1.000 | 0.086 | -0.435 | -0.143 |
| **3d MAX GW - Fal** | 0.397 | 0.329 | 0.266 | 0.050 | 0.872 | 0.266 | 0.827 | 0.397 | 0.704 | 0.266 | 0.266 | 0.827 | 0.397 | 0.266 | 0.208 | 0.544 | 0.957 | 0.397 | 0.461 | 0.208 | 0.872 | 1.000 | -0.319 | .886* |
| **7d MIN GW - Fal DOY** | 0.173 | 0.103 | 0.700 | 0.717 | 0.084 | 0.173 | 0.346 | 0.538 | 0.461 | 0.173 | 0.173 | 0.346 | 0.173 | 0.827 | 0.913 | 0.125 | 0.658 | 0.173 | 0.803 | 0.913 | 0.389 | 0.538 | 1.000 | -0.116 |
| **7d MIN GW - Fal** | 0.787 | 0.329 | 0.156 | 0.008 | 0.787 | 0.329 | 0.784 | 0.397 | 0.872 | 0.329 | 0.329 | 0.784 | 0.787 | 0.468 | 0.208 | 0.623 | 0.544 | 0.787 | 0.425 | 0.208 | 0.787 | 0.019 | 0.827 | 1.000 |

**. Correlation is significant at the 0.01 level (2-tailed).

*. Correlation is significant at the 0.05 level (2-tailed).

## Fall Kendall's Rank Analysis

| Fall Kendall's tau_b | Mean T | 7d MAX T - Fal DOY | 7d MAX T - Fal | 7d MIN T - Fal DOY | 7d MIN T - Fal | Total R-Fal | 3d MAX R - Fal DOY | 3d MAX R - Fal | 30d MIN R - Fal DOY | 30d MIN R - Fal | Water yield | 3d MAX Q - Fal DOY | 3d MAX Q - Fal | 7d MIN Q - Fal DOY | 7d MIN Q - Fal | BF yield | 3d MAX BF - Fal DOY | 3d MAX BF - Fal | 7d MIN BF - Fal DOY | 7d MIN BF - Fal | 3d MAX GW - Fal DOY | 3d MAX GW - Fal | 7d MIN GW - Fal DOY | 7d MIN GW - Fal |
|---|---|---|---|---|---|---|---|---|---|---|---|---|---|---|---|---|---|---|---|---|---|---|---|---|
| **Mean T** | 1.000 | 0.276 | 0.022 | 0.163 | .689** | 0.333 | 0.360 | 0.067 | 0.244 | 0.467 | 0.156 | 0.449 | 0.333 | -0.180 | -0.067 | -0.022 | 0.467 | 0.378 | -0.023 | -0.068 | .733* | 0.333 | -0.414 | 0.067 |
| **7d MAX T - Fal DOY** | 0.276 | 1.000 | -0.322 | 0.048 | 0.322 | 0.184 | 0.302 | 0.000 | 0.000 | .552* | 0.184 | 0.395 | 0.138 | -0.023 | 0.138 | 0.000 | 0.322 | 0.184 | 0.169 | 0.282 | 0.467 | 0.333 | -0.552 | 0.333 |
| **7d MAX T - Fal** | 0.929 | 0.204 | 1.000 | .535* | -0.022 | -0.022 | 0.000 | -0.111 | 0.244 | -0.067 | -0.022 | 0.090 | 0.067 | 0.000 | -0.067 | 0.067 | 0.200 | 0.022 | -0.256 | -0.205 | 0.200 | -0.200 | 0.138 | -0.467 |
| **7d MIN T - Fal DOY** | 0.523 | 0.853 | 0.036 | 1.000 | 0.256 | -0.210 | 0.330 | -0.163 | 0.349 | 0.070 | -0.163 | 0.471 | 0.023 | 0.000 | -0.303 | -0.116 | .535* | -0.023 | 0.171 | -0.143 | 0.276 | -0.690 | 0.214 | -.828* |
| **7d MIN T - Fal** | 0.006 | 0.204 | 0.929 | 0.316 | 1.000 | 0.289 | .494* | 0.111 | 0.022 | 0.422 | 0.111 | 0.405 | 0.289 | -0.045 | -0.289 | 0.022 | 0.422 | 0.333 | 0.116 | -0.205 | .733* | 0.067 | -0.552 | -0.200 |
| **Total R - Fal** | 0.180 | 0.468 | 0.929 | 0.412 | 0.245 | 1.000 | 0.135 | .644** | -0.244 | .600* | .644** | 0.135 | .556* | -0.360 | 0.244 | 0.467 | 0.156 | .600* | -.629* | 0.114 | 0.467 | 0.333 | -0.414 | 0.333 |
| **3d MAX R - Fal DOY** | 0.151 | 0.236 | 1.000 | 0.200 | 0.048 | 0.590 | 1.000 | 0.315 | 0.180 | 0.449 | 0.225 | .818** | .494* | -0.068 | -0.180 | 0.045 | .719** | 0.449 | 0.141 | -0.092 | .828* | 0.138 | -0.357 | -0.138 |
| **3d MAX R - Fal** | 0.788 | 1.000 | 0.655 | 0.523 | 0.655 | 0.009 | 0.209 | 1.000 | -0.333 | 0.333 | .556* | 0.225 | .644** | -0.449 | 0.067 | 0.378 | 0.244 | .600* | -0.442 | -0.068 | 0.600 | 0.200 | -0.138 | 0.200 |
| **30d MIN R - Fal DOY** | 0.325 | 1.000 | 0.325 | 0.171 | 0.929 | 0.325 | 0.472 | 0.180 | 1.000 | -0.022 | -0.156 | 0.180 | 0.022 | 0.045 | 0.244 | -0.156 | 0.244 | -0.022 | 0.163 | 0.296 | 0.067 | 0.200 | 0.276 | -0.067 |
| **30d MIN R - Fal** | 0.060 | 0.029 | 0.788 | 0.784 | 0.089 | 0.016 | 0.072 | 0.180 | 0.929 | 1.000 | .600* | 0.449 | .600* | -0.315 | 0.289 | 0.422 | 0.467 | .644** | -0.303 | 0.341 | 0.467 | 0.333 | -0.414 | 0.333 |
| **Water yield** | 0.531 | 0.468 | 0.929 | 0.523 | 0.655 | 0.009 | 0.369 | 0.025 | 0.531 | 0.016 | 1.000 | 0.135 | .733** | -.539* | 0.333 | .822** | 0.156 | .778** | -.582* | 0.296 | 0.467 | 0.333 | -0.414 | 0.333 |
| **3d MAX Q - Fal DOY** | 0.072 | 0.121 | 0.719 | 0.067 | 0.106 | 0.590 | 0.001 | 0.369 | 0.472 | 0.072 | 0.590 | 1.000 | 0.405 | -0.068 | -0.270 | -0.045 | .899** | 0.360 | 0.235 | -0.138 | .828* | 0.138 | -0.357 | -0.138 |
| **3d MAX Q - Fal** | 0.180 | 0.586 | 0.788 | 0.927 | 0.245 | 0.025 | 0.048 | 0.009 | 0.929 | 0.016 | 0.003 | 0.106 | 1.000 | -0.449 | 0.244 | .556* | 0.422 | .956** | -0.396 | 0.205 | .733* | 0.333 | -0.414 | 0.067 |
| **7d MIN Q - Fal DOY** | 0.472 | 0.927 | 1.000 | 1.000 | 0.857 | 0.151 | 0.787 | 0.072 | 0.857 | 0.209 | 0.031 | 0.787 | 0.072 | 1.000 | -0.225 | -0.360 | -0.180 | -.494* | 0.471 | -0.368 | -0.333 | -0.467 | 0.000 | -0.200 |
| **7d MIN Q - Fal** | 0.788 | 0.586 | 0.788 | 0.236 | 0.245 | 0.325 | 0.472 | 0.788 | 0.325 | 0.245 | 0.180 | 0.281 | 0.325 | 0.369 | 1.000 | 0.333 | -0.156 | 0.289 | -0.396 | .841** | -0.200 | 0.467 | 0.000 | 0.467 |
| **BF yield** | 0.929 | 1.000 | 0.788 | 0.649 | 0.929 | 0.060 | 0.857 | 0.128 | 0.531 | 0.089 | 0.001 | 0.857 | 0.025 | 0.151 | 0.180 | 1.000 | -0.022 | .600* | -.582* | 0.296 | 0.067 | 0.200 | -0.552 | 0.200 |
| **3d MAX BF - Fal DOY** | 0.060 | 0.204 | 0.421 | 0.036 | 0.089 | 0.531 | 0.004 | 0.325 | 0.325 | 0.060 | 0.531 | 0.000 | 0.089 | 0.472 | 0.531 | 0.929 | 1.000 | 0.378 | 0.163 | -0.023 | .867* | -0.067 | -0.138 | -0.333 |
| **3d MAX BF - Fal** | 0.128 | 0.468 | 0.929 | 0.927 | 0.180 | 0.016 | 0.072 | 0.016 | 0.929 | 0.009 | 0.002 | 0.151 | 0.000 | 0.048 | 0.245 | 0.016 | 0.128 | 1.000 | -0.396 | 0.250 | .733* | 0.333 | -0.414 | 0.067 |
| **7d MIN BF - Fal DOY** | 0.927 | 0.517 | 0.316 | 0.516 | 0.649 | 0.014 | 0.583 | 0.083 | 0.523 | 0.236 | 0.023 | 0.360 | 0.121 | 0.067 | 0.121 | 0.023 | 0.523 | 0.121 | 1.000 | -0.262 | -0.138 | -0.276 | 0.071 | -0.276 |
| **7d MIN BF - Fal** | 0.787 | 0.272 | 0.417 | 0.582 | 0.417 | 0.652 | 0.717 | 0.787 | 0.241 | 0.176 | 0.241 | 0.587 | 0.417 | 0.148 | 0.001 | 0.241 | 0.928 | 0.321 | 0.312 | 1.000 | -0.200 | 0.467 | 0.000 | 0.467 |
| **3d MAX GW - Fal DOY** | 0.039 | 0.188 | 0.573 | 0.444 | 0.039 | 0.188 | 0.022 | 0.091 | 0.851 | 0.188 | 0.188 | 0.022 | 0.039 | 0.348 | 0.573 | 0.851 | 0.015 | 0.039 | 0.702 | 0.573 | 1.000 | 0.067 | -0.276 | -0.200 |
| **3d MAX GW - Fal** | 0.348 | 0.348 | 0.573 | 0.056 | 0.851 | 0.348 | 0.702 | 0.573 | 0.573 | 0.348 | 0.348 | 0.702 | 0.348 | 0.188 | 0.188 | 0.573 | 0.851 | 0.348 | 0.444 | 0.188 | 0.851 | 1.000 | -0.276 | .733* |
| **7d MIN GW - Fal DOY** | 0.251 | 0.126 | 0.702 | 0.559 | 0.126 | 0.251 | 0.330 | 0.702 | 0.444 | 0.251 | 0.251 | 0.330 | 0.251 | 1.000 | 1.000 | 0.126 | 0.702 | 0.251 | 0.846 | 1.000 | 0.444 | 0.444 | 1.000 | -0.276 |
| **7d MIN GW - Fal** | 0.851 | 0.348 | 0.188 | 0.022 | 0.573 | 0.348 | 0.702 | 0.573 | 0.851 | 0.348 | 0.348 | 0.702 | 0.851 | 0.573 | 0.188 | 0.573 | 0.348 | 0.851 | 0.444 | 0.188 | 0.573 | 0.039 | 0.444 | 1.000 |

**. Correlation is significant at the 0.01 level (2-tailed).

*. Correlation is significant at the 0.05 level (2-tailed).

Appendix C – Correlation Result Tables

Note: grey indicates significance at 0.01, and no shading indicates significance at 0.05.

Annual correlation

| Annual Correlation | | Spearman's Rank | | Kendall's Rank | | Linear Regression | | |
|---|---|---|---|---|---|---|---|---|
| **Parameter 1** | **Parameter 2** | **ρ** | **p-value** | **τ** | **p-value** | **$R^2$** | **p-value** | **slope** |
| Mean T | 7d MIN T | 0.661 | 0.038 | 0.511 | 0.040 | 0.677 | 0.003 | + |
| Mean T | PET | 0.952 | 0.000 | 0.882 | 0.001 | 0.908 | <0.001 | + |
| Mean T | 10:90 exceed | -0.673 | 0.033 | -0.511 | 0.040 | 0.531 | 0.017 | - |
| Mean T | 3d MAX GW | -0.829 | 0.042 | -0.733 | 0.039 | 0.647 | 0.540 | - |
| 7d MAX T - DOY | 30d MIN R - DOY | -0.863 | 0.001 | -0.719 | 0.004 | 0.720 | 0.002 | - |
| 7d MIN T - DOY | Total P | 0.665 | 0.036 | 0.489 | 0.056 | 0.199 | 0.196 | + |
| 7d MIN T - DOY | Total R | 0.640 | 0.046 | 0.489 | 0.056 | 0.367 | 0.064 | + |
| 7d MIN T - DOY | 30d MIN R | 0.695 | 0.026 | 0.535 | 0.036 | 0.599 | 0.009 | + |
| 7d MIN T - DOY | CMI (P-PET) | 0.775 | 0.008 | 0.629 | 0.014 | 0.599 | 0.009 | + |
| 7d MIN T - DOY | 3d MAX GW - DOY | 0.829 | 0.042 | 0.733 | 0.039 | 0.773 | 0.021 | + |
| Total P | Total R | 0.964 | 0.000 | 0.911 | 0.000 | 0.149 | 0.271 | - |
| Total P | 3d MAX R | 0.661 | 0.038 | 0.511 | 0.040 | 0.441 | 0.036 | + |
| Total P | CMI (P-PET) | 0.867 | 0.001 | 0.689 | 0.006 | 0.888 | <0.001 | + |
| Total P | RBI | 0.624 | 0.054 | 0.511 | 0.040 | 0.357 | 0.068 | + |
| Total P | 3d MAX BF - DOY | 0.358 | 0.310 | 0.244 | 0.325 | 0.114 | 0.341 | + |
| Total P | 7d MIN GW | 0.943 | 0.005 | 0.867 | 0.015 | 0.577 | 0.080 | + |
| Total R | 3d MAX R | 0.600 | 0.067 | 0.511 | 0.040 | 0.361 | 0.066 | + |
| Total R | CMI (P-PET) | 0.794 | 0.006 | 0.600 | 0.016 | 0.798 | <0.001 | + |
| Total R | RBI | 0.564 | 0.090 | 0.511 | 0.040 | 0.366 | 0.064 | 0 |
| Total R | 7d MIN GW | 0.943 | 0.005 | 0.867 | 0.015 | 0.166 | 0.423 | + |
| 3d MAX R - DOY | 10:90 exceed | -0.818 | 0.004 | -0.689 | 0.006 | 0.517 | 0.019 | - |
| 3d MAX R - DOY | 3d MAX Q - DOY | -0.842 | 0.002 | -0.644 | 0.009 | 0.833 | <0.001 | - |
| 3d MAX R - DOY | 7d MIN Q - DOY | 0.600 | 0.067 | -0.511 | 0.040 | 0.468 | 0.029 | + |
| 3d MAX R - DOY | 3d MAX BF - DOY | -0.745 | 0.013 | -0.511 | 0.040 | 0.500 | 0.022 | - |
| 3d MAX R - DOY | 3d MAX BF | -0.745 | 0.013 | -0.600 | 0.016 | 0.385 | 0.055 | - |
| 3d MAX R - DOY | RBI | 0.879 | 0.001 | 0.733 | 0.003 | 0.848 | <0.001 | + |
| 3d MAX R - DOY | 3d MAX Q | 0.648 | 0.043 | 0.467 | 0.060 | 0.630 | 0.006 | + |
| 3d MAX R - DOY | 3d MAX BF - DOY | 0.418 | 0.229 | 0.289 | 0.245 | 0.295 | 0.105 | + |
| 3d MAX R - DOY | 3d MAX BF | 0.248 | 0.489 | 0.200 | 0.421 | 0.213 | 0.179 | + |
| 3d MAX R - DOY | 3d MAX GW - DOY | 1.000 | . | 1.000 | . | 0.520 | 0.106 | + |
| 30d MIN R - DOY | 3d MAX BF | 0.648 | 0.043 | 0.422 | 0.089 | 0.011 | 0.771 | + |
| PET | 10:90 exceed | -0.661 | 0.038 | -0.511 | 0.040 | 0.456 | 0.032 | - |
| CMI (P-PET) | Water yield | 0.661 | 0.038 | 0.511 | 0.040 | 0.492 | 0.024 | + |
| CMI (P-PET) | 7d MIN Q | 0.673 | 0.033 | 0.422 | 0.089 | 0.357 | 0.068 | 0 |
| CMI (P-PET) | BF yield | 0.648 | 0.043 | 0.511 | 0.040 | 0.419 | 0.043 | + |

| Annual Correlation | | Spearman's Rank | | Kendall's Rank | | Linear Regression | | |
|---|---|---|---|---|---|---|---|---|
| Parameter 1 | Parameter 2 | ρ | p-value | τ | p-value | $R^2$ | p-value | slope |
| CMI (P-PET) | 3d MAX BF - DOY | 0.467 | 0.174 | 0.378 | 0.128 | 0.284 | 0.113 | + |
| CMI (P-PET) | 7d MIN BF | 0.693 | 0.026 | 0.494 | 0.048 | 0.354 | 0.070 | + |
| RBI | 3d MAX Q | 0.806 | 0.005 | 0.644 | 0.009 | 0.749 | 0.001 | + |
| RBI | 3d MAX BF - DOY | 0.564 | 0.090 | 0.467 | 0.060 | 0.329 | 0.083 | + |
| RBI | 3d MAX BF | 0.455 | 0.187 | -0.333 | 0.348 | 0.312 | 0.093 | + |
| RBI | 3d MAX GW - DOY | 0.943 | 0.005 | 0.867 | 0.015 | 0.874 | 0.006 | + |
| 10:90 exceed | 3d MAX Q - DOY | 0.661 | 0.038 | 0.511 | 0.04 | 0.386 | 0.055 | + |
| 10:90 exceed | 7d MIN Q - DOY | -0.794 | 0.006 | -0.644 | 0.009 | 0.448 | 0.034 | - |
| 10:90 exceed | 7d MIN BF - DOY | -0.794 | 0.006 | -0.584 | 0.02 | 0.640 | 0.005 | - |
| 10:90 exceed | 7d MIN GW | -0.886 | 0.019 | -0.733 | 0.039 | 0.690 | 0.041 | - |
| Water yield | 7d MIN Q | 0.733 | 0.016 | 0.556 | 0.025 | 0.362 | 0.066 | + |
| Water yield | BF yield | 0.976 | 0.000 | 0.911 | 0.000 | 0.97 | <0.001 | + |
| Water yield | 3d MAX BF - DOY | 0.758 | 0.011 | 0.600 | 0.016 | 0.597 | 0.009 | + |
| Water yield | 7d MIN BF | 0.687 | 0.028 | 0.494 | 0.048 | 0.359 | 0.067 | + |
| Water yield | Mean GW | 0.886 | 0.019 | 0.733 | 0.039 | 0.453 | 0.143 | + |
| 3d MAX Q - DOY | 3d MAX BF - DOY | 0.927 | 0.000 | 0.867 | 0.000 | 0.563 | 0.012 | - |
| 3d MAX Q - DOY | 3d MAX BF | 0.709 | 0.022 | 0.511 | 0.040 | 0.295 | 0.105 | + |
| 3d MAX Q | 3d MAX BF - DOY | 0.709 | 0.022 | 0.556 | 0.025 | 0.522 | 0.018 | + |
| 3d MAX Q | 3d MAX BF | 0.782 | 0.008 | 0.644 | 0.009 | 0.721 | 0.002 | + |
| 7d MIN Q - DOY | 7d MIN BF - DOY | 0.964 | 0.000 | 0.911 | 0.000 | 0.737 | 0.001 | + |
| 7d MIN Q | BF yield | 0.806 | 0.005 | 0.644 | 0.009 | 0.388 | 0.054 | + |
| 7d MIN Q | 3d MAX BF - DOY | 0.152 | 0.676 | 0.289 | 0.245 | 0.046 | 0.553 | + |
| 7d MIN Q | 7d MIN BF | 0.985 | 0.000 | 0.944 | 0.000 | 0.987 | <0.001 | + |
| 7d MIN Q | Mean GW | 0.829 | 0.042 | 0.733 | 0.039 | 0.774 | 0.021 | + |
| BF yield | 3d MAX BF - DOY | 0.673 | 0.033 | 0.511 | 0.040 | 0.481 | 0.026 | + |
| BF yield | 7d MIN BF | 0.748 | 0.013 | 0.584 | 0.020 | 0.371 | 0.062 | + |
| BF yield | Mean GW | 0.886 | 0.019 | 0.733 | 0.039 | 0.517 | 0.107 | + |
| 3d MAX BF - DOY | 3d MAX BF | 0.782 | 0.008 | -0.644 | 0.009 | 0.613 | 0.007 | + |
| 3d MAX BF - DOY | 7d MIN BF | 0.413 | 0.235 | 0.270 | 0.281 | 0.043 | 0.567 | 0 |
| 3d MAX BF | Mean GW | 0.754 | 0.084 | 0.552 | 0.126 | 0.801 | 0.016 | + |
| Mean GW | 7d MIN GW - DOY | -0.821 | 0.023 | -0.619 | 0.051 | 0.595 | 0.042 | - |

*Correlation is significant only at 0.01 level (2-tailed)

**Correlation is not significant

Winter Correlation

| Winter (DJF) Correlation | | Spearman's Rank | | Kendall's Rank | | Linear Regression | | |
|---|---|---|---|---|---|---|---|---|
| Parameter 1 | Parameter 2 | ρ | p-value | τ | p-value | $R^2$ | p-value | slope |
| Mean T | 7d MIN T - Win | 0.764 | 0.006 | 0.636 | 0.006 | 0.756 | <0.001 | + |
| 7d MAX T - Win DOY | 3d MAX Q - Win DOY | -0.647 | 0.031 | -0.477 | 0.042 | 0.008 | 0.789 | + |
| 7d MAX T - Win DOY | 7d MIN BF - Win DOY | -0.409 | 0.212 | -0.315 | 0.183 | 0.022 | 0.666 | + |
| 7d MAX T - Win | 30d MIN R - Win | 0.618 | 0.043 | 0.418 | 0.073 | 0.284 | 0.113 | + |
| 7d MIN T - Win DOY | 7d MIN BF - Win | 0.621 | 0.041 | 0.519 | 0.032 | 0.623 | 0.004 | + |
| 7d MIN T - Win DOY | 3d MAX GW - Win | 0.829 | 0.042 | 0.600 | 0.091 | 0.396 | 0.181 | + |
| 7d MIN T - Win DOY | 7d MIN GW - Win | 0.829 | 0.042 | 0.600 | 0.091 | 0.391 | 0.184 | + |
| 30d MIN R - Win | 3d MAX Q - Win DOY | 0.626 | 0.039 | 0.492 | 0.044 | 0.163 | 0.217 | + |
| 30d MIN R - Win | 3d MAX BF - Win DOY | 0.683 | 0.021 | 0.531 | 0.030 | 0.168 | 0.211 | + |
| Water yield | 3d MAX Q - Win DOY | 0.720 | 0.012 | 0.531 | 0.03 | 0.035 | 0.584 | + |
| Water yield | 3d MAX Q - Win | 0.945 | 0.000 | 0.855 | 0.000 | 0.784 | <0.001 | + |
| Water yield | 7d MIN Q - Win | 0.800 | 0.003 | 0.600 | 0.010 | 0.526 | 0.012 | + |
| Water yield | BF yield - Win | 0.991 | 0.000 | 0.964 | 0.000 | 0.997 | <0.001 | + |
| Water yield | 3d MAX BF - Win DOY | 0.813 | 0.002 | 0.649 | 0.008 | 0.360 | 0.575 | + |
| Water yield | 3d MAX BF - Win | 0.882 | 0.000 | 0.782 | 0.001 | 0.830 | <0.001 | + |
| Water yield | 7d MIN BF - Win DOY | 0.647 | 0.031 | 0.477 | 0.042 | 0.000 | 0.965 | - |
| Water yield | 7d MIN BF - Win | 0.776 | 0.005 | 0.611 | 0.010 | 0.479 | 0.018 | + |
| 3d MAX Q - Win DOY | 3d MAX Q - Win | 0.776 | 0.006 | 0.570 | 0.020 | 0.014 | 0.730 | + |
| 3d MAX Q - Win DOY | BF yield - Win | 0.706 | 0.015 | 0.492 | 0.044 | 0.035 | 0.582 | + |
| 3d MAX Q - Win DOY | 3d MAX BF - Win DOY | 0.962 | 0.000 | 0.915 | 0.000 | 1.000 | <0.001 | + |
| 3d MAX Q - Win DOY | 3d MAX BF - Win | 0.706 | 0.015 | 0.570 | 0.020 | 0.019 | 0.685 | + |
| 3d MAX Q - Win DOY | 3d MAX GW - Win DOY | 1.000 | . | 1.000 | . | 0.932 | 0.002 | + |
| 3d MAX Q - Win | 7d MIN Q - Win | 0.782 | 0.004 | 0.600 | 0.010 | 0.247 | 0.120 | + |
| 3d MAX Q - Win | BF yield - Win | 0.918 | 0.000 | 0.818 | 0.000 | 0.744 | <0.001 | + |
| 3d MAX Q - Win | 3d MAX BF - Win DOY | 0.860 | 0.001 | 0.688 | 0.005 | 0.015 | 0.724 | + |
| 3d MAX Q - Win | 3d MAX BF - Win | 0.955 | 0.000 | 0.855 | 0.000 | 0.994 | <0.001 | + |
| 3d MAX Q - Win | 7d MIN BF - Win DOY | 0.674 | 0.023 | 0.550 | 0.019 | 0.000 | 0.987 | + |
| 3d MAX Q - Win | 7d MIN BF - Win | 0.772 | 0.005 | 0.611 | 0.010 | 0.254 | 0.114 | + |
| 7d MIN Q - Win DOY | 7d MIN Q - Win | 0.673 | 0.023 | 0.491 | 0.036 | 0.311 | 0.075 | + |
| 7d MIN Q - Win DOY | 7d MIN BF - Win DOY | 0.729 | 0.011 | 0.697 | 0.003 | 0.998 | <0.001 | + |
| 7d MIN Q - Win DOY | 7d MIN BF - Win | 0.708 | 0.005 | 0.537 | 0.023 | 0.389 | 0.040 | + |

| Winter (DJF) Correlation | | Spearman's Rank | | Kendall's Rank | | Linear Regression | | |
|---|---|---|---|---|---|---|---|---|
| Parameter 1 | Parameter 2 | ρ | p-value | τ | p-value | $R^2$ | p-value | slope |
| 7d MIN Q - Win | BF yield - Win | 0.755 | 0.007 | 0.564 | 0.016 | 0.520 | 0.012 | + |
| 7d MIN Q - Win | 3d MAX BF - Win DOY | 0.645 | 0.032 | 0.492 | 0.044 | 0.024 | 0.647 | 0 |
| 7d MIN Q - Win | 3d MAX BF - Win | 0.727 | 0.011 | 0.527 | 0.024 | 0.287 | 0.090 | + |
| 7d MIN Q - Win | 7d MIN BF - Win DOY | 0.825 | 0.002 | 0.661 | 0.005 | 0.325 | 0.067 | + |
| 7d MIN Q - Win | 7d MIN BF - Win | 0.986 | 0.000 | 0.945 | 0.000 | 0.983 | <0.001 | + |
| BF yield - Win | 3d MAX BF - Win DOY | 0.799 | 0.003 | 0.610 | 0.013 | 0.037 | 0.573 | + |
| BF yield - Win | 3d MAX BF - Win | 0.855 | 0.001 | 0.745 | 0.001 | 0.794 | <0.001 | + |
| BF yield - Win | 7d MIN BF - Win DOY | 0.615 | 0.044 | 0.440 | 0.061 | 0.002 | 0.899 | - |
| BF yield - Win | 7d MIN BF - Win | 0.731 | 0.011 | 0.574 | 0.015 | 0.466 | 0.021 | + |
| 3d MAX BF - Win DOY | 3d MAX GW - Win | 0.818 | 0.002 | 0.688 | 0.005 | 0.020 | 0.679 | + |
| 3d MAX BF - Win DOY | 7d MIN BF - Win | 0.610 | 0.046 | 0.441 | 0.075 | 0.022 | 0.660 | + |
| 3d MAX BF - Win DOY | 3d MAX GW - Win DOY | 0.941 | 0.005 | 0.857 | 0.020 | 0.870 | 0.007 | + |
| 3d MAX BF - Win | 7d MIN BF - Win DOY | 0.560 | 0.073 | 0.673 | 0.005 | 0.000 | 0.982 | - |
| 3d MAX BF - Win | 7d MIN BF - Win | 0.717 | 0.013 | 0.414 | 0.251 | 0.292 | 0.086 | + |
| 7d MIN BF - Win DOY | 7d MIN BF - Win | 0.824 | 0.002 | 0.673 | 0.005 | 0.406 | 0.035 | + |
| 7d MIN BF - Win | 3d MAX GW - Win | 0.841 | 0.036 | 0.690 | 0.056 | 0.470 | 0.640 | - |
| 7d MIN BF - Win | 7d MIN GW - Win | 0.841 | 0.036 | 0.690 | 0.056 | 0.278 | 0.282 | + |
| 3d MAX GW - Win | 7d MIN GW - Win | 1.000 | . | 1.000 | . | 0.914 | 0.003 | + |

*Correlation is significant only at 0.01 level (2-tailed)

**Correlation is not significant

Spring Correlation

| Spring (MAM) Correlation | | Spearman's Rank | | Kendall's Rank | | Linear Regression | | |
|---|---|---|---|---|---|---|---|---|
| Parameter 1 | Parameter 2 | ρ | p-value | τ | p-value | $R^2$ | p-value | slope |
| Mean T - Spr | BF yield - Spr | -0.733 | 0.016 | -0.511 | 0.040 | 0.376 | 0.035 | - |
| Mean T - Spr | 3d MAX GW - Spr | -0.900 | 0.037 | -0.800 | 0.050 | 0.717 | 0.071 | - |
| Mean T - Spr | 7d MIN GW - Spr DOY | -1.000 | . | -1.000 | . | 0.741 | 0.061 | - |
| 7d MIN T - Spr DOY | Total R - Spr | 0.665 | 0.036 | 0.523 | 0.038 | 0.193 | 0.204 | + |
| 7d MIN T - Spr DOY | 7d MIN Q - Spr DOY | 0.719 | 0.019 | 0.647 | 0.018 | 0.759 | 0.001 | + |

| Spring (MAM) Correlation | | Spearman's Rank | | Kendall's Rank | | Linear Regression | | |
|---|---|---|---|---|---|---|---|---|
| Parameter 1 | Parameter 2 | ρ | p-value | τ | p-value | $R^2$ | p-value | slope |
| 7d MIN T - Spr DOY | BF yield - Spr | 0.598 | 0.068 | 0.523 | 0.038 | -0.125 | 0.966 | + |
| 7d MIN T - Spr DOY | 3d MAX BF - Spr DOY | 0.689 | 0.028 | 0.523 | 0.038 | 0.25 | 0.141 | + |
| 7d MIN T - Spr | 3d MAX R - Spr | 0.661 | 0.038 | 0.556 | 0.025 | 0.337 | 0.079 | + |
| Total R - Spr | 3d MAX R - Spr | 0.709 | 0.022 | 0.556 | 0.025 | 0.807 | <0.001 | + |
| Total R - Spr | Water yield - Spr | 0.818 | 0.004 | 0.644 | 0.009 | 0.419 | 0.043 | + |
| Total R - Spr | 3d MAX Q - Spr DOY | 0.952 | 0.000 | 0.867 | 0.000 | 0.802 | <0.001 | + |
| Total R - Spr | 3d MAX Q - Spr | 0.612 | 0.060 | 0.511 | 0.040 | 0.734 | 0.002 | + |
| Total R - Spr | BF yield - Spr | 0.661 | 0.038 | 0.467 | 0.060 | 0.083 | 0.214 | + |
| Total R - Spr | 3d MAX BF - Spr DOY | 0.939 | 0.000 | 0.822 | 0.001 | 0.774 | <0.001 | + |
| Total R - Spr | 3d MAX BF - Spr | 0.830 | 0.003 | 0.689 | 0.006 | 0.621 | 0.007 | + |
| Water yield - Spr | 3d MAX Q - Spr DOY | 0.806 | 0.005 | 0.600 | 0.016 | 0.584 | 0.010 | + |
| Water yield - Spr | BF yield - Spr | 0.915 | 0.000 | 0.822 | 0.001 | 0.929 | <0.001 | + |
| Water yield - Spr | 3d MAX BF - Spr DOY | 0.818 | 0.004 | 0.644 | 0.009 | 0.619 | 0.007 | + |
| Water yield - Spr | 3d MAX BF - Spr | 0.855 | 0.002 | 0.689 | 0.006 | 0.698 | 0.003 | + |
| Water yield - Spr | 3d MAX GW - Spr | 0.900 | 0.037 | 0.800 | 0.050 | 0.625 | 0.112 | + |
| 3d MAX Q - Spr DOY | 3d MAX Q - Spr | 0.648 | 0.043 | 0.556 | 0.025 | 0.691 | 0.003 | + |
| 3d MAX Q - Spr DOY | BF yield - Spr | 0.636 | 0.048 | 0.422 | 0.089 | 0.352 | 0.070 | + |
| 3d MAX Q - Spr DOY | 3d MAX BF - Spr DOY | 0.988 | 0.000 | 0.956 | 0.000 | 0.997 | <0.001 | + |
| 3d MAX Q - Spr DOY | 3d MAX BF - Spr | 0.879 | 0.001 | 0.733 | 0.003 | 0.792 | <0.001 | + |
| 3d MAX Q - Spr | 3d MAX BF - Spr DOY | 0.721 | 0.019 | 0.600 | 0.016 | 0.679 | 0.003 | + |
| 3d MAX Q - Spr | 3d MAX BF - Spr | 0.855 | 0.002 | 0.733 | 0.003 | 0.753 | 0.001 | + |
| 7d MIN Q - Spr DOY | 7d MIN BF - Spr DOY | 0.877 | 0.001 | 0.758 | 0.003 | 0.327 | 0.084 | + |
| 7d MIN Q - Spr DOY | 7d MIN BF - Spr | 0.675 | 0.032 | 0.546 | 0.048 | 0.242 | 0.149 | + |
| 7d MIN Q - Spr DOY | 3d MAX GW - Spr DOY | -0.894 | 0.041 | -0.837 | 0.052 | 0.589 | 0.130 | - |
| 7d MIN Q - Spr DOY | 7d MIN GW - Spr | 0.894 | 0.041 | 0.837 | 0.052 | 0.828 | 0.032 | + |
| 7d MIN Q - Spr | 7d MIN BF - Spr DOY | 0.642 | 0.045 | 0.511 | 0.054 | 0.196 | 0.200 | + |
| 7d MIN Q - Spr | 7d MIN BF - Spr | 0.991 | 0.000 | 0.966 | 0.000 | 0.997 | <0.001 | + |
| BF yield - Spr | 3d MAX BF - Spr DOY | 0.648 | 0.043 | 0.467 | 0.060 | 0.339 | 0.077 | + |
| BF yield - Spr | 3d MAX BF - Spr | 0.673 | 0.033 | 0.511 | 0.040 | 0.441 | 0.036 | |
| BF yield - Spr | 3d MAX GW - Spr | 0.900 | 0.037 | 0.800 | 0.050 | 0.635 | 0.106 | + |
| 3d MAX BF - Spr DOY | 3d MAX BF - Spr | 0.915 | 0.000 | 0.778 | 0.002 | 0.818 | <0.001 | + |
| 3d MAX BF - Spr | 3d MAX GW - Spr | 1.000 | . | 1.000 | . | 0.968 | 0.003 | + |
| 3d MAX BF - Spr | 7d MIN GW - Spr DOY | 0.900 | 0.037 | 0.800 | 0.050 | 0.701 | 0.077 | + |
| 7d MIN BF - Spr DOY | 7d MIN BF - Spr | 0.665 | 0.036 | 0.529 | 0.051 | 0.223 | 0.168 | + |
| 7d MIN BF - Spr DOY | 3d MAX GW - Spr DOY | -0.894 | 0.041 | -0.738 | 0.077 | 0.513 | 0.174 | - |

| Spring (MAM) Correlation | | Spearman's Rank | | Kendall's Rank | | Linear Regression | | |
|---|---|---|---|---|---|---|---|---|
| **Parameter 1** | **Parameter 2** | **ρ** | **p-value** | **τ** | **p-value** | **$R^2$** | **p-value** | **slope** |
| 7d MIN BF - Spr DOY | 7d MIN GW - Spr | 0.894 | 0.041 | 0.316 | 0.448 | 0.741 | 0.061 | |
| 7d MIN BF - Spr | 3d MAX GW - Spr DOY | -0.872 | 0.054 | -0.738 | 0.077 | 0.75 | 0.026 | - |
| 3d MAX GW - Spr DOY | 7d MIN GW - Spr | -0.829 | 0.042 | -0.733 | 0.039 | 0.597 | 0.072 | - |

*Correlation is significant at the 0.01 level (2-tailed)

**Correlation is not significant

Summer Correlation

| Summer Correlation (JJA) | | Spearman's Rank | | Kendall's Rank | | Linear Regression | | |
|---|---|---|---|---|---|---|---|---|
| **Parameter 1** | **Parameter 2** | **ρ** | **p-value** | **τ** | **p-value** | **$R^2$** | **p-value** | **slope** |
| Mean T - Sum | 7d MAX T - Sum | 0.648 | 0.043 | 0.511 | 0.040 | 0.424 | 0.041 | + |
| 7d MAX T - Sum | 3d MAX Q - Sum DOY | 0.815 | 0.004 | 0.584 | 0.020 | 0.580 | 0.010 | + |
| 7d MAX T - Sum | 3d MAX BF - Sum DOY | 0.119 | 0.743 | 0.097 | 0.710 | 0.013 | 0.757 | + |
| 7d MIN T - Sum | 3d MAX R - Sum DOY | -0.669 | 0.032 | -0.539 | 0.031 | 0.508 | 0.021 | - |
| 7d MIN T - Sum | 7d MIN BF - Sum DOY | 0.652 | 0.041 | 0.432 | 0.087 | 0.049 | 0.538 | + |
| 7d MIN T - Sum | 7d MIN GW - Sum | 0.900 | 0.037 | 0.800 | 0.050 | 0.903 | 0.013 | + |
| Total R - Sum | 3d MAX R - Sum | 0.673 | 0.033 | 0.511 | 0.040 | 0.716 | 0.002 | + |
| Total R - Sum | 3d MAX Q - Sum | 0.648 | 0.043 | 0.511 | 0.040 | 0.506 | 0.021 | + |
| Total R - Sum | 3d MAX BF - Sum DOY | 0.564 | 0.090 | 0.378 | 0.128 | 0.272 | 0.122 | + |
| Total R - Sum | 3d MAX GW - Sum DOY | 0.894 | 0.041 | 0.837 | 0.052 | 0.942 | 0.006 | + |
| 3d MAX R - Sum DOY | 3d MAX R - Sum | -0.673 | 0.033 | -0.556 | 0.025 | 0.292 | 0.107 | - |
| 3d MAX R - Sum DOY | 30d MIN R - Sum | -0.818 | 0.004 | -0.644 | 0.009 | 0.696 | 0.003 | - |
| 3d MAX R - Sum DOY | Water yield - Sum | -0.818 | 0.004 | -0.644 | 0.009 | 0.512 | 0.012 | - |
| 3d MAX R - Sum DOY | 3d MAX Q - Sum | -0.842 | 0.002 | -0.644 | 0.009 | 0.595 | 0.009 | - |
| 3d MAX R - Sum DOY | 7d MIN Q - Sum DOY | -0.665 | 0.036 | -0.523 | 0.038 | 0.534 | 0.016 | - |
| 3d MAX R - Sum DOY | BF yield - Sum | -0.721 | 0.019 | -0.556 | 0.025 | 0.566 | 0.012 | - |
| 3d MAX R - Sum DOY | 3d MAX BF - Sum DOY | -0.867 | 0.001 | -0.689 | 0.006 | 0.578 | 0.011 | - |
| 3d MAX R - Sum DOY | 3d MAX GW - Sum | -0.900 | 0.037 | -0.800 | 0.050 | 0.824 | 0.033 | - |
| 3d MAX R - Sum | BF yield - Sum | 0.758 | 0.011 | 0.644 | 0.009 | 0.485 | 0.025 | + |
| 3d MAX R - Sum | 3d MAX Q - Sum | 0.842 | 0.002 | 0.733 | 0.003 | 0.647 | 0.005 | + |

| Summer Correlation (JJA) | | Spearman's Rank | | Kendall's Rank | | Linear Regression | | |
|---|---|---|---|---|---|---|---|---|
| **Parameter 1** | **Parameter 2** | **ρ** | **p-value** | **τ** | **p-value** | **$R^2$** | **p-value** | **slope** |
| 3d MAX R - Sum | BF yield - Sum | 0.576 | 0.082 | 0.467 | 0.060 | 0.495 | 0.025 | + |
| 3d MAX R - Sum | 3d MAX BF - Sum DOY | 0.830 | 0.003 | 0.689 | 0.006 | 0.539 | 0.016 | + |
| 30d MIN R - Sum DOY | 3d MAX Q - Sum DOY | 0.614 | 0.059 | 0.494 | 0.048 | 0.145 | 0.278 | + |
| 30d MIN R - Sum DOY | 3d MAX BF - Sum DOY | 0.069 | 0.850 | 0.467 | 0.060 | 0.022 | 0.681 | + |
| 30d MIN R - Sum | Water yield - Sum | 0.770 | 0.009 | 0.644 | 0.009 | 0.514 | 0.020 | + |
| 30d MIN R - Sum | 3d MAX Q - Sum | 0.721 | 0.019 | 0.556 | 0.025 | 0.380 | 0.058 | + |
| 30d MIN R - Sum | BF yield - Sum | 0.842 | 0.002 | 0.644 | 0.009 | 0.514 | 0.020 | + |
| 30d MIN R - Sum | 3d MAX BF - Sum DOY | 0.697 | 0.025 | 0.511 | 0.040 | 0.381 | 0.057 | + |
| Water yield - Sum | 3d MAX Q - Sum | 0.964 | 0.000 | 0.911 | 0.000 | 0.856 | <0.001 | + |
| Water yield - Sum | 7d MIN Q - Sum DOY | 0.774 | 0.009 | 0.659 | 0.009 | 0.407 | 0.047 | + |
| Water yield - Sum | 7d MIN Q - Sum | 0.636 | 0.048 | 0.511 | 0.040 | 0.510 | 0.020 | + |
| Water yield - Sum | BF yield - Sum | 0.939 | 0.000 | 0.822 | 0.001 | 0.987 | <0.001 | + |
| Water yield - Sum | 3d MAX BF - Sum DOY | 0.855 | 0.002 | 0.778 | 0.002 | 0.546 | 0.015 | + |
| Water yield - Sum | 7d MIN BF - Sum DOY | 0.614 | 0.059 | 0.494 | 0.048 | 0.311 | 0.094 | + |
| Water yield - Sum | 7d MIN BF - Sum | 0.687 | 0.028 | 0.539 | 0.031 | 0.561 | 0.013 | + |
| Water yield - Sum | 3d MAX GW - Sum DOY | 0.894 | 0.041 | 0.837 | 0.052 | 0.261 | 0.379 | + |
| Water yield - Sum | 3d MAX GW - Sum | 0.900 | 0.037 | 0.800 | 0.050 | 0.585 | 0.132 | + |
| Water yield - Sum | 7d MIN GW - Sum DOY | 0.900 | 0.037 | 0.800 | 0.050 | 0.926 | 0.009 | + |
| 3d MAX Q - Sum DOY | 3d MAX BF - Sum DOY | 0.138 | 0.703 | 0.147 | 0.575 | 0.010 | 0.785 | + |
| 3d MAX Q - Sum | 7d MIN Q - Sum DOY | 0.671 | 0.034 | 0.568 | 0.024 | 0.328 | 0.084 | + |
| 3d MAX Q - Sum | BF yield - Sum | 0.855 | 0.002 | 0.733 | 0.003 | 0.806 | <0.001 | + |
| 3d MAX Q - Sum | 3d MAX BF - Sum DOY | 0.952 | 0.000 | 0.867 | 0.000 | 0.76 | 0.001 | + |
| 3d MAX Q - Sum | 3d MAX GW - Sum DOY | 0.894 | 0.041 | 0.837 | 0.052 | 0.564 | 0.143 | + |
| 3d MAX Q - Sum | 3d MAX GW - Sum | 0.900 | 0.037 | 0.800 | 0.050 | 0.672 | 0.089 | + |
| 3d MAX Q - Sum | 7d MIN GW - Sum DOY | 0.900 | 0.037 | 0.800 | 0.050 | 0.808 | 0.038 | + |
| 7d MIN Q - Sum DOY | 7d MIN Q - Sum | 0.695 | 0.026 | 0.523 | 0.038 | 0.152 | 0.265 | + |
| 7d MIN Q - Sum DOY | BF yield - Sum | 0.756 | 0.011 | 0.568 | 0.024 | 0.412 | 0.045 | + |
| 7d MIN Q - Sum DOY | 3d MAX BF - Sum DOY | 0.579 | 0.079 | 0.477 | 0.058 | 0.250 | 0.141 | + |

| Summer Correlation (JJA) | | Spearman's Rank | | Kendall's Rank | | Linear Regression | | |
|---|---|---|---|---|---|---|---|---|
| **Parameter 1** | **Parameter 2** | **ρ** | **p-value** | **τ** | **p-value** | **$R^2$** | **p-value** | **slope** |
| 7d MIN Q - Sum DOY | 7d MIN BF - Sum DOY | 0.948 | 0.000 | 0.851 | 0.001 | 0.784 | <0.001 | + |
| 7d MIN Q - Sum DOY | 7d MIN BF - Sum | 0.725 | 0.018 | 0.552 | 0.030 | 0.149 | 0.27 | + |
| 7d MIN Q - Sum DOY | 3d MAX BF - Sum DOY | 0.918 | 0.028 | 0.882 | 0.046 | 0.564 | 0.154 | + |
| 7d MIN Q - Sum DOY | 3d MAX GW - Sum | 0.975 | 0.005 | 0.949 | 0.023 | 0.858 | 0.024 | + |
| 7d MIN Q - Sum | BF yield - Sum | 0.648 | 0.043 | 0.511 | 0.040 | 0.557 | 0.013 | + |
| 7d MIN Q - Sum | 7d MIN BF - Sum | 0.997 | 0.000 | 0.989 | 0.000 | 0.970 | <0.001 | + |
| BF yield - Sum | 3d MAX BF - Sum DOY | 0.733 | 0.016 | 0.600 | 0.016 | 0.532 | 0.017 | + |
| BF yield - Sum | 7d MIN BF - Sum DOY | 0.620 | 0.056 | 0.405 | 0.106 | 0.316 | 0.091 | + |
| BF yield - Sum | 7d MIN BF - Sum | 0.699 | 0.024 | 0.539 | 0.031 | 0.621 | 0.007 | + |
| BF yield - Sum | 3d MAX GW - Sum DOY | 0.224 | 0.718 | 0.120 | 0.782 | 0.138 | 0.538 | + |
| BF yield - Sum | 3d MAX GW - Sum | 0.300 | 0.624 | 0.200 | 0.624 | 0.565 | 0.143 | + |
| BF yield - Sum | 7d MIN GW - Sum DOY | 0.700 | 0.188 | 0.600 | 0.142 | 0.951 | 0.005 | + |
| 3d MAX BF - Sum DOY | 3d MAX GW - Sum DOY | 0.918 | 0.028 | 0.882 | 0.046 | 0.995 | <0.001 | + |
| 3d MAX BF - Sum | 3d MAX GW - Sum DOY | 0.894 | 0.041 | 0.837 | 0.052 | 0.497 | 0.184 | + |
| 3d MAX BF - Sum | 3d MAX GW - Sum | 1.000 | . | 1.000 | . | 0.964 | 0.003 | + |
| 3d MAX BF - Sum | 7d MIN GW - Sum DOY | 0.700 | 0.188 | 0.600 | 0.142 | 0.770 | 0.050 | + |
| 7d MIN BF - Sum DOY | 3d MAX GW - Sum DOY | 0.918 | 0.028 | 0.882 | 0.046 | 0.348 | 0.265 | + |
| 7d MIN BF - Sum DOY | 3d MAX GW - Sum | 0.975 | 0.005 | 0.949 | 0.023 | 0.913 | 0.011 | + |
| 7d MIN BF - Sum DOY | 7d MIN GW - Sum | 0.564 | 0.322 | 0.527 | 0.207 | 0.758 | 0.055 | + |
| 3d MAX GW - Sum DOY | 3d MAX GW - Sum | 0.894 | 0.041 | 0.837 | 0.052 | 0.311 | 0.329 | + |

*Correlation is significant only at 0.01 level (2-tailed)

** Correlation not significant

Fall Correlation

| Fall (SON) Correlation | | Spearman's Rank | | Kendall's Rank | | Linear Regression | | |
|---|---|---|---|---|---|---|---|---|
| Parameter 1 | Parameter 2 | ρ | p-value | τ | p-value | $R^2$ | p-value | slope |
| Mean T - Fal | 7d MIN T - Fal | 0.867 | 0.001 | 0.689 | 0.006 | 0.034 | 0.609 | + |
| Mean T - Fal | 3d MAX GW - Fal DOY | 0.829 | 0.042 | 0.733 | 0.039 | 0.645 | 0.054 | + |
| 7d MAX T - Fal DOY | 30d MIN R - Fal | 0.706 | 0.023 | 0.552 | 0.029 | 0.515 | 0.020 | + |
| 7d MAX T - Fal DOY | 7d MIN T - Fal | 0.720 | 0.019 | 0.535 | 0.036 | 0.448 | 0.034 | + |
| 7d MIN T - Fal DOY | 3d MAX BF - Fal DOY | 0.702 | 0.024 | 0.535 | 0.036 | 0.368 | 0.063 | + |
| 7d MIN T - Fal DOY | 3d MAX GW - Fal | -0.812 | 0.050 | -0.690 | 0.056 | 0.433 | 0.156 | - |
| 7d MIN T - Fal DOY | 7d MIN GW - Fal | -0.928 | 0.008 | -0.828 | 0.022 | 0.797 | 0.017 | - |
| 7d MIN T - Fal | 3d MAX R - Fal DOY | 0.669 | 0.035 | 0.494 | 0.048 | 0.315 | 0.091 | + |
| 7d MIN T - Fal | 30d MIN R - Fal | 0.636 | 0.048 | 0.422 | 0.089 | 0.282 | 0.114 | + |
| 7d MIN T - Fal | 3d MAX Q - Fal DOY | 0.681 | 0.030 | 0.405 | 0.106 | 0.314 | 0.092 | + |
| 7d MIN T - Fal | 3d MAX BF - Fal DOY | 0.673 | 0.033 | 0.422 | 0.089 | 0.359 | 0.067 | + |
| 7d MIN T - Fal | 3d MAX GW - Fal DOY | 0.886 | 0.019 | 0.733 | 0.039 | 0.579 | 0.079 | + |
| Total R - Fal | 3d MAX R - Fal | 0.794 | 0.006 | 0.644 | 0.009 | 0.577 | 0.011 | + |
| Total R - Fal | 30d MIN R - Fal | 0.733 | 0.016 | 0.600 | 0.016 | 0.560 | 0.013 | + |
| Total R - Fal | Water yield - Fal | 0.794 | 0.006 | 0.644 | 0.009 | 0.491 | 0.024 | + |
| Total R - Fal | 3d MAX Q - Fal | 0.770 | 0.009 | 0.556 | 0.025 | 0.370 | 0.062 | + |
| Total R - Fal | BF yield - Fal | 0.673 | 0.033 | 0.467 | 0.060 | 0.325 | 0.085 | + |
| Total R - Fal | 3d MAX BF - Fal | 0.794 | 0.006 | 0.600 | 0.016 | 0.380 | 0.058 | + |
| Total R - Fal | 7d MIN BF - Fal DOY | -0.732 | 0.016 | -0.629 | 0.014 | 0.339 | 0.078 | - |
| 3d MAX R - Fal DOY | 3d MAX Q - Fal DOY | 0.915 | 0.000 | 0.818 | 0.001 | 0.885 | <0.001 | + |
| 3d MAX R - Fal DOY | 3d MAX Q - Fal | 0.584 | 0.077 | 0.494 | 0.048 | 0.492 | 0.024 | + |
| 3d MAX R - Fal DOY | 3d MAX BF - Fal DOY | 0.875 | 0.001 | 0.719 | 0.004 | 0.576 | 0.011 | + |
| 3d MAX R - Fal DOY | 3d MAX GW - Fal DOY | 0.899 | 0.015 | 0.828 | 0.022 | 0.756 | 0.024 | + |
| 3d MAX R - Fal | Water yield - Fal | 0.697 | 0.025 | 0.556 | 0.025 | 0.488 | 0.025 | + |
| 3d MAX R - Fal | 3d MAX Q - Fal | 0.733 | 0.016 | 0.644 | 0.009 | 0.853 | <0.001 | + |
| 3d MAX R - Fal | BF yield - Fal | 0.467 | 0.174 | 0.378 | 0.128 | 0.155 | 0.260 | + |
| 3d MAX R - Fal | 3d MAX BF - Fal | 0.721 | 0.019 | 0.600 | 0.016 | 0.861 | <0.001 | + |
| 3d MAX R - Fal | 7d MIN BF - Fal DOY | -0.585 | 0.076 | -0.442 | 0.083 | 0.243 | 0.147 | - |
| 30d MIN R - Fal | Water yield - Fal | 0.733 | 0.016 | 0.600 | 0.016 | 0.461 | 0.031 | + |
| 30d MIN R - Fal | 3d MAX Q - Fal | 0.745 | 0.013 | 0.600 | 0.016 | 0.160 | 0.252 | + |
| 30d MIN R - Fal | BF yield - Fal | 0.588 | 0.074 | 0.422 | 0.089 | 0.429 | 0.040 | + |
| 30d MIN R - Fal | 3d MAX BF - Fal | 0.806 | 0.005 | 0.644 | 0.009 | 0.173 | 0.231 | + |
| Water yield - Fal | 3d MAX Q - Fal | 0.867 | 0.001 | 0.733 | 0.003 | 0.435 | 0.038 | + |
| Water yield - Fal | 7d MIN Q - Fal DOY | -0.717 | 0.020 | -0.539 | 0.031 | 0.181 | 0.220 | - |

| Fall (SON) Correlation | | Spearman's Rank | | Kendall's Rank | | Linear Regression | | |
|---|---|---|---|---|---|---|---|---|
| Parameter 1 | Parameter 2 | ρ | p-value | τ | p-value | $R^2$ | p-value | slope |
| Water yield - Fal | BF yield - Fal | 0.915 | 0.000 | 0.822 | 0.001 | 0.837 | <0.001 | + |
| Water yield - Fal | 3d MAX BF - Fal | 0.915 | 0.000 | 0.778 | 0.002 | 0.491 | 0.024 | + |
| Water yield - Fal | 7d MIN BF - Fal DOY | -0.714 | 0.020 | -0.582 | 0.023 | 0.242 | 0.149 | |
| 3d MAX Q - Fal DOY | 3d MAX BF - Fal DOY | 0.960 | 0.000 | 0.899 | 0.000 | 0.682 | 0.003 | + |
| 3d MAX Q - Fal DOY | 3d MAX GW - Fal DOY | 0.899 | 0.015 | 0.828 | 0.022 | 0.877 | 0.006 | + |
| 3d MAX Q - Fal | BF yield - Fal | 0.733 | 0.016 | 0.556 | 0.025 | 0.091 | 0.396 | + |
| 3d MAX Q - Fal | 3d MAX BF - Fal | 0.988 | 0.000 | 0.956 | 0.000 | 0.995 | <0.001 | + |
| 3d MAX Q - Fal | 7d MIN BF - Fal DOY | -0.579 | 0.080 | -0.396 | 0.121 | 0.092 | 0.395 | - |
| 3d MAX Q - Fal | 3d MAX GW - Fal DOY | 0.829 | 0.042 | 0.733 | 0.039 | 0.365 | 0.204 | + |
| 7d MIN Q - Fal DOY | BF yield - Fal | -0.511 | 0.132 | -0.360 | 0.151 | 0.129 | 0.307 | - |
| 7d MIN Q - Fal DOY | 3d MAX BF - Fal | -0.638 | 0.047 | -0.494 | 0.048 | 0.120 | 0.326 | - |
| 7d MIN Q - Fal DOY | 7d MIN BF - Fal DOY | -0.554 | 0.097 | 0.471 | 0.067 | 0.918 | <0.001 | + |
| 7d MIN Q - Fal | 7d MIN BF - Fal DOY | 0.921 | 0.000 | 0.841 | 0.001 | 0.839 | <0.001 | + |
| BF yield - Fal | 3d MAX BF - Fal | 0.770 | 0.009 | 0.600 | 0.016 | 0.230 | 0.161 | + |
| BF yield - Fal | 7d MIN BF - Fal DOY | -0.745 | 0.013 | -0.582 | 0.023 | 0.215 | 0.177 | |
| 3d MAX BF - Fal DOY | 3d MAX GW - Fal DOY | 0.943 | 0.005 | 0.867 | 0.015 | 0.893 | 0.004 | + |
| 3d MAX BF - Fal | 3d MAX GW - Fal DOY | 0.829 | 0.042 | 0.733 | 0.039 | 0.377 | 0.195 | + |
| 3d MAX GW - Fal | 7d MIN GW - Fal | 0.886 | 0.019 | 0.733 | 0.039 | 0.686 | 0.042 | + |

*Correlation is significant only at the 0.01 level (2-tailed)

** Correlation not significant

Appendix D – Neebing River Hydrographs 2008-2016

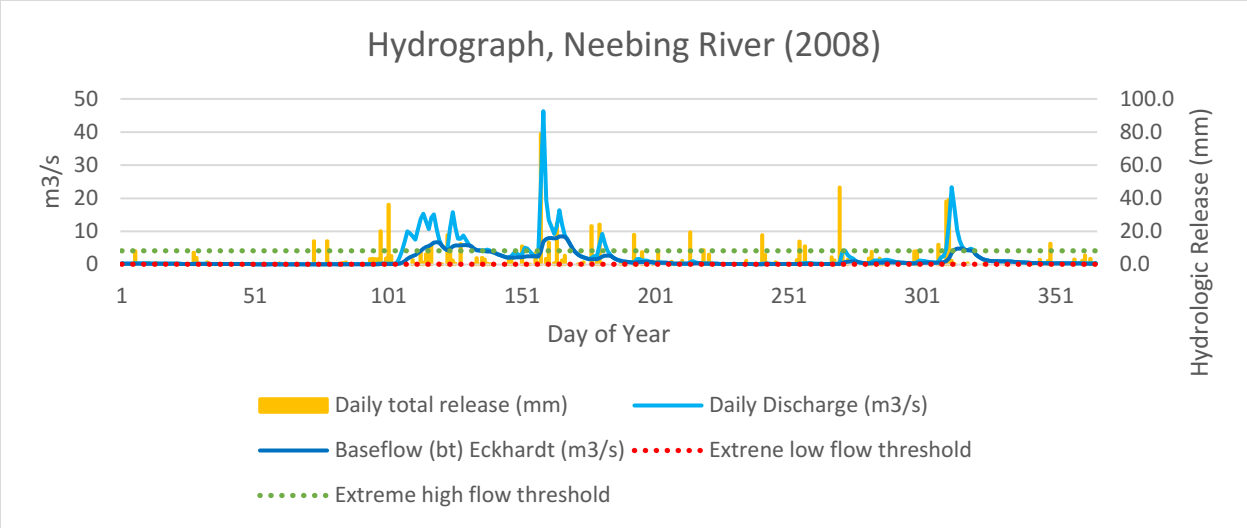
Hydrograph, Neebing River (2008)
m3/s
Hydrologic Release (mm)
Day of Year
Daily total release (mm)
Daily Discharge (m3/s)
Baseflow (bt) Eckhardt (m3/s)
Extrene low flow threshold
Extreme high flow threshold

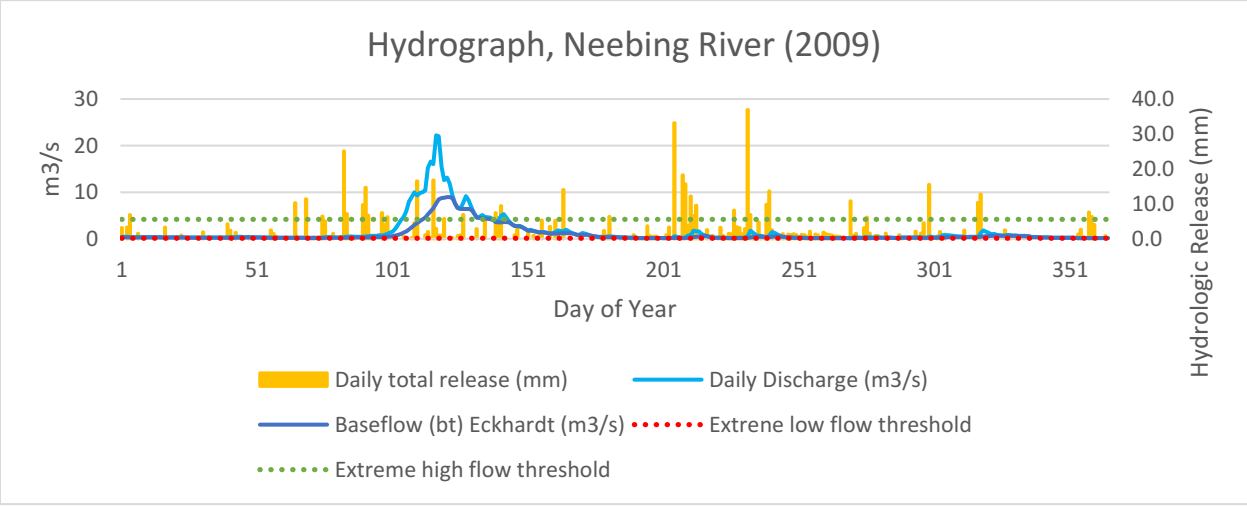
Hydrograph, Neebing River (2009)
m3/s
Hydrologic Release (mm)
Day of Year
Daily total release (mm)
Daily Discharge (m3/s)
Baseflow (bt) Eckhardt (m3/s)
Extrene low flow threshold
Extreme high flow threshold

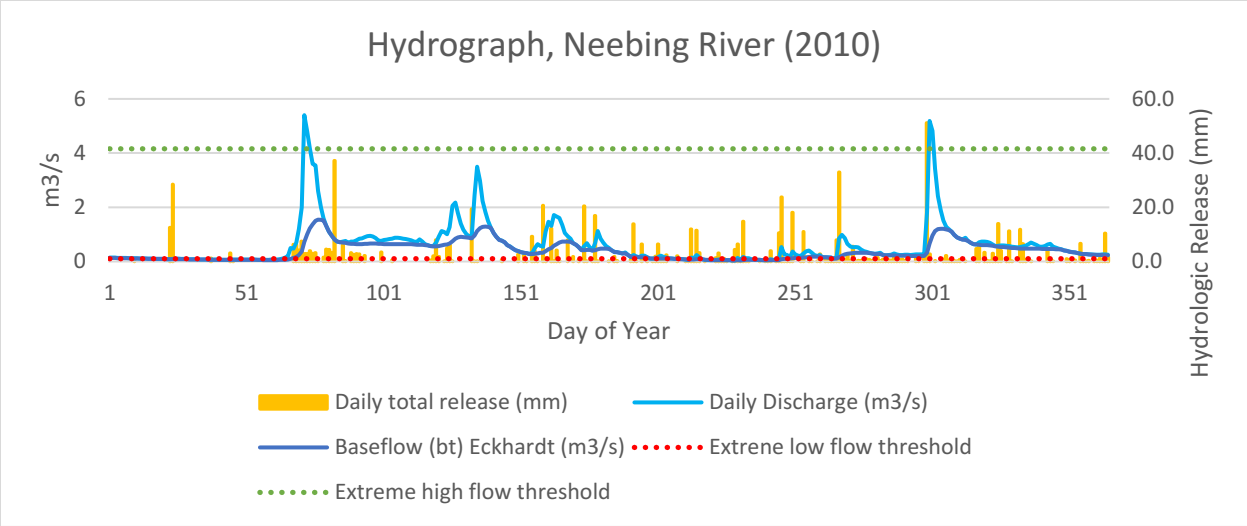
Hydrograph, Neebing River (2010)
m3/s
Hydrologic Release (mm)
Day of Year
Daily total release (mm)
Daily Discharge (m3/s)
Baseflow (bt) Eckhardt (m3/s)
Extrene low flow threshold
Extreme high flow threshold

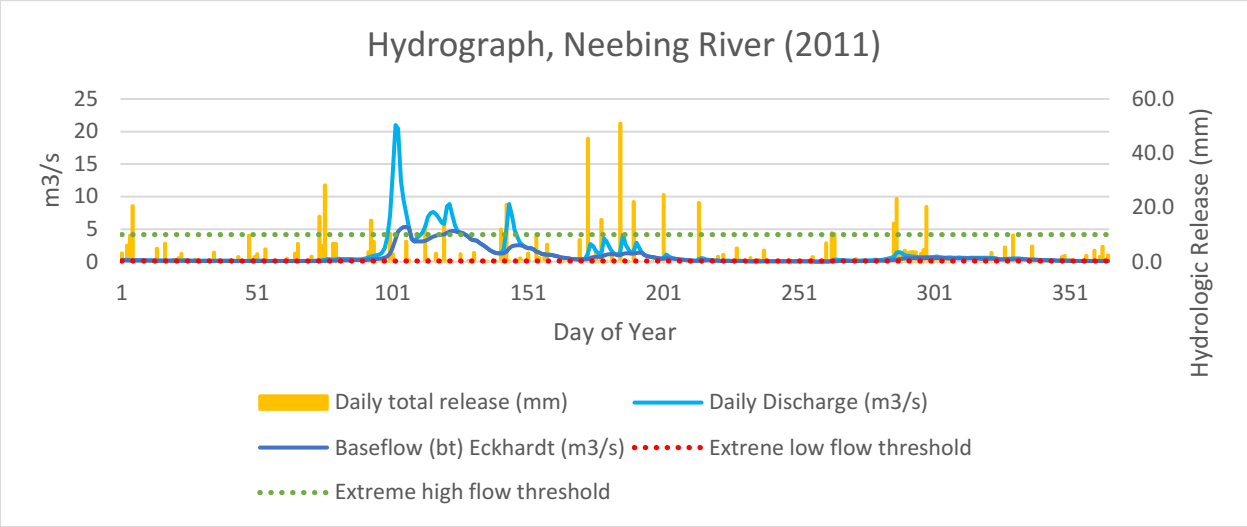
Hydrograph, Neebing River (2011)
m3/s
Hydrologic Release (mm)
Day of Year
Daily total release (mm)
Daily Discharge (m3/s)
Baseflow (bt) Eckhardt (m3/s)
Extrene low flow threshold
Extreme high flow threshold

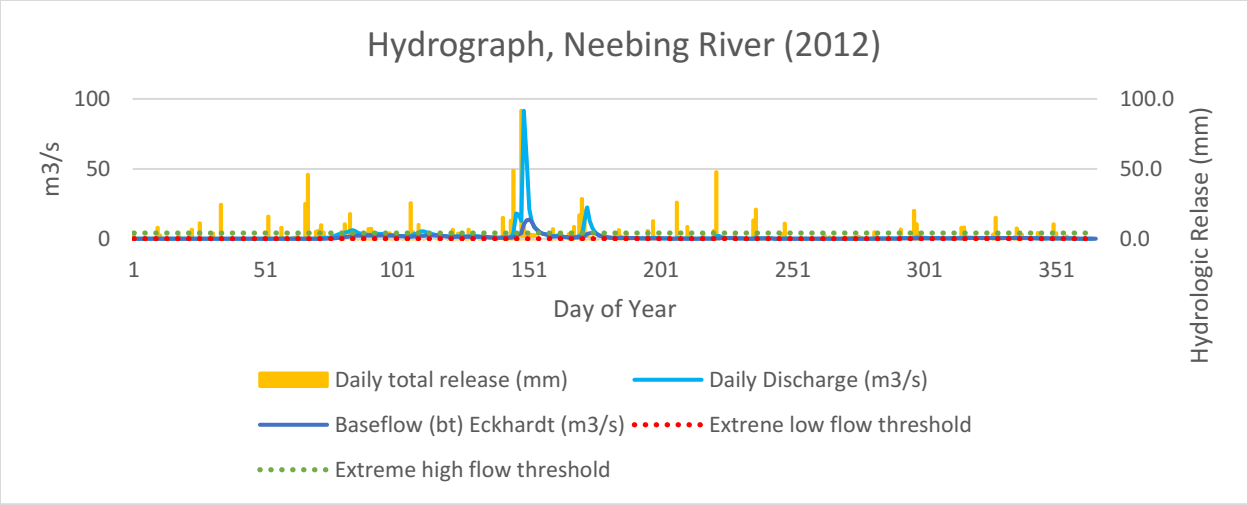
Hydrograph, Neebing River (2012)
m3/s
100
50
0
100.0
50.0
0.0
Hydrologic Relase (mm)
1
51
101
151
201
251
301
351
Day of Year
Daily total release (mm)
Daily Discharge (m3/s)
Baseflow (bt) Eckhardt (m3/s)
Extrene low flow threshold
Extreme high flow threshold

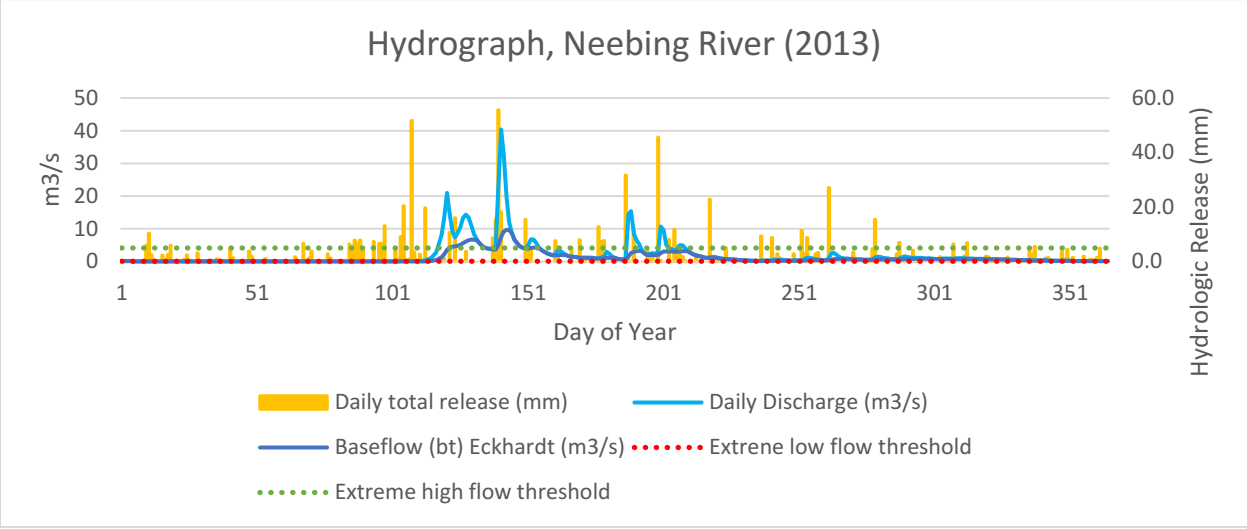
Hydrograph, Neebing River (2013)
m3/s
50
40
30
20
10
0
60.0
40.0
20.0
0.0
Hydrologic Release (mm)
1
51
101
151
201
251
301
351
Day of Year
Daily total release (mm)
Daily Discharge (m3/s)
Baseflow (bt) Eckhardt (m3/s)
Extrene low flow threshold
Extreme high flow threshold

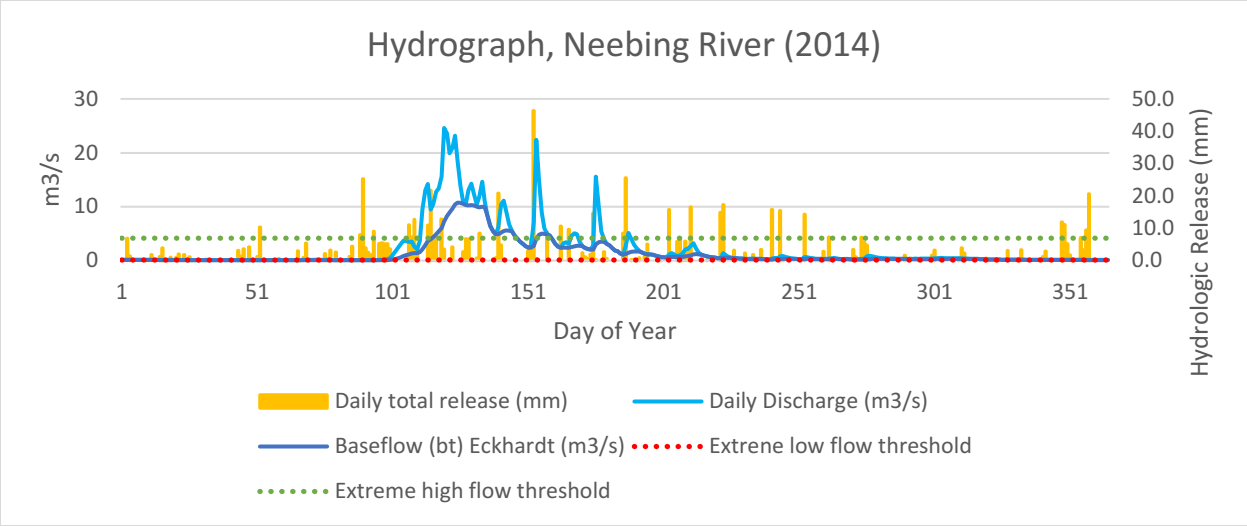
Hydrograph, Neebing River (2014)
m3/s
30
20
10
0
50.0
40.0
30.0
20.0
10.0
0.0
Hydrologic Release (mm)
1
51
101
151
201
251
301
351
Day of Year
Daily total release (mm)
Daily Discharge (m3/s)
Baseflow (bt) Eckhardt (m3/s)
Extrene low flow threshold
Extreme high flow threshold

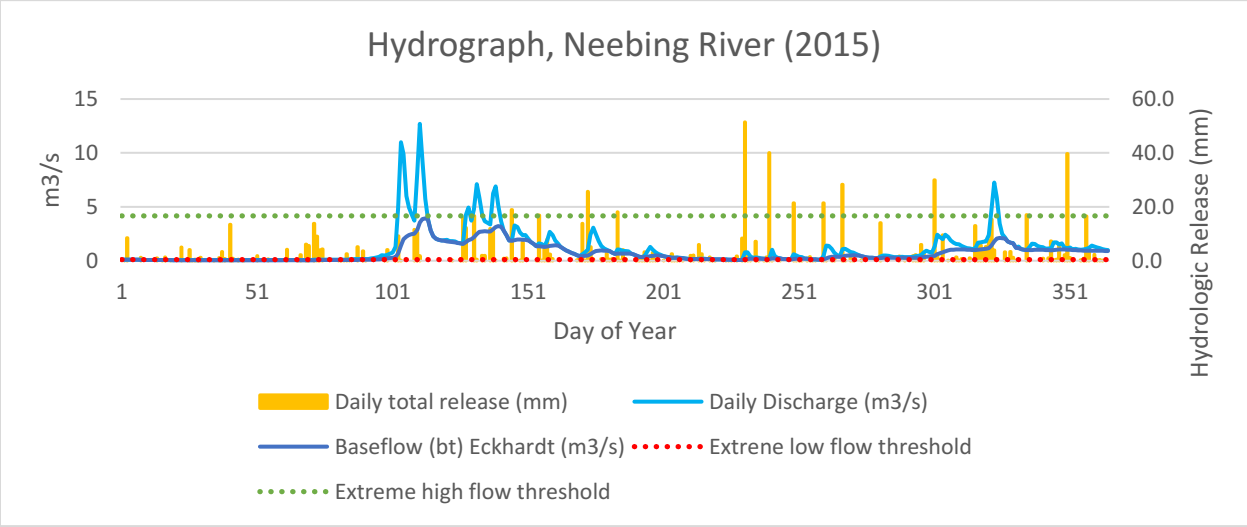
Hydrograph, Neebing River (2015)
m3/s
15
10
5
0
60.0
40.0
20.0
0.0
Hydrologic Release (mm)
1
51
101
151
201
251
301
351
Day of Year
Daily total release (mm)
Daily Discharge (m3/s)
Baseflow (bt) Eckhardt (m3/s)
Extrene low flow threshold
Extreme high flow threshold

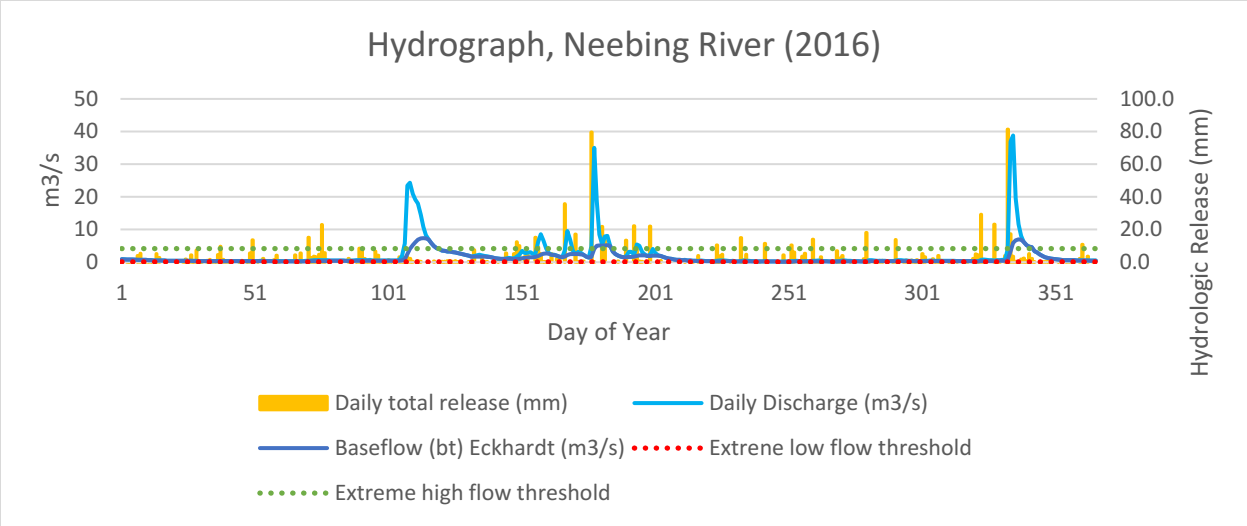


Appendix E – Mann-Kendall Trend Test Results Table

The highlighted rows indicate different levels of confidence, from very confident (VC) p-values <0.025, to potentially trending (PT) p-values <0.05, to warning (W) p-values <0.1.

| Parameter | tau | 2-sided p-value | Confidence | Note |
|---|---|---|---|---|
| Mean T | 0.111 | 0.72051 | | |
| Mean T - Win | 0.11 | 0.69622 | | |
| Mean T - Spr | 0.0667 | 0.85803 | | |
| Mean T - Sum | -0.0222 | 1 | | |
| Mean T - Fal | 0.244 | 0.37109 | | |
| 7d MAX T - DOY | 0.225 | 0.41896 | | |
| 7d MAX T | 0.225 | 0.41896 | | |
| 7d MAX T - Win DOY | 0.514 | 0.035001 | PT | |
| 7d MAX T - Win | 0.527 | 0.029273 | PT | |
| 7d MAX T - Spr DOY | -0.0227 | 1 | | |
| 7d MAX T - Spr | 0.289 | 0.28313 | | |
| 7d MAX T - Sum DOY | 0.225 | 0.41896 | | |
| 7d MAX T - Sum | 0.225 | 0.41896 | | |
| 7d MAX T - Fal DOY | 0.414 | 0.12275 | | |
| 7d MAX T - Fal | -0.2 | 0.47427 | | |
| 7d MIN T - DOY | 0.442 | 0.10082 | | |
| 7d MIN T | -0.289 | 0.28313 | | |
| 7d MIN T - Win DOY | 0.359 | 0.15516 | | |
| 7d MIN T - Win | -0.127 | 0.64043 | | |
| 7d MIN T - Spr DOY | 0.159 | 0.58851 | | |
| 7d MIN T - Spr | 0 | 1 | | |
| 7d MIN T - Sum DOY | 0.27 | 0.32324 | | |

| Parameter | tau | 2-sided p-value | Confidence | Note |
|---|---|---|---|---|
| 7d MIN T - Sum | 0.315 | 0.24303 | | |
| 7d MIN T - Fal DOY | -0.21 | 0.46583 | | |
| 7d MIN T - Fal | -0.0667 | 0.85803 | | |
| Total P | 0.511 | 0.049098 | PT | |
| Total R | 0.511 | 0.49098 | PT | |
| Total R - Win | 0.382 | 0.11947 | | |
| Total R - Spr | -0.0222 | 1 | | |
| Total R - Sum | -0.111 | 0.72051 | | |
| Total R - Fal | 0.289 | 0.28313 | | |
| 3d MAX R - DOY | 0.0222 | 1 | | |
| 3d MAX R | 0.111 | 0.72051 | | |
| 3d MAX R - Win DOY | 0.22 | 0.39036 | | |
| 3d MAX R - Win | 0.2 | 0.43627 | | |
| 3d MAX R - Spr DOY | -0.111 | 0.72051 | | |
| 3d MAX R - Spr | -0.0222 | 1 | | |
| 3d MAX R - Sum DOY | -0.0111 | 0.72051 | | |
| 3d MAX R - Sum | 0.2 | 0.47427 | | |
| 3d MAX R - Fal DOY | -0.225 | 0.41896 | | |
| 3d MAX R - Fal | -0.0667 | 0.8503 | | |
| 30d MIN R - DOY | -0.0222 | 1 | | |
| 30d MIN R | 0.733 | 0.0042075 | VC | |
| 30d MIN R - Win DOY | -0.183 | 0.48219 | | |
| 30d MIN R - Win | 0.673 | 0.0050693 | VC | |
| 30d MIN R - Spr DOY | 0.584 | 0.024764 | VC | |
| 30d MIN R - Spr | 0.422 | 0.1074 | | |
| 30d MIN R - Sum DOY | 0.0222 | 1 | | |
| 30d MIN R - Sum | 0.111 | 0.72051 | | |
| 30d MIN R - Fal DOY | 0.111 | 0.72051 | | |
| 30d MIN R - Fal | 0.244 | 0.37109 | | |
| PET | 0.0222 | 1 | | |
| CMI (P-PET) | 0.467 | 0.073638 | W | |
| RBI | 0.135 | 0.65342 | | |
| 10:90 exceed | -0.0667 | 0.85803 | | |
| Water Yield | 0.244 | 0.37109 | | |
| Water Yield - Win | 0.2 | 0.43627 | | |
| Water Yield - Spr | 0.156 | 0.59151 | | |
| Water Yield - Sum | 0.2 | 0.47427 | | |
| Water Yield - Fal | 0.2 | 0.47427 | | |
| 3d MAX Q - DOY | -0.2 | 0.47427 | | |

| Parameter | tau | 2-sided p-value | Confidence | Note |
|---|---|---|---|---|
| 3d MAX Q | -0.0667 | 0.85803 | | |
| 3d MAX Q - Win DOY | 0.413 | 0.10742 | | |
| 3d MAX Q - Win | 0.273 | 0.27576 | | |
| 3d MAX Q - Spr DOY | 0.111 | 0.72051 | | |
| 3d MAX Q - Spr | 0.111 | 0.72051 | | |
| 3d MAX Q - Sum DOY | 0.135 | 0.65342 | | |
| 3d MAX Q - Sum | 0.111 | 0.72051 | | |
| 3d MAX Q - Fal DOY | -0.0449 | 0.92844 | | |
| 3d MAX Q - Fal | 0.0222 | 1 | | |
| 7d MIN Q - DOY | -0.111 | 0.72051 | | |
| 7d MIN Q | 0.23 | 0.4139 | | |
| 7d MIN Q - Win DOY | -0.0545 | 0.87627 | | |
| 7d MIN Q - Win | 0.204 | 0.43347 | | |
| 7d MIN Q - Spr DOY | 0.2 | 1 | | |
| 7d MIN Q - Spr | 0.2 | 1 | | |
| 7d MIN Q - Sum DOY | 0.477 | 0.071335 | W | |
| 7d MIN Q - Sum | 0.341 | 0.20683 | | |
| 7d MIN Q - Fal DOY | -0.18 | 0.5296 | | |
| 7d MIN Q - Fal | 0.341 | 0.20683 | | |
| BF yield | 0.244 | 0.37109 | | |
| BF yield - Win | 0.164 | 0.53342 | | |
| BF Yield - Spr | 0.0667 | 0.85803 | | |
| BF Yield - Sum | 0.111 | 0.72051 | | |
| BF Yield - Fal | 0.111 | 0.72051 | | |
| 3d MAX BF - DOY | -0.0667 | 0.8503 | | |
| 3d MAX BF | 0.0222 | 1 | | |
| 3d MAX BF - Win DOY | 0.452 | 0.076578 | W | |
| 3d MAX BF - Win | 0.2 | 0.43627 | | |
| 3d MAX BF - Spr DOY | 0.156 | 0.59151 | | |
| 3d MAX BF - Spr | 0.111 | 0.72051 | | |
| 3d MAX BF - Sum DOY | -0.0484 | 0.92581 | | |
| 3d MAX BF - Sum | 0.156 | 0.59151 | | |
| 3d MAX BF - Fal DOY | -0.111 | 0.72051 | | |
| 3d MAX BF - Fal | 0.0667 | 0.85803 | | |
| 7d MIN BF - DOY | -0.0222 | 1 | | |
| 7d MIN BF | 0.225 | 0.41896 | | |
| 7d MIN BF - Win DOY | -0.0367 | 0.93776 | | |
| 7d MIN BF - Win | 0.204 | 0.43347 | | |
| 7d MIN BF - Spr DOY | 0 | 1 | | |

| Parameter | tau | 2-sided p-value | Confidence | Note |
|---|---|---|---|---|
| 7d MIN BF - Spr | 0 | 1 | | |
| 7d MIN BF - Sum DOY | 0.449 | 0.087961 | W | |
| 7d MIN BF - Sum | 0.315 | 0.24303 | | |
| 7d MIN BF - Fal DOY | -0.116 | 0.71538 | | |
| 7d MIN BF - Fal | 0.341 | 0.20683 | | |
| Mean GW | 0.619 | 0.071505 | W | <10 years of data |
| 3d MAX GW - DOY | -0.524 | 0.13313 | | <10 years of data |
| 3d MAX GW | -0.143 | 0.76389 | | <10 years of data |
| 3d MAX GW - Win DOY | 0.276 | 0.56609 | | <10 years of data |
| 3d MAX GW - Win | 0.867 | 0.024171 | VC | <10 years of data |
| 3d MAX GW - Spr DOY | -0.733 | 0.060289 | W | <10 years of data |
| 3d MAX GW - Spr | -0.467 | 0.25966 | | <10 years of data |
| 3d MAX GW - Sum DOY | 0.12 | 1 | | <10 years of data |
| 3d MAX GW - Sum | 0.2 | 0.8065 | | <10 years of data |
| 3d MAX GW - Fal DOY | 0.2 | 0.70711 | | <10 years of data |
| 3d MAX GW - Fal | 0.6 | 0.13285 | | <10 years of data |
| 7d MIN GW - DOY | -0.238 | 0.54801 | | <10 years of data |
| 7d MIN GW | 0.524 | 0.13313 | | <10 years of data |
| 7d MIN GW - Win DOY | 0.2 | 1 | | <10 years of data |
| 7d MIN GW - Win | 0.867 | 0.024171 | VC | <10 years of data |
| 7d MIN GW - Spr DOY | 0.0667 | 1 | | <10 years of data |
| 7d MIN GW - Spr | 0.733 | 0.060289 | W | <10 years of data |
| 7d MIN GW - Sum DOY | -0.2 | 0.8065 | | <10 years of data |
| 7d MIN GW - Sum | 0.6 | 0.22067 | | <10 years of data |
| 7d MIN GW - Fal DOY | -0.69 | 0.085168 | W | <10 years of data |
| 7d MIN GW - Fal | 0.6 | 0.13285 | | <10 years of data |